SCIENCE CHINA
Life Sciences

•REVIEW•

August 2021 Vol.64 No.8: 1236–1280
https://doi.org/10.1007/s11427-020-1915-y

Biodiversity-based development and evolution: the emerging research systems in model and non-model organisms

Long Zhao[1,3†], Feng Gao[1,2,3†], Shan Gao[1,2,4†], Yujun Liang[1,4†], Hongan Long[1,2,3†], Zhiyi Lv[1,4†], Ying Su[1,4†], Naihao Ye[5†], Liusuo Zhang[2,6†], Chengtian Zhao[1,2,4†], Xiaoyu Wang[1,4], Weibo Song[1,2,3*], Shicui Zhang[1,2,4*] & Bo Dong[1,2,4*]

[1]*Institute of Evolution and Marine Biodiversity (IEMB), Ocean University of China, Qingdao 266003, China;*
[2]*Laboratory for Marine Biology and Biotechnology, Qingdao National Laboratory for Marine Science and Technology, Qingdao 266237, China;*
[3]*College of Fisheries, Ocean University of China, Qingdao 266003, China;*
[4]*College of Marine Life Sciences, Ocean University of China, Qingdao 266003, China;*
[5]*Yellow Sea Fisheries Research Institute, Chinese Academy of Fishery Sciences, Qingdao 266071, China;*
[6]*CAS Key Laboratory of Experimental Marine Biology, Institute of Oceanology, Chinese Academy of Sciences, Qingdao 266071, China*

Received December 25, 2020; accepted March 16, 2021; published online April 22, 2021

Evolutionary developmental biology, or Evo-Devo for short, has become an established field that, broadly speaking, seeks to understand how changes in development drive major transitions and innovation in organismal evolution. It does so via integrating the principles and methods of many subdisciplines of biology. Although we have gained unprecedented knowledge from the studies on model organisms in the past decades, many fundamental and crucially essential processes remain a mystery. Considering the tremendous biodiversity of our planet, the current model organisms seem insufficient for us to understand the evolutionary and physiological processes of life and its adaptation to exterior environments. The currently increasing genomic data and the recently available gene-editing tools make it possible to extend our studies to non-model organisms. In this review, we review the recent work on the regulatory signaling of developmental and regeneration processes, environmental adaptation, and evolutionary mechanisms using both the existing model animals such as zebrafish and *Drosophila*, and the emerging non-standard model organisms including amphioxus, ascidian, ciliates, single-celled phytoplankton, and marine nematode. In addition, the challenging questions and new directions in these systems are outlined as well.

Evo-Devo, regeneration, epigenetic, mutation, environmental adaptation, biodiversity

Citation: Zhao, L., Gao, F., Gao, S., Liang, Y., Long, H., Lv, Z., Su, Y., Ye, N., Zhang, L., Zhao, C., et al. (2021). Biodiversity-based development and evolution: the emerging research systems in model and non-model organisms. Sci China Life Sci 64, 1236–1280. https://doi.org/10.1007/s11427-020-1915-y

Introduction

To answer fundamental questions of life and to decipher underlying mechanisms of numerous biological phenomena, investigations using model and non-model organisms play a determinative role. The studies on development, regeneration, and evolution have been the most attractive topics for centuries. Continually, along with the emerging discoveries of genetic regulation, these formed a solid basis for modern life science studies, including the fast progress of medical research.

Evolutionary developmental biology (Evo-Devo) is highly relevant for human beings, in order to understand the origin and genesis of life on the earth. In the past decades, we

†Contributed equally to this work
*Corresponding authors (Weibo Song, email: wsong@ouc.edu.cn; Shicui Zhang, email: sczhang@ouc.edu.cn; Bo Dong, email: bodong@ouc.edu.cn)

gained more in-depth understanding of developmental processes through model organism systems, especially the molecular and cellular mechanisms of organogenesis, morphogenesis, and metabolic homeostasis. However, we still cannot resolve the current problems related to developmental biology, such as birth defects, aging, and natural or disease-caused death. This indicates that the knowledge that we gained is still insufficient to fully understand the complexity and dynamics of life. We might have to expand our studies from several model systems to more non-model systems. Indeed, milestone breakthroughs are more often coming from studies using non-model organisms. For example, Cyclin, the key regulatory factor of cell cycle, was discovered using sea urchins, which lay a huge number of eggs at the same time, allowing biochemical assays (Evans et al., 1983). Another exciting finding is the telomere, which was identified by Elizabeth Blackburn when she studied the chromosome of a unicellular ciliate organism *Tetrahymena* (Szostak and Blackburn, 1982; Greider and Blackburn, 1985; Greider and Blackburn, 1989). The increasing large-scale genomic sequencing of diverse species and the application of CRISPR/Cas9-based gene-editing tools made it possible to extend the current Evo-Devo studies onto non-model organisms (Wei, 2020).

Regeneration is a fascinating ability to replacement of lost body parts, which has captured human imagination since ancient times. The regenerative capacities of metazoans vary, from the level of the whole body, mainly in invertebrates, to the organs/tissues in vertebrates. The knowledge of regeneration obtained via animal studies not only fulfill the gaps in knowledge of basic biology, but also provide valuable clues for developing clinical strategies to restore damaged organs or tissues in humans. Human hearts do not regenerate upon mechanical or pathological injuries, causing most of the deaths worldwide. However, recent studies indicate that human cardiomyocytes are renewable at a low but detectable rate throughout life (Bergmann et al., 2009; Bergmann et al., 2015). This significantly raises the importance of cardiac regeneration studies using animal models, such as zebrafish and mouse, and made them inimitably valuable especially in the medical research field. Another example is the ability to regenerate appendages, which naturally occurs in salamanders but is no longer present in mammals, including human. Researchers revealed mechanisms involving blastema and associated molecules during limb regeneration in axolotls (Joven et al., 2019). Information about regeneration is revealed by studies using different animals. Comparative analyses are performed to illustrate an entire blueprint of regeneration, by identifying pivotal genetic determinants during evolutionary processes.

Genetic regulation administrates the collective outcome of individual genes, thus governing the biological processes and cellular phenotypes. On the one hand, some regulatory type mechanisms are highly conserved across eukaryotes, like histone post-translational modifications and RNA N^6-adenosine methylation (m^6A). Other mechanisms display a patchier distribution and highly diversified functions, such as DNA N^6-adenine methylation (6mA). On the other hand, even the most conserved regulatory mechanisms, such as cellular signaling pathways and protein modifications, are distinct in relevant components, intersecting pathways, and biological outputs. All these factors require investigation, not only in model organisms that already provided deep insights into genetic regulation, but also in non-model organisms that harbor a rich pool of unexplored phenomena and mechanisms.

Evolution is defined as a spatio-temporal change of allele frequency, focusing on mechanisms changing or maintaining allele frequencies at the population level, such as mutation, natural selection, genetic drift, and recombination. With the benefits of "omics" and bioinformatics, more and more high-quality reference genomes have been published from various model and non-model organisms, especially those at population level. Combined with theoretical advances, they have revealed tremendous diversity in all aspects of genome architecture. They broadly promoted our understanding of horizontal gene transfer, genetic admixture, genome rearrangement, as well as mutation and adaptation upon environmental changes. In addition, many interdisciplinary studies demonstrate great potentials in solving long standing questions, such as applying evolutionary genetic methods to evaluation of toxicity, phage display from experimental evolution to immunotherapy.

In this review, we aim to highlight the recent progress in diverse and active studies utilizing representative model and non-model organisms, to illustrate the progress of discoveries in the fields of development, regeneration, genetic regulation, and evolution.

Molecular evolution

Growth hormone/insulin-like growth factor axis in the basal chordate amphioxus (Figure 1)

All vertebrate brains have a hypothalamus, which forms the ventral part of the diencephalon. One of the most important functions of the hypothalamus is to link the nervous system to the endocrine system via the pituitary gland. For example, the hypothalamus secretes growth hormone releasing hormone (GHRH), which triggers production of growth hormone (GH) from the pituitary gland. GH is delivered by a high-affinity GH-binding protein (GHBP) to the cytoplasmic membrane of hepatocytes and interacts with the specific receptor, GH receptor (GHR), on this membrane, resulting in the production of insulin-like growth factor I (IGF-I). IGF-I is finely regulated by a family of high-affinity IGF-binding

proteins (IGFBPs) in the circulation. It plays a key role in the regulation of proliferation, differentiation and anti-apoptosis of bone and muscle cells, by binding to IGF-I receptor (IGFR-I) located on the cell surface of the target tissues. This complicated system, mainly consisting of GH, GHR, IGF-I, and IGFR-I, is referred to as the GH/IGF axis or pituitary-liver axis, which comprises a key part of the neuroendocrine system in vertebrates. The GH/IGF system has been documented in all groups of vertebrates including lamprey (Kawauchi and Sower, 2006), but its evolutionary origin remains enigmatic. Amphioxus, a basal chordate, is the best available stand-in for the proximate invertebrate ancestor of vertebrates, and thus provides an ideal model for studying the origin of the GH/IGF system. It has been our pet model animal for more than 30 years and has been used to investigate the origin and evolution of vertebrates in our laboratory. Below we briefly discuss the state-of-the-art understanding of the origin and evolution of the GH/IGF system.

A functional GH-like hormone is present in amphioxus

GH has long been regarded as an evolutionary innovation in vertebrates. But we show for the first time that a functional GH-like polypeptide, GHl, exists in amphioxus (Li et al., 2014; Li et al., 2017). First, we have cloned a cDNA encoding a protein of 208 amino acids, which belongs to the class-I cytokine superfamily, and bears a 3-dimensional structure sharing a high degree of similarity with human GH. In addition, we found that GHl was predominantly distributed in Hatschek's pit, a tissue homologous to the vertebrate pituitary gland. Second, both recombinant amphioxus GHl (rGHl) and zebrafish GH (rGH) have a similar capacity to bind to the GH receptors (GHRs) from the livers of zebrafish, prepared and partially purified through a wheat-germ agglutinin (WGA)-agarose column, in a dose-dependent manner. Third, we proved that amphioxus GHl as well as human GH share some conserved amino acids, such as R70 and R175, which are critical for the interaction with GHRs. Fourth, rGHl stimulates the expression of *igf-i* in the liver and muscle, as GH does in vertebrates; this gene expression-stimulating effect is abolished by the pre-incubation of rGHl with the recombinant GHl receptor (rGH/PRLlBP). Fifth, rGHl, like zebrafish rGH, is able to promote growth in zebrafish. Supplementation of amphioxus rGHl as well as zebrafish rGH can rescue abnormal morphogenesis caused by GH deficiency in *tbx5* knockdown zebrafish embryos. Lastly, rGHl is capable of mediating osmoregulation through the same mechanisms as vertebrate GH. Collectively, these data provide compelling evidence for the existence of a functional GH-like hormone in the basal chordate amphioxus.

Amphioxus GHl is an ancestral hormone

Structurally related pituitary hormones in vertebrates contain GH, prolactin (PRL) and somatolactin (SL), which are believed to have evolved from a common ancestral gene through duplication and subsequent divergence. GHs have been identified in all vertebrates, including jawless vertebrates. However, there is no evidence that PRL is present or functional in extant jawless vertebrates, including lamprey and hagfish. Based on these data, it has been suggested that in the pituitary hormone family, GH is the closest to the ancestral hormone. We found that amphioxus GHl is the only member of the pituitary hormone family in amphioxus. Phylogenetic analysis shows that amphioxus GHl is positioned at the base of the vertebrate pituitary hormone GH and PRL, suggesting it is the archetype of the vertebrate pituitary hormone family. It is highly likely that amphioxus GHl is the ancestral peptide that first originated in the molecular evolution of the pituitary hormone family in chordates, and the emergence of PRL and SL resulted from gene duplication events during vertebrate evolution (Li et al., 2014).

Amphioxus has an interacting partner of GHl hormone

GH functions by binding to its specific receptor. As amphioxus GHl has been shown to be functional, we thus set out to explore its receptor. We identified an amphioxus GH/PRLlBP peptide by cDNA cloning, consisting of 224 amino acids, from by, which contains the entire hormone binding domain of GH/PRL receptors. It is widely expressed among the different amphioxus tissues, including the hepatic caecum, gill, hindgut, notochord, and testis. Such a wide expression pattern is consistent with the pleiotropic actions of GH peptides in vertebrates. Importantly, we have shown that recombinant GH/PRLlBP (rGH/PRLlBP) specifically interacted with amphioxus rGHl as well as zebrafish rGH, and that the interaction of rGH/PRLlBP with rGHl suppressed the biological activity of GHl. This clearly indicates that GH/PRLlBP is a partner molecule capable of interacting with GHl in amphioxus. It is evident that, like in vertebrates, amphioxus GHl also functions by binding to its interacting partner. It is interesting to note that GH gene expression is not confined to the pituitary gland, which is consistent with its occurrence in many extrapituitary tissues in vertebrates. In addition, autocrine/paracrine GH actions are also known in vertebrates. Notably, amphioxus GHl is also distributed in a number of tissues, such as the Hatschek's pit, muscle, and notochord, suggesting that autocrine/paracrine actions of GHl may be present in amphioxus. This hypothesis was further corroborated by the fact that the gene encoding GH/PRLlBP, an interacting partner of GHl, is widely expressed in different tissues of amphioxus. Thus, we propose that the autocrine/paracrine GH actions may have emerged in basal chordates, and remained throughout vertebrate evolution (Li et al., 2014).

Amphioxus has a GH/GH receptor-like system

In amphioxus, the Hatschek's pit is regarded as the homolog

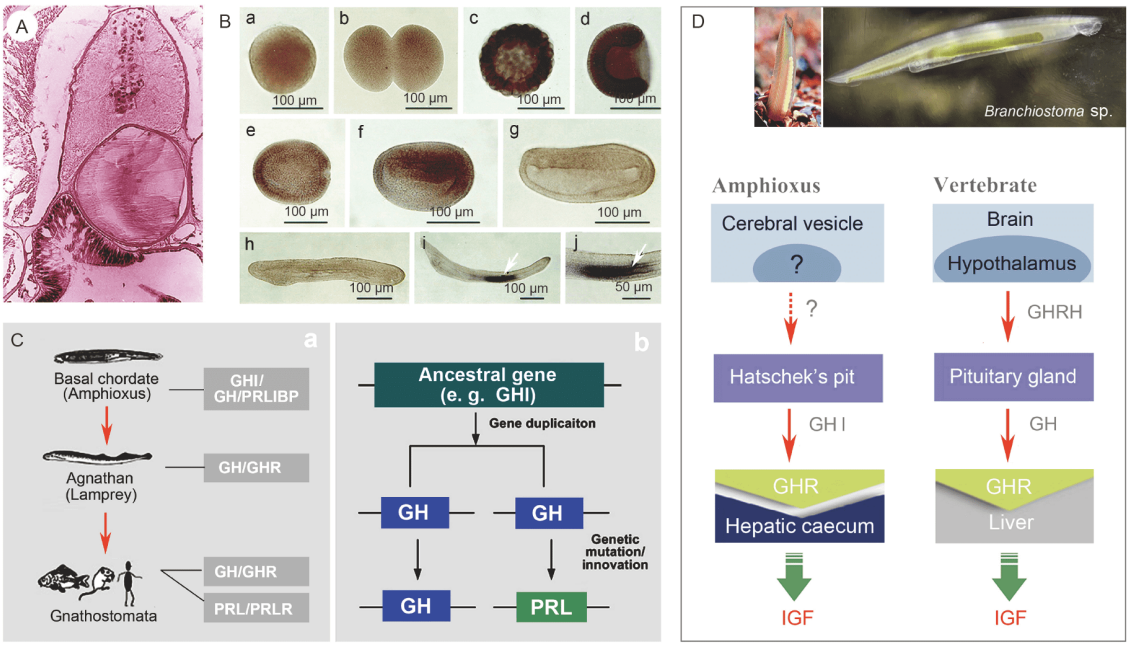

Figure 1 Presence of a vertebrate-like GH/IGF system in the basal chordate amphioxus *Branchiostoma*. A, Hatschek's groove, a tissue equivalent to vertebrate pituitary gland. B, Different stages of amphioxus embryos with the developing hepatic caecum marked by the liver-specific gene encoding cathepsin L; the arrows in (Bi) and (Bj) indicate larval gut. C, Diagrams showing the origin and evolution of GH/GHR as well as the emergence of prolactin (PRL) gene via genetic mutation and innovation of ancestral GH gene. D, GH/IGF systems (i.e. pituitary-liver axis) in vertebrate and amphioxus. Note the presence of hypothalamus-like structure in amphioxus remains to be tested. GH, growth hormone; GHl, GH-like; GHR, GH receptor; GHRH, growth hormone releasing hormone; IGF, insulin-like growth factor.

of vertebrate pituitary gland. This is further supported by the localization of vertebrate-like gonadotropic hormone in Hatschek's pit, and the expression patterns of the pituitary-specific transcription factors, *Pit-1* and *Pax6* in the preoral pit, the primordium of Hatschek's pit. We demonstrated that GHl is abundantly distributed in Hatschek's pit. Moreover, we have shown the presence of a GH receptor-like protein, with the entire hormone binding domain of GH/PRL receptors, which is predominantly expressed in the liver-like tissue of amphioxus, the hepatic caecum. It is capable of interacting with GHl in amphioxus, analogous to vertebrate GH receptors (Li et al., 2014). Therefore, it seems that a vertebrate-like neuroendocrine axis setting emerged in amphioxus, providing additional evidence for the functional homology between the Hatschek's pit and vertebrate pituitary gland.

Amphioxus has an IGF/IGF receptor-like system

IGF-I is the pivot of the GH/IGF system, and the primary action of IGF-I, mediated by binding to its specific receptor IGFI-R, is present in a wide range of tissues. Chan and colleagues cloned and characterized a cDNA encoding an insulin-like peptide (ILP) from the cephalochordate amphioxus Branchiostoma californiensis (Chan et al., 1990). The deduced amino acid of ILP is a hybrid peptide that shows features characteristic of both insulin and IGFs, suggesting that ILP may represent the common ancestral form of vertebrate insulin and IGFs. Moreover, a gene coding for ILP receptor has also been identified in the same species, and the deduced amino acid sequence shares features of both the insulin receptor and IGF-I receptor (Pashmforoush et al., 1996). Together, these data suggest that evolutionarily ILP and its receptor already emerged in primitive chordates. This is further strengthened by our study showing the presence of an insulin/IGF hybrid polypeptide in another cephalochordate species, *B. japonicum* (Guo et al., 2009). Interestingly, we demonstrated that the recombinant insulin/IGF peptide, is able to stimulate the flounder gill cell proliferation, thereby resembling vertebrate IGF. However, it cannot reduce blood glucose levels like insulin, suggesting that *B. japonicum* insulin/IGF may be a molecule functionally similar to vertebrate IGF. In addition, we have established a primary culture system of mouse muscle satellite cells as an *in vitro* model to investigate the effects of amphioxus IGF-like molecule on muscle cell development. We revealed that the recombinant IGF-like molecule, like human IGF, is able to stimulate the proliferation of mouse muscle cells. Besides, it is able to bind to the cells and the partially purified IGF receptors from mouse muscle cells. Importantly, recombinant amphioxus IGF-like molecules are capable of activating the MAPK and PI3K/Akt pathways by stimulating phosphorylation of MAPK and Akt (Liu and Zhang, 2011). This interaction of amphioxus IGF-like molecule with mammalian (mouse) IGF receptors, and its ability of indu-

cing similar downstream signaling pathways, clearly supports the presence of an IGF/IGF receptor in amphioxus.

The acquisition of the hypothalamic-pituitary system, which is specific to vertebrates, is considered to be a seminal event that led to physiological divergence, including reproduction, growth, metabolism, stress, and osmoregulation. Of note, a brain-Hatschek's pit connection has been suggested in amphioxus (Gorbman et al., 1999). It is probable that the emergence of Hatschek's pit represents one of the most important events during evolution of the endocrine network, providing the basis for the subsequent formation of a hypothalamic-pituitary system in vertebrates. This is further supported by our recent identification of a GHRH-like gene (Bb_267100R; http://genome.bucm.edu.cn/lancelet/) and its receptor gene (XP_019638674.1; https://www.ncbi.nlm.nih.gov/protein/) from amphioxus genome data. The functional characterization of the GHRH-like hormone and its receptor in amphioxus are being now under way in our laboratory.

A rediscovered epigenetic mark, DNA N^6-adenine methylation, in unicellular eukaryotic ciliates (Figure 2)

6mA are widely distributed and functionally diversified in eukaryotes

DNA 6mA is a recently rediscovered modification in eukaryotes. In contrast to the widely-present and well-characterized 5-methylcytosine (5mC) (Breiling and Lyko, 2015), 6mA in eukaryotes remained largely neglected for a long time due to the fact that 6mA is present at a low level and has been undetectable in most eukaryotes (Bird, 1992; Hattman, 2005; Hattman et al., 1978). Recent studies, however, have significantly advanced our knowledge of 6mA in eukaryotes, facilitated by modern technologies such as ultrasensitive high-performance liquid chromatography coupled with mass spectrometry (UHPLC-QQQ-MS/MS) and Single Molecule, Real-Time (SMRT) sequencing (Fu et al., 2015; Greer et al., 2015; Zhang et al., 2015a). 6mA is required for transcription regulation in many organisms (Fu et al., 2015; Liang et al., 2018; Wang et al., 2018), developmental modulation in *Drosophila* (Zhang et al., 2015a), epigenetic information transmission in *Caenorhabditis elegans* (Greer et al., 2015), stress response in the mouse brain (Yao et al., 2017), carcinogenesis in human glioblastoma (Xie et al., 2018), hypoxia response in human mitochondria (Hao et al., 2020), etc. So far, 6mA was reported in more than 20 eukaryotes, from protists and fungi (Fu et al., 2015; Gorovsky et al., 1973; Mondo et al., 2017; Salvini et al., 1986; Wang et al., 2017), to plants and animals (Greer et al., 2015; Koziol et al., 2016; Liang et al., 2018; Liu et al., 2016; Schiffers et al., 2017; Wang et al., 2018; Wu et al., 2016; Xiao et al., 2018; Zhang et al., 2015a; Zhou et al., 2018), revealing a patchy yet wide presence of 6mA and corroborating its biological relevance in eukaryotes. Of note, eukaryotic 6mA is highly divergent in abundance and function, suggesting a complex evolutionary history of 6mA, and providing a novel perspective for understanding eukaryote diversification.

Ciliates are ideal model systems to study evolutionary diversification of 6mA

As a major, successful, and diversified evolutionary lineage of unicellular eukaryotes, ciliates were among the first eukaryotes reported to contain 6mA (Cummings et al., 1974; Gorovsky et al., 1973; Rae and Spear, 1978). The most distinguishing feature of ciliates is the two types of nuclei in a single cell, including the smaller, diploid, germline-like micronucleus (MIC) and the larger, polyploid, soma-like macronucleus (MAC) (Prescott et al., 1971). Ciliate 6mA was investigated in about ten ciliate species during the 1970s and 80s (Ammermann et al., 1981; Cummings et al., 1974; Gorovsky et al., 1973; Palacios et al., 1994; Pratt and Hattman, 1981; Rae and Spear, 1978; Salvini et al., 1986). The ciliates *Tetrahymena thermophila* (Ciliophora, Oligohymenophorea) (Wang et al., 2017) and *Oxytricha fallax* (Spirotrichea) (Beh et al., 2019) (referred to as *Tetrahymena* and *Oxytricha* hereafter, respectively) were reinvestigated with modern technologies. Notably, 6mA is the only detectable methylated nucleotide base in *Tetrahymena* so far discovered (Gorovsky et al., 1973; Wang et al., 2017), making it an ideal system for the study of 6mA. 6mA is also the sole DNA methylation during its asexual stage in *Oxytricha* (~0.4%) (Beh et al., 2019), but was reported to have 5mC during conjugation the sexual stage of ciliates (Bracht et al., 2012).

Genomic and sequence features of ciliate 6mA

The amount of 6mA in *Tetrahymena* is ~0.6%–1%, as detected by paper chromatography, SMRT sequencing, and mass spectrometry (Gorovsky et al., 1973; Wang et al., 2017). This is orders of magnitude higher than in most other eukaryotes. In *Tetrahymena*, 6mA is only present in the transcriptionally-active MAC and is absent in the inert MIC (Gorovsky et al., 1973; Wang et al., 2017), indicating its correlation with gene expression (see below) (Harrison et al., 1986; Harrison and Karrer, 1985; Wang et al., 2017). The 6mA level in the MAC is relatively stable during different stages of the asexual division (Gorovsky et al., 1973; Wang et al., 2017), suggesting that maintenance methylation occurs quickly and efficiently after DNA replication. During conjugation, the new MAC differentiated from the 6mA-free zygotic MIC (Martindale et al., 1982), which necessitates the occurrence of *de novo* methylation.

Most 6mA (>90%) are located in the sequence of 5′-AT-3′, approximately 3% of which are in 5′-GATC-3′ (Gorovsky et al., 1973; Wang et al., 2017), suggesting that primary DNA sequences *per se* provide necessary information to locate 6mA. However, given that the *Tetrahymena* MAC genome is

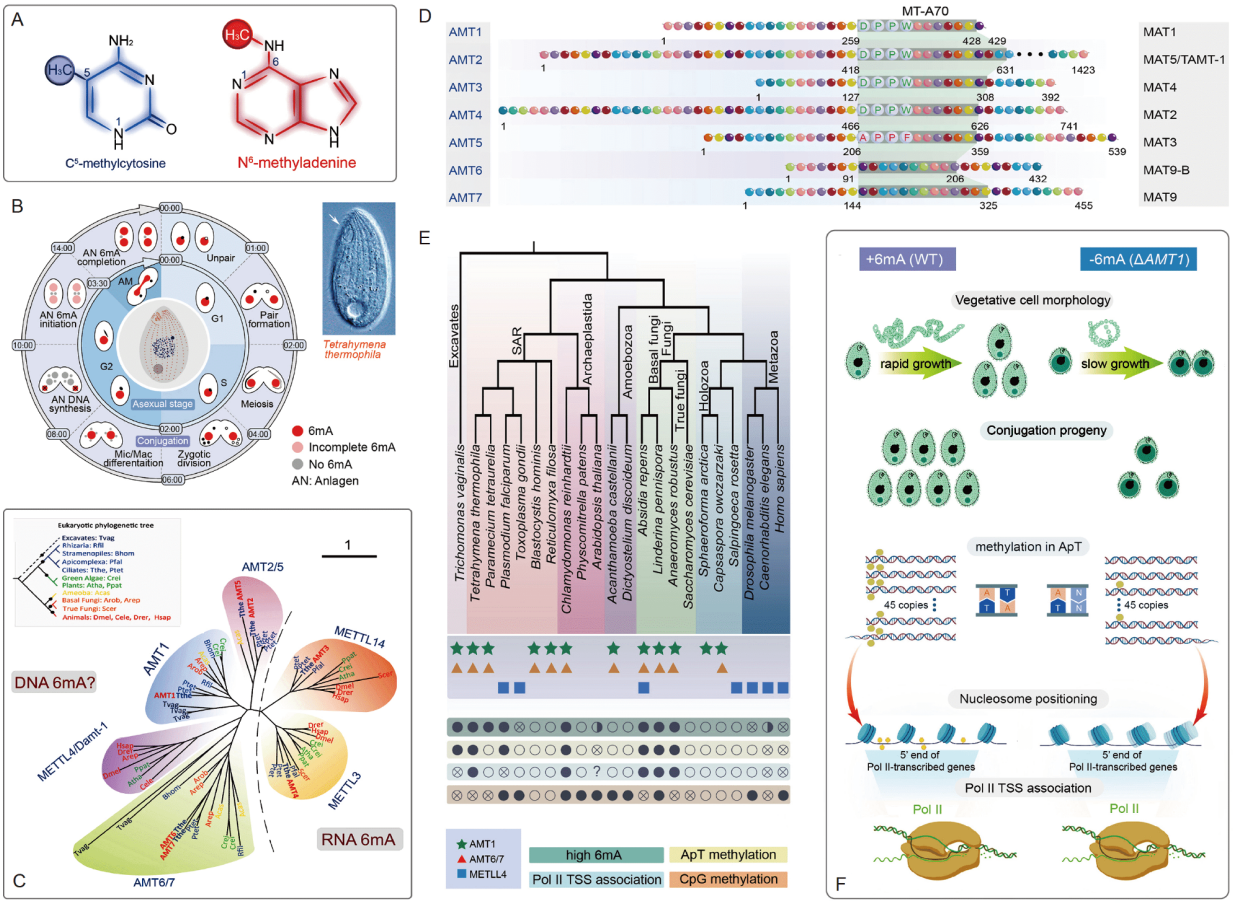

Figure 2 N^6-methyladenine (6mA) and its methyltransferase (MTase) in the unicellular eukaryote *Tetrahymena thermophila*. A, Chemical structure of C^5-metylcytosine (5mC) and 6mA. B, 6mA dynamics during the asexual growth and the sexual development. C, Phylogenetic analysis of MT-A70 family proteins. D, Conserved domains and motifs in AMTs 1–7. E, Phyletic distribution of MT-A70 family genes (*AMT1*, *AMT6/7*, and *METTL4* clades) and features of DNA methylation. F, Summary of AMT1's roles.

highly AT-rich (~75% A and T, ~39% AT dinucleotides) (Sheng et al., 2020), one 6mA per 165 bp DNA (corresponding to 0.8% 6mA level) indicates that other factors beyond sequence are also required for 6mA distribution (Karrer and VanNuland, 2002). Indeed, the genome-wide analysis revealed a preferential localization of 6mA in the linker DNA region, which is flanked by the well-positioned and/or nucleosome containing histone variant H2A.Z (Wang et al., 2017). Meanwhile, 6mA shares a similar distribution pattern to that of the histone variant H2A.Z, toward the 5′ end of the gene body (Wang et al., 2017). *Oxytricha* 6mA is also located in the consensus sequence of 5′-AT-3′ in linker DNA regions at the 5′ end of the gene body (Beh et al., 2019). Together, these results suggest that 6mA is an integral part of the chromatin environment.

Correlation of 6mA and transcription

The correlation of 6mA with transcription is intensively studied, inspired by the well-established 5mC regulation on gene expression (Bird, 2002). In *Tetrahymena*, 6mA is exclusively present in the transcriptionally-active MAC (Gorovsky et al., 1973; Wang et al., 2017); thus, 6mA was proposed to be required for gene expression. Several lines of evidence support this, such as that 6mA is preferentially associated with RNA Polymerase II (Pol II)-transcribed genes, accumulated downstream of transcription start sites (TSS) and strongly correlated with two transcription activation marks (H3K4 methylation and H2A.Z) (Guillemette et al., 2005; Stargell et al., 1993; Strahl et al., 1999; Wang et al., 2019; Wang et al., 2017). The similar distribution pattern between 6mA and the two marks also suggests that 6mA methyltransferases (MTases) are likely to be recruited to the promoter region, in a similar way to H3K4 methyltransferase and ATP-dependent chromatin remodelers responsible for the removal and incorporation of H2A.Z (Billon and Côté, 2012; Okitsu et al., 2010). During conjugation, however, in the meiotic MIC and early developing MAC, both of which feature strong transcription activities (Chalker and Yao, 2001), 6mA is either absent or initiates after the onset of transcription (Chicoine and Allis, 1986; Harrison and Karrer, 1985; Wang et al., 2017). Moreover, 6mA levels are only weakly correlated with transcription levels in the MAC.

There are a number of highly expressed genes with low 6mA levels and many minimally expressed genes with high 6mA levels (Wang et al., 2017). It should also be noted that unlike metazoan 6mA (Greer et al., 2015; Hao et al., 2020; Xie et al., 2018; Yao et al., 2017; Zhang et al., 2015a), *Tetrahymena* 6mA is not enriched on genes of a specific pathway (Wang et al., 2019; Wang et al., 2017). Given that >90% *Tetrahymena* genes are decorated with 6mA (Wang et al., 2019), 6mA in unicellular eukaryotes may not have evolved to regulate specific pathways. A likely scenario is that 6mA fine-tunes Pol II transcription as an integral part of the chromatin environment.

6mA methyltransferase in ciliates

The identity of MTase in *Tetrahymena* has been a mystery for more than 40 years (Gorovsky et al., 1973; Harrison et al., 1986; Hattman et al., 1978). Recent studies identified AMT1 (adenine methyltransferase 1, referred to as MTA1 in Beh et al., 2019) as the major MTase in *Tetrahymena* (Wang et al., 2019). This breakthrough was largely facilitated by comprehensive phylogenomic analyses that predicted seven-candidate 6mA MTases belonging to the MT-A70 family, which was evolved from the bacterial M.MunI- like DNA 6mA MTase (Iyer et al., 2011; Iyer et al., 2016). AMT1 represents a distinct and uncharacterized subclade (Beh et al., 2019; Wang et al., 2019), generally found in protists and basal fungi, featuring ApT hyper-methylation associated with transcription of Pol II-transcribed genes (Wang et al., 2019). In strong contrast, in animals, plants, and true fungi that are using METTL4 orthologs—a different subclade of the eukaryotic MT-A70 family—as their 6mA methyltransferases (Iyer et al., 2011; Iyer et al., 2016), 6mA levels are usually much lower than unicellular eukaryotes and their 6mA are not associated with ApT dinucleotides and Pol II transcription (Wang et al., 2019). This dichotomy of 6mA functions and cognate MTases may have implications in eukaryotic diversification. AMT7 (referred to as MAT9B in Beh et al., 2019), which mirrored the distribution of AMT1 in early-branching eukaryotes, was identified as an AMT1-associated partner required for its catalytic activity. AMT2 (referred to as TAMT1) was also reported to regulate 6mA levels (Luo et al., 2018), but this result was not corroborated by later findings (Wang et al., 2019).

AMT1 depletion significantly reduced 6mA level in the MAC of the vegetative cells and in the new developing MAC of the conjugating cells, strongly arguing that 6mA levels in *Tetrahymena* are mainly dependent on AMT1 throughout its life cycle (Wang et al., 2019). In particular, symmetrically methylated 6mA (methylated on both strands in the ApT nucleotides) was almost abolished, leaving an even distribution of 6mA on four types of ApN dinucleotides, indicating that AMT1 is specifically required for symmetric 6mA. AMT1-catalyzed 6mA is required for cell growth and development; Δ*AMT1* cells took longer to duplicate, moved slower, and contained an abnormally large contractile; conjugating Δ*AMT1* cells could barely enter the anlagen stage and produced very few viable progenies. These severe phenotypes could be attributable to the dramatic change of transcription profile upon *AMT1* deletion. In particular, reduced expression of *RAB46*, which encodes a Rab family GTPase involved in membrane trafficking, could partially account for the large vacuole phenotype in Δ*AMT1* cells. Similarly, loss of function of AMT1 (referred to as MTA1 in Beh et al., 2019) in *Oxytricha* resulted in a genome-wide loss of 6mA, particularly abolished the dimethylated ApT motif, and caused complete lethality in the sexual cycle (Beh et al., 2019).

Correlation of 6mA and nucleosomes

The correlation between 6mA and nucleosomes is a typical "chicken or egg" paradox. On the one hand, 6mA and nucleosomes could act as barriers for each other. It was reported that 6mA disfavors nucleosome occupancy, by comparing *in vitro* nucleosome occupancy on identical DNA sequences in *Tetrahymena*, with or without 6mA (Luo et al., 2018). This may be attributed to the intrinsic structural rigidity of DNA containing 6mA, which hinders its wrapping around the histone octamer (Luo et al., 2018; Ngo et al., 2016). Meanwhile, 6mA is preferentially located in linker DNA regions, and levels of 6mA are higher when 6mA sites are farther away from the nucleosome dyads (Wang et al., 2017), possibly due to the steric hindrance of 6mA MTases by nucleosomes. On the other hand, 6mA and nucleosomes could reinforce each other. *Tetrahymena* genes with 6mA showed more orderly nucleosome arrays than genes without 6mA (Luo et al., 2018; Wang et al., 2017; Cheng et al., 2019); a similar trend was revealed in *Oxytricha* (Beh et al., 2019), *Chlamydomonas* (Fu et al., 2015) and rice *Oryza* (Zhou et al., 2018). Meanwhile, *in vitro* nucleosome assembly using *Tetrahymena* genomic DNA with 6mA can recapitulate the *in vivo* nucleosome array downstream of TSS, more so than using unmethylated DNA (Beh et al., 2019). In the Δ*AMT1* cells, in which the 6mA level was dramatically reduced, the nucleosome positioning degree was significantly lower (Wang et al., 2019), strongly arguing that 6mA could promote nucleosome positioning. A positive feedback loop is likely to exist between 6mA and nucleosomes, in order to maintain the chromatin landscape.

Perspectives

Investigating the basal eukaryotic ciliate system has made great contributions to the understanding of 6mA function and regulation. Several questions still need systematic investigations for ciliate 6mA in the future: (i) are there other MTases that deposit asymmetric and/or non-ApT 6mA, and how do they function in coordination with AMT1? (ii) What

are the roles of partners of AMT1, such as AMT7, p1, and p2 (Beh et al., 2019), and are there other components required? (iii) Are members of AlkB family involved in the demethylation of 6mA? If not, what are the 6mA demethylases? (iv) What is the reader(s) of 6mA? (v) How is the 6mA pattern transmitted to the next generation? (vi) How does 6mA interact with other histone modifications, in particular H3K4 methylation? (vii) What is the division of labor for distinct MTases and demethylases during different developmental stages? Studies in ciliates will help to further establish 6mA as a physiologically relevant epigenetic marker.

Developmental evolution

Notochord tubulogenic, a novel type of biological tube formation in the ascidians (Figure 3)

Urochordates (tunicates), cephalochordates (lancelets or amphioxus), and vertebrates constitute the chordate phylum. These subphyla share four anatomical features, namely notochord, a dorsal hollow neural tube, somites, and a postanal tail (Satoh, 2008; Satoh, 2009). Among the chordates, cephalochordates are thought to be the most basal, while tunicates are the group most closely related to vertebrates (Bourlat et al., 2006; Delsuc et al., 2006; Holland et al., 2008). Marine ascidians, one of three main tunicate groups, have been used for more than 100 years as a model organism to study embryogenesis. They are also ideal models to understand the mechanisms of morphogenesis because of their evolutionary position, and characteristics such as the transparency of eggs and embryos, a simple body plan, a characterized larval cell lineage, and mosaic development (Lv et al., 2019). In the past decade, new approaches allowed developmental biologists to use ascidian species such as *Ciona robusta*, *C. savignyi*, and *Phallusia mammillata* to address the basic questions of embryogenesis, evolutionary developmental biology, and cell biology. New approaches and technologies include: genomic and single-cell sequencing (Dehal et al., 2002; Cao et al., 2019), TALEN- and CRISPR/Cas9-based gene-editing tool development (Stolfi et al., 2014; Treen et al., 2014), supra-resolution time-lapse imaging (Sladitschek et al., 2020), and application of biophysical modeling (Hashimoto et al., 2015; Lu et al., 2020). Using marine ascidian models, exciting findings and new knowledge was obtained recently, such as discovery of neural crest like cells in invertebrates (Abitua et al., 2012; Stolfi et al.,

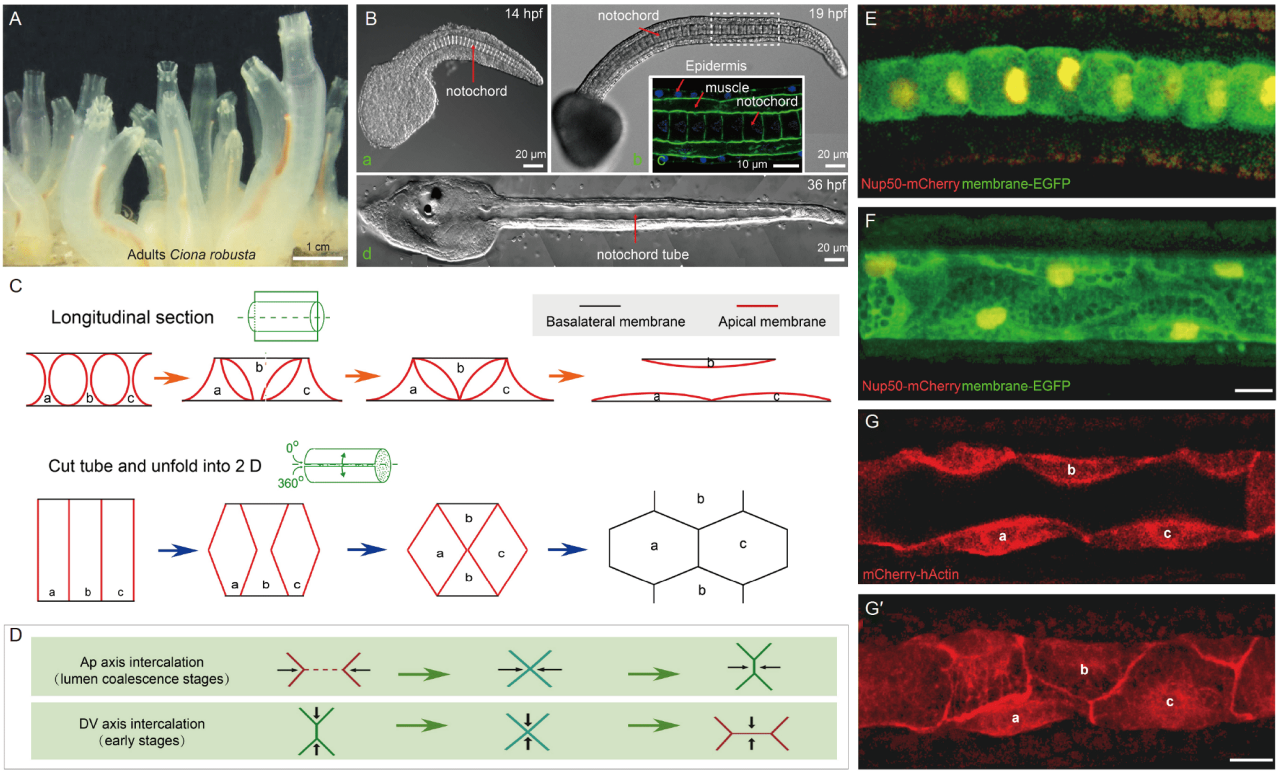

Figure 3 Notochord tube formation via a unique cellular process in urochordate *Ciona robusta*. A, A small population of adult *Ciona robusta*. B, Early tailbud larva of *Ciona robusta* at 14 h post fertilization (Ba); late tailbud larva at 19 h post fertilization (Bb); inset is the notochord cells stained by phalloidin (Bc); swimming tailbud larva at 36 h post fertilization (Bd). C, Schematic representation of longitudinal section of notochord cell shape change (up panel) and the intercalation of notochord cells along the AP axis (bottom panel). D, Schematic representation of junction remodeling of notochord cell junctions at lumen coalescence stages (up panel) and early stages (bottom panel), respectively. E and F, Project of notochord cell before lumen formation (E) and lumen coalescence (F), respectively. G and G′, Cross section (G) and projection (G′) of notochord cells labelled by mCherry-hActin. Scale bars in (E–G′) represent 10 μm.

2015).

Tubulogenesis in the ascidian notochord

Biological tubes such as the gut, the pancreatic duct, the lung, the kidney, the vascular and lymphatic system, are fundamental structures of internal organs in animals, playing essential roles in metabolism and homeostasis. The biological tubes consist of polarized epithelial or endothelial tubes, and many of them undergo branching morphogenesis. Tubulogenesis, formation of these of tubes, involves a series of cellular processes and distinct molecular mechanisms, which have been reviewed in previous publications (Lubarsky and Krasnow, 2003; Baer et al., 2009). Recently, mechanical forces are also demonstrated to be involved actively in tubulogenesis (Iruela-Arispe and Beitel, 2013; Luschnig and Uv, 2014; Hayashi and Dong, 2017; Dumortier et al., 2019). Dysfunction of biological tubes causes severe diseases in human. Therefore, the study of the cellular and developmental mechanisms of tubulogenesis is essential for our understanding of a number of biological tube-related human diseases. Several model systems have already been established for tubulogenesis studies, such as MDCK cell-based induced tube, the zebrafish vascular system, the *Drosophila* tracheal system, and the *Caenorhabditis elegans* secretion organ.

The notochord is an ideal organ system to study cell biological processes, for example, the regulation and control of cell shape (Lu et al., 2019), and establishment and maintenance of cell polarity (Peng et al., 2020b). Recently, the notochord was found to form a tubular structure via a novel cellular process (Dong et al., 2009), which provides an excellent model to study molecular mechanisms and geometry control of the biological tube. Here, we will review our current understanding of cellular processes and the underlying molecular mechanisms that govern notochord cell shape change, extracellular lumen emergence and coalescence, and cell-cell junction remodeling.

Cellular steps for notochord tube formation

The notochord is a characteristic rod-like midline organ in chordate embryos that supports the body structure and produces positioning signaling for surrounding organs (Corallo et al., 2015; Stemple, 2005). For example, the notochord only exists in the tail part of swimming larvae and disappears after metamorphosis in urochordates such as ascidians (Cloney, 1982; Matsunobu and Sasakura, 2015). In the development of ascidian *Ciona* embryos, notochord cells are found to secrete the extracellular matrix (ECM) into the space between two adjacent cells, forming the extracellular lumen for cavitation. The separated pocket lumens then expand and join together, forming a single lumen. Thus, the notochord forms a tubular structure. The cellular processes of notochord tube formation are unique and distinct from previously reported ones (Dong et al., 2009; Ettensohn, 2013). There are three main phases of notochord tube formation: (i) initiation of apical domain and establishment of apical-basal (AB) polarity, (ii) lumen expansion, and (iii) bidirectional migration and junction remodeling.

Ascidian notochord is composed of 40 cells from the A and B lineages driven by the T-box family gene *brachyury*. At the end of cell division, these 40 notochord cells invaginate, medially intercalate, and then converge and extend along the anterior-posterior (AP) axis, forming a single-cell-diameter-wide line. Next, an actomyosin contractile ring appears at the anterior edge of notochord cells, and drives further elongation of notochord (Dong et al., 2011; Sehring et al., 2015). When AP length of one notochord cell reaches the diameter of the cylinder disc, a lumen appears between two adjacent cells. A new apical domain emerges in the notochord cells. Thus, notochord cells experience a typical mesenchymal-epithelial transition (Dong et al., 2009). *De novo* formation of new apical domain means the establishment of AB polarity in notochord cells. The Par3-Par6-aPKC polarity complex initially appears at the center of two opposite lateral domains of the notochord cell. Loss-of-function of Par3 causes the failure of apical domain formation, indicating the requirement of this signaling pathway for the establishment of AB polarity (Denker et al., 2013). As a result of apical membrane formation, diffusible ECM is secreted into this surface area (Wei et al., 2017). ZO-1, as an important component of the tight junction, co-localizes and interacts with the Par3-Par6-aPKC polarity complex, to avoid leaking of the lumen (Denker et al., 2013). Another interesting point is that each *Ciona* notochord cell has two apical domains, although they eventually merge into one.

The lumen expands continually after the establishment of AB polarity. Expansion of lumen space requires at least three cellular processes: membrane biogenesis, filling of the lumen with liquid, and remodeling of cell cell junctions. Trafficking and fusion of vesicles is one of mechanisms of membrane growth mechanism. Based on meticulous measurements, it has been reported that the amount of liquid through vesicle fusion is not sufficient to fill the newly increased membrane space. This indicates that liquid must be added into the lumen space through additional mechanisms. Osmotic pressure and ion transporters are potential mechanisms to regulate lumen size (Datta et al., 2011). In the notochord, lumen shape changes during expansion (Denker et al., 2015), indicating that the membrane biogenesis and addition of liquid are two separate regulatory processes. It is been known that AB polarity and vesicle trafficking are required for apical membrane biogenesis and ECM secretion in *Ciona* notochord tubulogenesis (Mizotani et al., 2018; Bhattachan et al., 2020). SLC26aα is a transmembrane ion transporter protein, located at the apical membrane to control the osmotic pressure in the lumen cavity (Deng et al., 2013). Ac-

tomyosin forms disc structures in the lateral domains and has been demonstrated to regulate apical membrane tension required for expansion during notochord lumen expansion (Denker et al., 2015). Using electron microscopy, apical lumen was observed to present with a relatively lower density, indicating the diffusible property of lumen matrix components (Wei et al., 2017). However, none of the ECM components have been identified in the *Ciona* notochord. Caveolin is a structure transmembrane protein found specifically in the apical membrane in the notochord cells. It has showed the ability to induce the curvature at the plasma membrane, forming vertebrate-like caveolae structures. Caveolin-GFP vesicles traffic to the apical domains. Disruption of its function leads to failure of lumen formation and expansion (Bhattachan et al., 2020). The invaginated curvature structures therefore provide redundant membrane and are assumed to serve as the mechanosensor to respond to tension in the apical membrane. The regulatory feedback mechanism seems to be essential for notochord lumen expansion.

Following the development of the notochord lumen, the apical membrane surface areas increase, along with the decrease of the lateral domains. During this process, pocket lumens grow. At a certain time point, after the pocket lumens reach the largest volume, notochord cells become motile and extend bi-directionally on the notochord sheath at leading edges. Meanwhile, the opposite edges retract. Thus, each notochord cell has two leading edges and two trailing edges. The two trailing edges will eventually meet and thus two apical domains will join together and merge into one single apical domain. At the merging site, the two leading edges from anterior and posterior neighbor cells, respectively, meet and form new cell-cell junctions. The neighbor cells show opposite migration behaviors. As a consequence, the coordinated collective migration leads to the fusion of adjacent luminal pockets, forming a single lumen in the notochord. In this process, the notochord cell shape and cell-cell junction undergos striking remodeling, reversing the initial intercalation phase. It is therefore termed as “reverse intercalation”. Thus, notochord cells experience dramatic cell rearrangement, but the underlying molecular mechanism for this process is still unknown. It has been shown that the microtubule might be involved in the regulatory process. After disruption of microtubule polymerization, the migration behaviors of notochord cells become inconsistent and the lumen fails to fuse (Dong et al., 2011).

The challenging questions in notochord tubulogenesis

Ascidian notochord develops into hydrostatic skeleton for larval swimming via luminogenesis. It is worth noting that not all ascidians develop a luminal notochord (Jiang and Smith, 2007). In addition, in other chordates the notochord develops into hydrostatic skeleton via formation of intracellular vacuoles (Jiang and Smith, 2007). Thus, from the evolutionary perspective, formation of extracellular lumen in the notochord is not conserved. On the other hand, the type of *Ciona* notochord tube formation occurs not only in ascidians. Recent studies have shown that the similar processes are also present in vascular anastomosis (Herwig et al., 2011) and gut tube formation in zebrafish (Alvers et al., 2014), suggesting that it is a universally novel type of biological tube formation. As an intriguing model for biological tube formation, several questions remain to be resolved.

First, how is the initial apical domain position determined? As we discussed before, Par3-Par6- aPKC complex localizes at this position before lumen opening. However, the upstream signaling that induces the localization of this complex remains a mystery. Recent studies showed that centrosome (Feldman and Priess, 2012) and Rho signaling pathway components (Schmidt et al., 2018) could be involved in this process. Elucidation of their roles in notochord cells might provide cues to reveal how AB polarity is initially induced.

Second, what is the mechanical mechanism that drives the lumen expansion? During notochord development, ECM components are secreted, forming the extracellular lumen at the anterior and posterior edges of notochord cells. Growth and expansion of the lumen is essential for lumen coalescence. Osmotic pressure is thought to be the main force, which needs to be highly coordinated with actomyosin activity and junction remodeling. Among the potential upstream signaling pathways to regulate this process, Rho signaling is a promising candidate and awaits to be verified in the future.

Third, how are the collective migration behaviors in notochord cells coordinated? During notochord tube formation, there are several lumen coalescence regions from the anterior to the posterior axis, and the appearance of the earliest connected lumen region seems to be random, suggesting that the upstream regulatory factors might not be gradient signaling. Mechanical signaling could be a possible mechanism, which is transmitted through cell-cell contact within a short range, and guides lumen coalescence. It will be intriguing to experimentally verify these self-organized mechanisms for organogenesis in future studies.

Cilia and ciliopathies, what can we learn from zebrafish? (Figure 4)

Cilia are microtubule-based, evolutionary conserved organelles present in various phyla ranging from protozoa to vertebrates. Cilia can be classified as motile and primary cilia. The motile cilia are essential for the swimming of single-celled animals, as well as directing fluid flow over the cell surface in multicellular cell organisms. Primary cilia function as cell antennae to receive extracellular signals, which are essential for cell proliferation, differentiation and migration (Ishikawa and Marshall, 2011). According to the

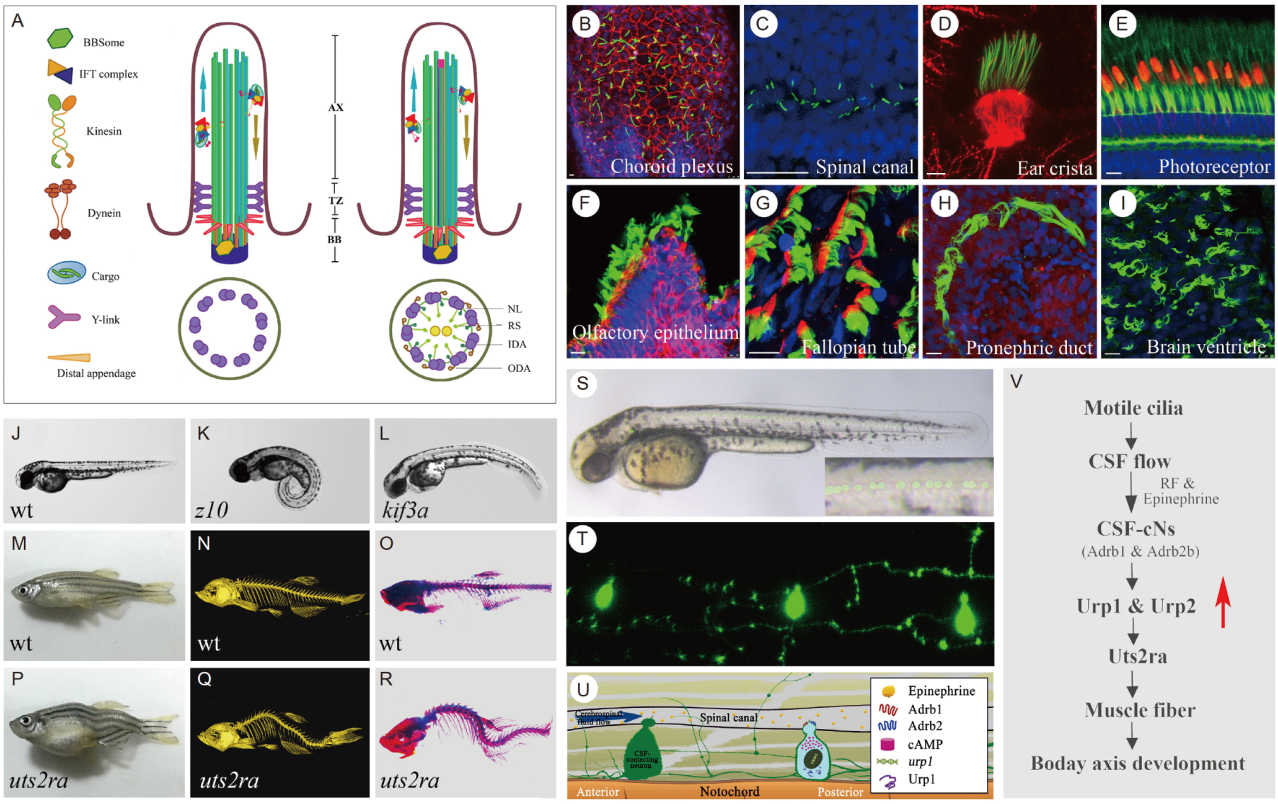

Figure 4 Cilia diversity in zebrafish and their roles during body axis development. A, Schematic diagrams of primary and motile cilia. B–I, Cilia in different zebrafish organs visualized by immunofluorescence analysis. Scale bar=10 μm. J–L, External phenotypes of wild-type and ciliary mutant embryos at 72 hpf. M–R, Micro-CT and Alizarin red staining results showing bone morphology of wild-type and *uts2ra* mutants. S, Distribution of CSF-cNs as visualized using Tg (*urp1*:GAL4; *UAS*:Kaede) double transgenic zebrafish larvae. T, High magnification views showing the morphology of CSF-cNs at 10 dpf zebrafish larvae. U, Model illustrating the activation of urotensin neuropeptide (Urp1) by epinephrine signals from CSF. V, Molecular mechanisms underlying cilia-driven CSF controlled body axis straightening. CSF, cerebrospinal fluid; CSF-cNs, CSF-contacting neurons.

structure and position, cilia can be divided into a basal body, transition zone, and axonemal region. Generally, motile cilia contain nine peripheral doublet microtubules and a central pair of singlet microtubules, i.e., the "9+2" configuration. The central pair of microtubules is absent in primary cilia, forming "9+0" configuration (Song et al., 2016).

The morphology of cilia can be highly diverse in different organisms. In the nematode *Caenorhabditis elegans*, for example, cilia display morphologically different shapes, including rod-type, wing-like, and branched. In the marine ciliate *Euplotes vannus*, the cilia are specialized as an adoral zone of membranelles (membrane-like, around the cell mouth, or cytostome, to obtain food) and cirrus/cirri (tuft-shaped organelles formed by bundles of cilia that have a locomotion function). In vertebrates, the cone- or rod-shape outer segments of photoreceptors are sensory cilia that are essential for converting light stimuli into neurological responses. Interestingly, albeit with very diverse morphology, cilia preserve highly conserved structural components. In addition, the signaling pathways regulating ciliogenesis are similar among different species. For example, ZMYND10 and C21ORF59, two ciliary dynein assembly proteins, regulate cilia motility in *Euplotes vannus,* zebrafish and human.

Defects in ciliary structure and/or function have been linked to a wide range of human diseases, known as ciliopathies. Cilia are present almost in every cell of the human body, so it is not surprising that dysfunction of cilia will affect nearly all the vital organs. Currently, more than 35 ciliopathies have been classified, including primary ciliary dyskinesia (PCD), also known as immobile cilia syndrome, polycystic kidney disease, Bardet-Biedl syndrome and retinal degeneration disease, affecting more than 12 million people worldwide (Hildebrandt et al., 2011). Till now, approximately 200 genes have been acknowledged to cause ciliopathies. The pathogenesis of genes involved in ciliopathies is quite complex, not only because of the diversity of pathogenic genes, but also the complexity of the regulatory signaling pathways (Reiter and Leroux, 2017). Exploring the roles of these ciliary genes in different model systems will help us decipher the pathogenicity of genes involved in human ciliopathies.

Over the last decades, zebrafish has become a classic vertebrate model to study human diseases, due to its transparent embryos and rapid development. More than 72% of human genes have at least one distinct homologous gene in the zebrafish genome, and orthologs of over 82% of human

disease causative genes have been identified in zebrafish (Amores et al., 1998; Howe et al., 2013). Cilia develop in nearly all in zebrafish cell types, and can be observed through either transgenic live imaging or immunofluorescence analysis (Song et al., 2016). The external development of zebrafish embryos also makes it easy to characterize organogenesis defects for modeling human ciliopathies. For example, cystic kidney develops consistently in the glomeruli and the proximal tubules region in ciliary mutants and morphants (embryos injected with morpholino antisense oligos) (Zhao and Malicki, 2007). Organogenesis defects in many human ciliopathies can be mimicked in zebrafish, including cystic kidney, photoreceptor degeneration, hydrocephalus and laterality defects (Song et al., 2016).

The most apparent feature of zebrafish ciliary mutants is the presence of a ventral curly body axis. In wild-type zebrafish embryos, as well as the embryos of many other vertebrate species, the body axis is initially curved ventrally around the yolk, then gradually straightening out and finally forming a straight, longitudinal body axis. In contrast, zebrafish cilia mutants develop a ventral body axis, while the elongation of the trunk process normally. The severity of body axis defects varies among ciliary mutants. Mutation of the *zmynd10* gene, one of the human PCD causative genes, results in severe body axis defects in zebrafish. Surprisingly, the body curvature is rather minor in both *kif3a* and *ift88* mutants, two essential genes required for ciliogenesis (Feng et al., 2017; Tsujikawa and Malicki, 2004). Maternal contributions of Kif3a and Ift88 proteins, inherited from the oocytes, maybe the main reason accounting for such differences. In ciliary mutants, body axis defects become apparent from 28 h post fertilization (hpf), when the maternal proteins are still present in the embryos and may partially compensate for the loss of zygotic proteins. In fact, most cilia are still present in *kif3a* and *ift88* mutants at 24 hpf. In contrast, body axis defects are evident in *MZift88* mutants, which lack both maternal and zygotic proteins (Huang and Schier, 2009).

Cilia regulate body axis straightening at larval stages but are also essential for the maintenance of a straight body axis during later development. Overexpression of wild-type mRNA in mutants with ciliary motility defects, can rescue early embryonic lethality, while mutants still developed a late-onset spinal curvature (Grimes et al., 2016). Surprisingly, the spinal curvature in these ciliary mutants closely resembles human Idiopathic scoliosis (IS), one of the most common spinal diseases (Grimes et al., 2016). In IS patients, instead of growing straight, the spine develops into an elongated “S” or “C” shape and their bones are twisted or rotated, which affect the position of internal organs, gait changes and respiratory functions. IS is by far the most common type of scoliosis appearing in later childhood and adolescence, and is also called Adolescent Idiopathic Scoliosis (Weinstein, 2019). Currently, the etiology of the development of scoliosis remains largely unknown. The lack of appropriate animal models to mimic these diseases is one of the main reasons for our delayed understanding of the mechanisms underlying scoliosis. Human beings have an upright posture and a bipedal ambulation, which differ considerably with popular lab animal models. For example, mice are quadrupedal mammals, and the direction of gravity is perpendicular to the AP axis of the spine, which is different from humans. It has been proposed that the upright posture will incur natural biomechanical strains on the human spine, which may contribute to the formation of scoliosis (Boswell and Ciruna, 2017; Fadzan and Bettany-Saltikov, 2017). The quadrupedal posture in mouse might compensate the imbalance defects caused by abnormal biomechanical forces imposed on the vertebrae, making it difficult to mimic human scoliosis in mice. In contrast, spine curvature is a common morphological deformity in teleost fish. The architecture and structure of the spine is well conserved between fish and humans (Boswell and Ciruna, 2017). Similar to human, the spine of teleost fish may also be susceptible to mechanical forces generated by swimming. Actually, scoliosis and kyphosis are common in zebrafish both in natural and genetic mutants, making zebrafish a preferable model for studying scoliosis compared to traditional quadrupedal models.

Based on the work on zebrafish, several recent studies have linked cilia-driven cerebrospinal fluid (CSF) flow to the etiology of IS. CSF is a colorless, nutrient-rich fluid in the brain ventricles and neural tube, essential for embryonic development and homeostasis of the central nervous system. Cilia are widely distributed in the brain ventricles and spinal canal, where forces are generated through beating of these motile cilia, to drive CSF flow. Removal of CSF by manually draining the fluid from early embryos led to curly body axis phenotype, suggesting that CSF is involved in the regulation of body axis straightening (Zhang et al., 2018). Abnormal ciliogenesis in the brain ventricles causes CSF flow defects, which further affect downstream signaling and finally lead to scoliosis during late development (Grimes et al., 2016).

The role of CSF underlying scoliosis remains to be elucidated. Recently, we compared body axis development between *zmynd10*, *kif3a* and *ift88* mutants, and found that the severity of body curvature defects is causally linked to the flow rate of CSF (Zhang et al., 2018). Through RNA-Seq transcriptome analysis, we identified *urp1* and *urp2*, which encode two urotensin neuropeptides that are substantially downregulated in ciliary mutants. Overexpression of these genes rescued ventral bending defects in ciliary mutants, suggesting a critical role of urotensin neuropeptides during body axis development. Importantly, both *urp1* and *urp2* are expressed in a special type of neurons, CSF-contacting neurons (CSF-cNs), which are present along the entire central canal. CSF-cN are atypical spinal sensory neurons with a

unique morphology. The apical extension of each CSF-cNs is composed of a single motile cilium surrounded by actin-based protrusions that can contact CSF directly (Desban et al., 2019). Such protrusions help CSF-cNs to detect mechanical stimuli associated with CSF flow. Other development cues, including pH and osmolarity, can also be sensed by these neurons (Jalalvand et al., 2016).

Through small molecule compound screening, we identified CSF epinephrine as one of the key signals that can be sensed by CSF-cNs. Mechanically, CSF adrenergic signals activate CSF-cNs through binding to the β-adrenergic receptors, Adrb1 and Adrb2b, which further initiate downstream signals through the cAMP pathway and activate the expression of urotensin neuropeptides (Wang et al., 2020b). CSF-cNs develop long anterior extended axons with multiple dorsal projected branches during development of zebrafish larvae. This morphology is closely related to the role of CSF-cNs during embryonic development: they are involved in the postural control during locomotion of zebrafish larvae through interacting with motor and sensory interneurons. It is currently still unknown how urotensins are secreted from these neurons. In contrast, urotensin receptors are specifically expressed in the dorsal muscle fiber cells, suggesting that these neurons can regulate muscle fiber contraction directly (Zhang et al., 2018).

Altogether, CSF flow driven by spinal canal motile cilia transfers the adrenergic signals down to the CSF-cNs and activates the expression of urotensin neuropeptides. These stimulate the contraction of muscle fibers and trigger the ventral curve of the trunk to gradually straighten out. Surprisingly, malfunction of the urotensin receptor results in strong scoliosis during later development, suggesting that this signal pathway is also crucial for the maintenance of a straight body axis. The high prevalence of scoliosis in people with Parkinson's disease, characterized by the gradual loss of dopaminergic neurons, further suggests the essentials roles of adrenergic signals during scoliosis (Doherty et al., 2011). Considering that urotensin receptor is specifically expressed in the muscle fiber cells, it is possible that neuromuscular defects may also get involved in scoliosis. In line with this, neuroinflammatory signals are highly activated in zebrafish *ptk7* scoliosis mutants, and prevention of the inflammation in the central nervous system can partially reduce the severity of scoliosis (Van Gennip et al., 2018).

Reissner fiber (RF) is a filamentous structure extending caudally from the brain ventricles to the central canal of the spinal cord. It forms by aggregation of a glycoprotein called SCO-spondin (Sspo). Zebrafish *sspo* mutants develop strong scoliosis (Rose et al., 2020). Oscillation of motile cilia drives the smooth flow of CSF to help maintain a normal diameter and internal pressure of the central canal, which is essential for the assembly of RF (Orts-Del'Immagine et al., 2020). The RF can regulate the transmission of the CSF adrenergic signals to the CSF-cNs (Caprile et al., 2003), thus affecting the expression of downstream neuropeptides.

In summary, zebrafish provides an ideal model to study human ciliopathies, especially for IS. Compared with the quadrupedal mouse model, zebrafish has inherent advantages in modeling scoliosis. Recent studies provide new insight in the pathogenesis of the disease. Further analysis using zebrafish will definitely help us understand the biological processes underlying spinal curve formation in IS patients.

Cellular dynamics and morphogenesis: lessons from Drosophila (Figure 5)

Drosophila melanogaster is one of the most successful model organisms. The fast generation time, easy lab maintenance with low cost, and relatively simple genome of *Drosophila* enabled decades of genetic screens to identify many of the key genes involved in tissue architecture formation and maintenance, pattern formation, and organogenesis. The convenience of using *Drosophila* to answer the fundamental biological questions attracted many researchers, which led the further development of genetic tools and resources for *Drosophila*.

In addition to the advanced genetic tools, another feature highlighting the experimental tractability of *Drosophila* embryos is their amenability to live imaging and non-invasive optical interference. Selective-plane illumination microscopy allows rapid and complete imaging of live embryos, and reliable tracking of nuclear and cell movements during development (Krzic et al., 2012). High-speed imaging makes it feasible to uncover the cellular dynamics at second and sub-second scale (Mann et al., 2019; Winkler et al., 2015). Optogenetic and optochemical tools have been successfully implemented. Application of optogenetic methods modulating the Rho signaling pathway (Izquierdo et al., 2018) can trigger local inhibition or activation of apical constriction in a group of cells. Alternatively, contractility in single-cell resolution was achieved with the optical-chemical approach of Ca^{2+} uncaging (Kong et al., 2019). Meanwhile, newly developed imaging techniques and image processing algorithms opened opportunities to address the protein/mRNA localization and dynamics in living organisms on nanoscale level (Godin et al., 2014).

Cytoskeletal dynamics during syncytial blastoderm

Drosophila embryogenesis has been studied for nearly half a century, resulting in a broad understanding of fundamental biological processes, such as the logic of gene regulation and cellular behavior during morphogenesis (Sullivan and Theurkauf, 1995). Nevertheless, the early embryogenesis of *Drosophila melamogaster* presents some common features among insects. The most prominent feature is the early

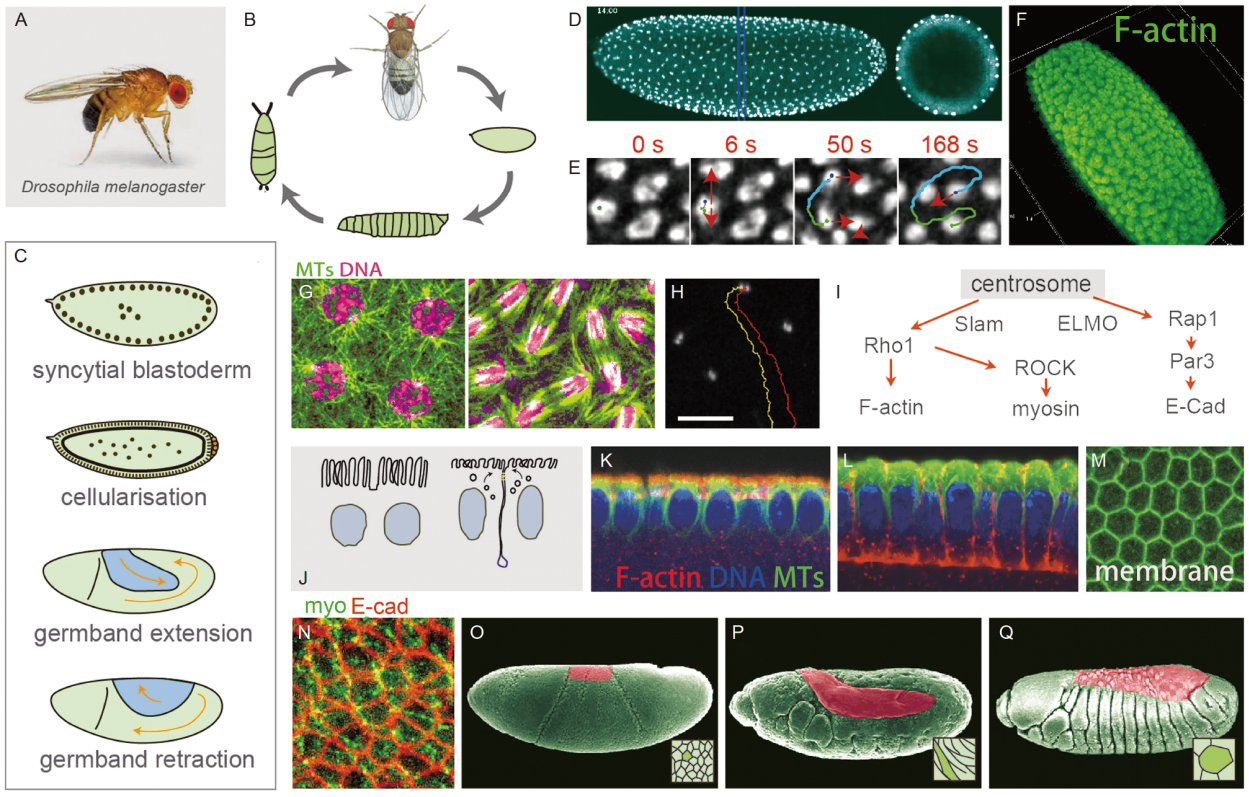

Figure 5 The cellular dynamics in early embryogenesis of *Drosophila melanogaster*. A and B, *Drosophila melanogaster* and its life cycle. C, Embryogenesis of *Drosophila*. D, *In toto* image of a syncytial blastoderm expressing Histone-GFP. E, Nuclear yo-yo movement. F, F-actin cap structure. G, Microtubules form an interwoven network in interphase and participate the spindle formation during mitosis. H, Centrosomes fluctuate in prophase. I, Centrosomes control cortical actin remodelling. J, Membrane material is added by exocytosis during cellularization. K and L, Cellularization in early (K) and late stage (L). M, Surface of a cellularizing embryo. The cell-cell contact forms regular hexagons. N, The top view of epidermis of an embryo undergoing gastrulation movement. O–Q, The scan electron microscope (EM) images of *Drosophila* embryos by courtesy of Flybase. The truck epidermis is masked in green and amnioserosa is in red. The inserts reveal the dramatic shape change of amnioserosa cells during germband extension (P) and retraction (Q).

embryo developing as a syncytium.

After fertilization, the *Drosophila* embryo undergoes 13 rounds of nuclear division without cytokinesis in the first two hours, constituting a syncytium. The nuclei share a common intracellular space of an ellipsoid with ~500 μm in length and ~180 μm in width. During the first 7 mitotic cycles, the nuclei divide deep in the center of the embryo. During cycles 8 and 9, most nuclei migrate toward the periphery of the embryo. The yolk nuclei maintain their positions in the deep yolk, will become polyploid and undergo apoptosis later in embryogenesis. After the ninth mitotic cycle, the nuclear migration is completed, leading to the so-called blastoderm. The blastoderm embryo undergoes four rounds of nuclear division (cycles 10–13), giving rise to about 6,000 nuclei arranged at the cortex of the embryo (Sullivan and Theurkauf, 1995).

In the blastoderm, F-actin and microtubules are highly dynamic and coupled with cell cycle progression. During interphase, F-actin is organized into caps that reside between the plasma membrane and the nuclei. Microtubules emitted from adjacent centrosomes overlap with each other, forming an interwoven network across the whole embryo. During mitosis, the actin caps resolve. F-actin is then enriched at the metaphase furrow that separates adjacent mitotic spindles, and thus blocks the interaction between neighboring nuclei mediated by microtubules.

The cyclical reorganization in cycle 10 to 13, accompanied with the rise and fall of the minuscule interaction of cytoskeletal components in a minute -scale, leads to the stereotypic flow movements of nuclei and cytoplasm following the nuclear division. The terminal nuclei enter mitosis earlier than the nuclei in the trunk region, resulting in a propagating wave across the embryo (Deneke et al., 2016). A stereotypic nuclear movement is associated with the mitotic wave (Lv et al., 2020). The unbiased spindle expansion during mitosis is followed by a directional nuclear flow in the opposite direction of the mitotic wave progression. During the next interphase, after approximately three minutes, the collective movement slows down and turns to the original position. Phenomenologically, this movement has been referred as "yo-yo". The underlying mechanism driving this collective nuclear movement involves an interaction between the microtubule and the actin cytoskeletons, both of which undergo large-scale turnover throughout the division cycle. The nu-

clear movement is less pronounced in the embryo with a shorter spindle, suggesting that the spindle elongation in anaphase drives the "yo-yo" movement. (Lv et al., 2020).

Furthermore, as cortical actin undergoes cyclic remodeling, the total amount of F-actin decreases in anaphase, which probably reduces the cytosolic material stiffness in regions close to the cortex. As spindle elongation generates isotropic compressive stress, it leads to larger deformations in regions where material is probably softer. Following anaphase, nuclei are merely displaced as part of a collective material deformation of the cytoplasm near the cortex. Interestingly, cortical F-actin steadily increases after reaching the lowest density in anaphase, probably caused by the maturation of newly formed centrosomes, which in turn induce F-actin accumulation. F-actin is involved in restricting nuclear displacement and dampening the movements, since in the mutant embryo with impaired cortical F-actin, the nuclei are moving farther away, and cannot regain their initial positions. These measurements indicate that cortical actin likely acts as a viscoelastic medium, not only to dampen the movements but also to restore the initial nuclei positions. It might be an important mechanical property of actin to assure the effective positional information provided by morphogens. It is likely that the nuclear "yo-yo" movement also occurs in other insect syncytial embryos. It has been reported that nuclear division asynchrony was observed in the beetle *Tribolium castaneum*, suggesting this might be a conserved mechanism in insect syncytial embryos.

Cellular blastoderm formation

At the onset of interphase 14, mitosis is blocked for about 1 h. The membrane between adjacent nuclei invaginates and encircles the single nuclei, forming a columnar epithelium with an intact cellular structure. This process is called cellularization. The surface area of the plasma membrane increases about 25-fold (Lecuit and Wieschaus, 2000). The microvilli, that decorate the surface of the embryo before cellularization, provide membrane for cellularization. Microvilli are depleted while membrane furrows between adjacent nuclei invaginate, suggesting that microvilli act as a source of membrane during cellularization. The second source for cellular membrane is the apical exocytosis. Mutations in membrane traffic and exocytic machinery cause cellularization defects. Sec5, the exocytic component, is enriched apically, and Golgi bodies move to the apical cell surface during cellularization (Román-Fernández and Bryant, 2016), suggesting that the membrane materials are added to the apical cell surface by exocytosis.

Another striking feature during cellularization is that the membrane differentiates into distinct domains, including apical, subapical, lateral, and basal. F-actin plays a central role in the formation of cortical domains during cellularization. When F-actin is depleted genetically or by small molecule inhibitors, the boundary between distinct domains is missing. Recently, excellent reviews have been published on this topic (Flores-Benitez and Knust, 2016; Schmidt and Grosshans, 2018).

Amnioserosa tissue undergoes dramatic cell shape change

Following cellularization, the gastrulation starts. The cells and tissues in different regions show distinct morphogenetic movements. The single row of cells at the boundary between head and embryonic trunk (germband) shortens, initiating the formation of the cephalic furrow (Leptin and Grunewald, 1990). On the ventral side of the embryo, a stripe of cells, about 18 cells wide and 60 cells long, constitutes the mesodermal anlage, and invaginates at the beginning of gastrulation (Leptin and Grunewald, 1990). The germband, located laterally in the embryo, elongates along the AP axis. Meanwhile, the germband shortens along the dorsal-ventral axis, and the left-side and right-side germbands join at the ventral midline, covering the invaginated mesoderm. The dorsal-most epidermis (about 6 cells wide) that does not participate in germband extension, develops into the extra-embryonic amnioserosa (Leptin and Grunewald, 1990). The amnioserosa anlage cells are specified by the expression of *zerknüllt*, which is regulated by the morphogens Dpp and Dorsal. The amnioserosa anlage is composed of ~200 cells, which do not enter mitosis, so that the cell number remains the same. During germband extension, the amnioserosa cells become extremely elongated, which is mediated by the growth and reorganization of microtubules (Pope and Harris, 2008). By the end of germband extension, the amnioserosa cells are 10 times their initial length and 1/5 their original diameter. To what extent the amnioserosa cell shape change contributes to the germband extension, is unknown.

After the segments are formed during the extension, the germband shortens during a process called germband retraction. The amnioserosa cells concurrently shorten and become squamous, with a diameter of 15 μm but only 3 μm in height at the end of germband retraction (Kong et al., 2019). The amnioserosa is essential for germband retraction. Mutant embryos with premature amnioserosa apoptosis display a defective germband retraction. The morphogenetic movements of germband and amnioserosa tissue are highly coordinated during germband extension and retraction. How these two tissues communicate, what triggers the amnioserosa cell elongating and shortening, and the transition between the two reverse behaviors, are largely unknown.

Unlike *Drosophila*, the extra-embryonic tissue of the red flour beetle *Tribolium castaneum* and mosquito *Anopheles gambiae* is constituted by two tissues: amnion, and serosa. The morphogenetic flow, i.e., the overall cellular movement, during germband extension and retraction represents an evolutionary diversity in insects.

We gained deep insight in pattern formation during the past

decades. Nevertheless, we know much less about cell dynamic properties and morphogenesis. We expect that the studies in *Drosophila* and the embryogenesis other insects will reveal fundamental principles of how cells and tissues mechanically interact with each other, and collectively drive embryo development.

Growth and patterning: molecular insights from Drosophila wing development (Figure 6)

How a developing organ grows and patterns to its final size and shape is an important question in developmental biology. As a classic animal model in genetics, *Drosophila melanogaster* has also contributed a lot to our knowledge of developmental biology. Particularly, the studies in *Drosophila* wing in the past 30 years have provided valuable insights into our understanding of growth and patterning control.

Overview of Drosophila wing development

The adult wing of the fruit fly *Drosophila* is derived from the imaginal primordium, commonly described as "wing imaginal disc", which is initially specified in the ectoderm of the embryo and has flattened into a disc shape by the larval stage. The wing disc grows and patterns during larval development. Through ~10–11 rounds of cell division, the cell number in a wing disc increases from around 30 in the embryo stage to 30,000–50,000 at the end of the third larval instar (Matamoro-Vidal et al., 2015). At the pupal stage, the wing disc goes through dramatic morphogenesis into a fully formed adult wing. The most visible characteristic of adult wing are the veins, ectodermal tubular structures, providing rigidity of the wing and serving as vessels for trachea, nerves, and hemolymph. The pattern of the veins is highly stereotyped and specific among species (De Celis and Diaz-Benjumea, 2003), providing an intriguing model to study developmental patterning. The well-studied *Drosophila melanogaster* adult wing shows a simple pattern with five longitudinal veins (L1 to L5) and two transverse veins.

The mature wing disc consists of two distinct domains, according to their developmental fates: the notum and the wing appendage. At the center of wing appendage domain, the oval shaped wing pouch will give rise to the adult wing blade. The ring of cells surrounding the wing pouch will become the proximal hinge, which develops from the notum domain of the wing disc and connects the adult wing blade to the adult thorax. Due to its relatively flat geometry and its integrity of developmental fate, numerous studies for organ growth and patterning have concentrated on the wing pouch. The establishment of the three body-axes (AP; dorsal-ventral (DV); proximal-distal (PD)) and pre-patterning of five vein

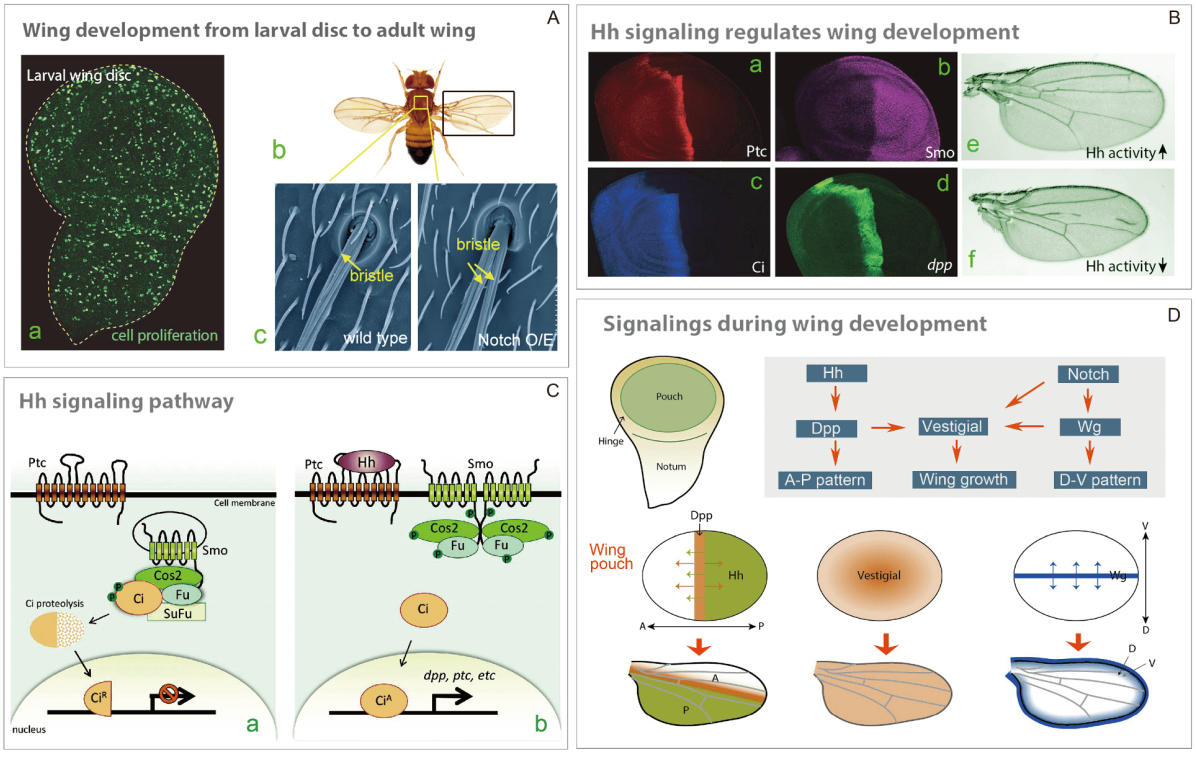

Figure 6 The major signaling pathways controlling wing growth and patterns in *Drosophila melanogaster*. A, A larval wing disc (Aa), the precursor of an adult wing (Ab), and the EM images of notum bristles (Ac). B, The expression patterns of Hedgehog (Hh) pathway components, including the receptor Ptc (Ba), activator Smo (Bb), transcription factor Ci (Bc), target gene *dpp* (Bd), in the larval wing discs, and the adult wing phenotypes caused by the altered Hh signaling activities (Be and Bf). C, The diagram of Hh signaling pathway in the absence (Ca) or the presence of Hh ligand (Cb). D, Major morphogens and factors in the larval wing pouch controlling the wing growth and patterns.

territories have been well characterized within the wing pouch. Many critical cellular signaling pathways and transcription factors have been demonstrated to regulate these developmental events.

It has been widely recognized that morphogens pay a fundamental role in generating tissue and organ patterns. Morphogens are secreted factors, controlling tissue/organ patterning in a dose-dependent manner. Several morphogens, such as Wnt/Wingless (Wg), BMP family member Decapentaplegic (Dpp), and Hedgehog (Hh), precisely define patterning of *Drosophila* wing disc, including the generation of the three axes and pre-patterning of vein territories. In addition, the non-morphogen molecular signals, such as Notch and epidermal growth factor receptor (EGFR) signals, also play critical roles in determining cell fate during wing development.

Anterior-posterior patterning

The wing pouch can be divided into two distinct compartments, the anterior (A) and posterior (P) compartments, conferred by the expression of *engrailed* (*en*) in the posterior cells (Basler and Struhl, 1994). The Hh morphogen secreted from the P compartment and the Dpp morphogen from the AP boundary, are both required to pattern the wing blade along the AP axis. They act in coordination with the EGFR signaling pathway to position and maintain vein territories in the developing wing.

In the P compartment, Hh protein is produced under the control of En, a homeo-box containing transcription factor in *Drosophila* (Tabata et al., 1992). After secretion, Hh morphogen spreads into the A compartment, forming a concentration gradient. In the Hh-receiving cells, the binding of Hh ligand with the receptor Patched (Ptc) releases the Smo protein from Ptc inhibition and allows the activation of Smo protein. The activated Smo triggers a cascade of downstream signal transduction events. Eventually, the transcription factor Ci switches on the transcription of target genes, including *ptc* and *dpp* (Jiang and Hui, 2008; Zhao et al., 2017). The activation of *ptc* transcription requires a high threshold of Hh signaling; therefore, it is expressed in a stripe at the AP border, where the cells receive the highest level of Hh signal. The overexpressed Ptc proteins in turn, sequester the Hh ligand and limit Hh spreading to A cells, thus mediating a negative feedback loop to restrict the over-activated Hh signaling. Another target gene, *dpp*, encodes the BMP family protein Dpp. Unlike *ptc*, a medium level of Hh signal is enough to activate the expression of *dpp*, which reveals a similar but wider stripe pattern than *ptc* in the center of the wing disc. The wing disc AP boundary is corresponding to the adult wing area between L3 and L4. Consistently, increasing Hh signaling activity results in expanded space between L3 and L4 in the adult wing, whereas repressed Hh signaling can narrow this space and disrupt L3 formation (Johnson et al., 1995). Thus, Hh signaling controls the patterning of the central region of the wing, including the vein L3.

Dpp, a homolog of vertebrate BMP2/4, acts as another morphogen to control AP patterning in the wing disc (Hamaratoglu et al., 2014). The Hh-induced Dpp protein is secreted from the central region of the wing disc. It diffuses toward both A and P compartments, to generate an approximately symmetrical gradient. In the signal-receiving cells, Dpp preferentially binds to type I receptor Thickveins (Tkv), triggering the phosphorylation and activation of Tkv. *Mothers against Dpp* (Mad) is then phosphorylated by Tkv. Together with the Smad4 homolog Medea, the phosphorylated Mad (pMad) translocates to the nucleus and regulates the expressions of target genes. Dpp signaling activity inhibits the *brinker* (*brk*) expression, resulting in a gradient of Brk inverse in shape to the Dpp gradient. Brk protein functions as a transcription repressor for Dpp target genes. The relative levels of Dpp signaling and Brk protein pattern the expression of target genes such as *daughters against dpp* (*dad*), *spalt* (*sal*), and *optomotor blind* (*omb*). It has been noted that the Dpp exerts a long-range effect organizing the lateral domains flanking the Hh-effective central domain of the wing pouch (Nellen et al., 1996). In the cells near the AP boundary, which receive both Hh and Dpp morphogens, Hh signaling is found to repress Tkv levels (Funakoshi et al., 2001), implying a possible mechanism by which Hh signaling in these cells is protected from the Dpp signaling interference (Chen, 2019).

As a consequence of the Dpp/Brk patterning, in brief, vein L2 is induced at the border of *sal* expression in the anterior compartment, and vein L5 is positioned at the border of *omb* and *brk* expressions in the posterior compartment. Actually, the complex regulatory interactions downstream of Dpp signaling might precisely position the wing veins. For example, the gene *knirps* is expressed in the presumptive L2 vein of the wing disc. Four Dpp target genes *aristaless* (*al*), two *sal* genes (*spalt major* (*salm*) and *spalt-related* (*salr*)), and *optix*, encode the transcription factors. A positive input from Al and negative inputs from Sal and Optix together restrict the *knirps* expression to the L2 territory (Martín et al., 2017). EGFR signaling acts downstream of Hh and Dpp signaling to establish and maintain the perspective vein domains in an AP pattern (De Celis, 2003).

Dorsal-ventral patterning

In the wing disc, dorsal (D) and ventral (V) compartments are conferred by the expression of *apterous* (*ap*) in dorsal cells (Diaz-Benjumea and Cohen, 1993). It has been found that Notch signaling and Wg morphogen play important roles in controlling the DV patterning in the wing pouch.

Notch signaling plays a fundamental role in governing cell fate determination (Bray, 2006). Different from the mor-

phogen signal, Notch signaling is a communication between two neighboring cells. Once the ligand, located at the signal-sending cell membrane, binds with the Notch receptor at the signal-receiving cell membrane, Notch protein is cleaved to generate the Notch intracellular domain, which in turn translocates to the nucleus to facilitate the transcription of target genes. The Notch signaling is active in the DV border cells, controlling the adult wing margin formation; and inducing the expression of *wg* at the DV boundary.

At the early larval stage, Wg is expressed broadly in the wing pouch, to specify the wing appendage fate, while the EGFR signal specifies the notum fate in the proximal domain of the disc. Later, Wg expression becomes restricted to two rows of cells at the DV boundary, regulated by Notch signaling. Wg morphogens spread toward both the D and V compartments, to activate the expression of target genes such as *senseless* and *Distal-less (Dll)*, in a concentration-dependent manner (Neumann and Cohen, 1997). It has been shown that Wg acts over a distance of up to 11 cell diameters to induce signaling in the wing disc (Chaudhary et al., 2019).

Proximal-distal patterning

In the wing pouch, the cells are roughly organized in a radial pattern from the center (distal) toward the periphery (proximal), generating a PD axis. The Vestigial (Vg) transcription factor and its target gene network control the PD pattern in the wing disc. Dpp, Notch, and Wg signaling cooperate to regulate the expression of *vg* (Klein and Arias, 1998). Two enhancers, the quadrant enhancer (VgQE) and the boundary enhancer (VgBE), together drive the expression of *vg* throughout the wing pouch. VgBE is active along the DV and AP boundaries, controlled by Notch and Wg signaling. VgQE is active in the rest area of the pouch, regulated by Dpp signaling. Vg interacts with Scalloped (Sd) to form a transcription factor complex (Halder et al., 1998). Vg induces the expression of *four-jointed* (*fj*) and represses the expression of *dachsous* (*ds*) (Cho and Irvine, 2004), therefore causing the expression of Fj and Ds as opposing gradients, oriented radially with respect to the pouch. These two gradients are necessary to localize the atypical myosin Dachs at the cell junction perpendicular to the direction of Fj-Ds gradients. The localization of Dachs controls the orientation of cell division in the pouch, to establish a radial pattern (Matamoro-Vidal et al., 2015).

Wing growth

It has been suggested that patterning and growth are coupled. In addition to the patterning roles, the Hh, Dpp, and Wg morphogens are also playing important roles in promoting growth (Barrio and Milán, 2020; Jiang and Hui, 2008). They can increase wing size when overexpressed through a downstream transcriptional network. In addition to these intrinsic signals, there are extrinsic factors from other tissues, regulating wing growth and final size. For example, the insulin-like signal produced in the brain and the fat body, is able to promote wing disc growth (Boulan et al., 2015). The muscle-derived Myoglianin, an Activin/TGFβ family member, has recently been demonstrated to modulate wing size (Upadhyay et al., 2020).

Wg is clearly required for wing growth, since the wing fails to grow in the absence of Wg, hence obtaining its name (Bejsovec, 2018). Wg signaling contributes positively to cell proliferation. However, around the DV boundary, a high level of Wg signaling prevents proliferation and promotes differentiation. Dpp signaling is also important for regulating the growth of the wing imaginal disc, particularly in the wing pouch. Ubiquitous Dpp expression results in disc overgrowth (Schwank et al., 2008), and the loss of Dpp signaling leads to wing defects (Burke and Basler, 1996). It has been shown that the cells in the Dpp gradient target field are highly proliferative, leading to a continuous increase in size of the wing disc. To fit the growing wing disc size, Dpp and its activity gradient are adjusted to expand accordingly (Ben-Zvi et al., 2011; Zhu et al., 2020).

Dpp and Wg signals cooperate to induce and maintain gene expression that promotes cell survival and proliferation such as *vg*. In the central region of the wing pouch, where AP and DV boundaries intersect, Vg is most highly expressed, leading to a higher proliferation rate in the center than the periphery region during early larval stages. This difference changes the global tensions in the wing pouch, which stimulates proliferation at the periphery and suppresses proliferation at the center. This feedback regulation leads to homogenous growth throughout the wing pouch at later stages. Between the pouch and the hinge, there are also different proliferation rates, which cause cell stretching and then induce hinge cell division, oriented tangentially to the hinge/pouch boundary (Matamoro-Vidal et al., 2015).

In summary, in the specified wing pouch, the Hh-Dpp and the Notch-Wg signal cascades define the AP and DV pattern, respectively, and collectively form a coordinate system to pattern the veins and PD orientation. The Hh, Dpp, and Wg signaling pathways are also required for wing growth and size control. Importantly, these signaling pathways, identified and characterized in *Drosophila*, show conserved growth and patterning functions during vertebrate appendage development, especially during limb development. Recently, much effort has been made to unravel the crosstalk and downstream transcriptional network of these signaling pathways. These signaling networks may possess a robustness to guarantee proper tissue patterning and growth in response to various genetic and environmental perturbations (Chaudhary et al., 2019; Lander et al., 2020; Zhang et al., 2020). In addition to cellular signaling, the roles of mechanical stresses during wing growth and patterning are currently attracting a lot of attention in the field. Even so, the

mechanisms by which these signals and their networks construct the complete 3D wing structure, are still poorly known in detail, and future investigation is needed.

Regenerative evolution

Cardiac regeneration: storytelling from fish, mouse and more (Figure 7)

Cardiovascular diseases (CVD) have long been the leading cause of morbidity and mortality worldwide. In China, CVD is the cause of 40% of deaths in the population and a major burden on health care resources (Zhao et al., 2019a). In response to myocardial infarction (MI) or heart attack, which results in acute loss of myocardial cells and eventual progression to heart failure, adult mammals including humans fail to restore the lost cardiomyocytes (CMs). Instead, they form scar tissues without a contractile function. In contrast to adult mammals, certain fish, amphibians and neonatal mammals can completely regenerate cardiac tissue architecture after injury, both structurally and functionally. The human heart indeed possesses regenerative capacity, although it is constrained. The homeostatic CMs can turnover at the estimated rate of 1% annually, but this rate drops progressively to 0.45% from the age of 25 to 75 years old (Bergmann et al., 2009; Bergmann et al., 2015). This low renewal rate cannot sufficiently restore the massive loss of CMs after MI. Therefore, it would behoove us to explore the natural cardiac regeneration processes and decipher their intrinsic and extrinsic determinants, in order to develop a strategy for *in vivo* reactivating or boosting human heart regenerative capacity after MI. More and more fascinating insights into cardiac regeneration have already been offered from comparative analyses, using well-established model animals, such as zebrafish, mice, and salamanders; or non-model organisms, for example, cavefish (Price et al., 2019; Vivien et al., 2016). Over the last two decades, based on numerous studies using model and non-model animals, a tremendous achievement has been reached in elucidating the evolutionarily conserved cellular and molecular mechanisms

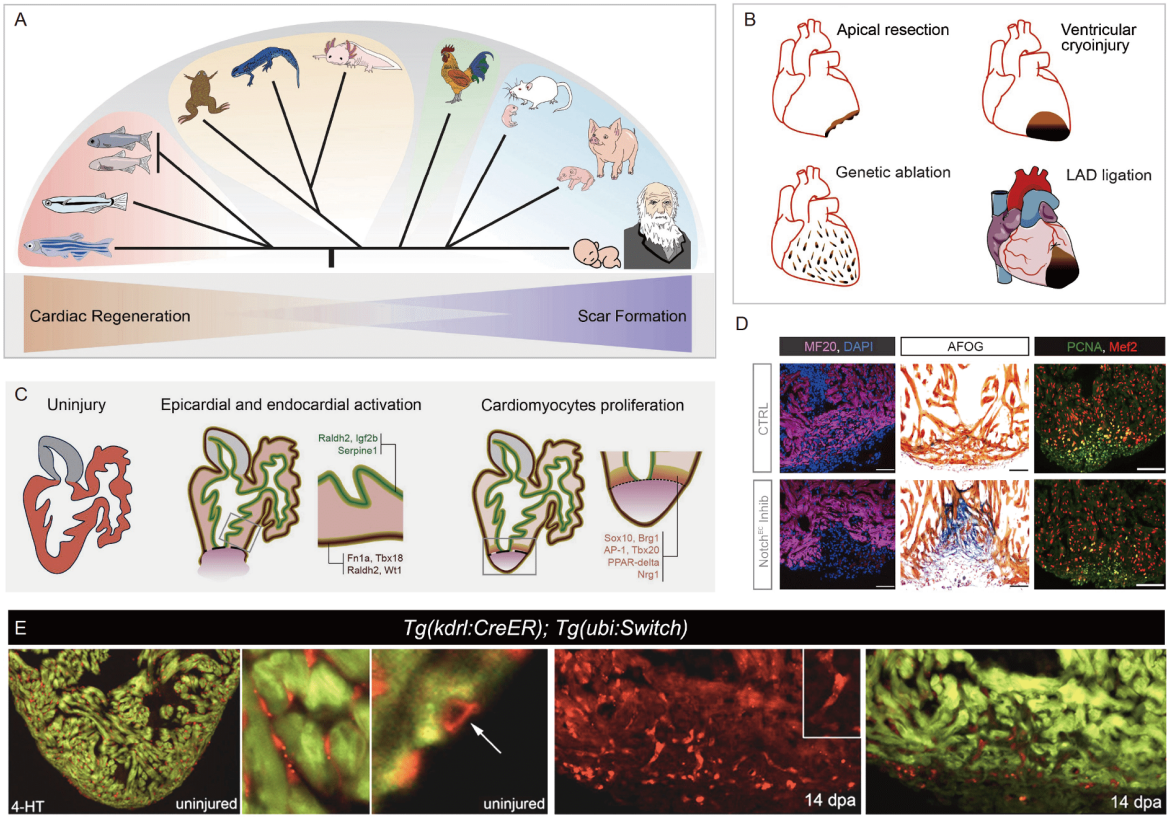

Figure 7 Cardiac regeneration in model and non-model organisms. A, Vertebrate phylogeny of representative animals with various cardiac regenerative capacities. From left to right, zebrafish (*Danio rerio*), medaka (*Oyzias latipes*), Mexican tetra (or cave blindfish) (*Astyanax mexicanus*), *Xenopus* (*Xenopus laevis* or *Xenopus tropicalis*), newt (*Notophthalmus viridescens*), axolotls (*Ambystoma mexicanum*), chicken (*Gallus gallus*), mouse (*Mus musculus*), pig (*Sus scrofa*), human (*Homo sapiens*). B, Typical approaches for induction of cardiac injury in vertebrate heart regeneration studies. C, Schematic diagrams of cellular and molecular events during heart regeneration in zebrafish. D, Endocardial Notch signaling is required for cardiomyocytes proliferation and heart regeneration in adult zebrafish. The immunostainings reveal the cardiomyocytes (MF20; magenta), CM nucleus (Mef2; red), cycling cells (PCNA; green), and nucleus (DAPI; blue). Histochemical staining with AFOG shows the muscle (brown), fibrin (red) and collagen (blue). E, Regenerated coronary endothelium derives from preexisting endothelial cells during zebrafish heart regeneration. The arrow indicates coronary vessel. CM, cardiomyocyte; EC, endocardial cells; dpa, days post-amputation; 4-HT, 4-hydrocytamoxifen. Scale bars: 50 μm.

on the biological processes of cardiac regeneration.

Zebrafish

Zebrafish (*Danio rerio*) is a widely used fish model in developmental biology studies. It holds regenerative capacity of heart tissues, as well as other adult tissues, such as brain, spinal cord, kidney, fin, liver, and retinae, during its entire life. (Marques et al., 2019). A pioneering study demonstrated that adult zebrafish could fully regenerate an injured heart following surgical removal of 20% ventricular apex in 30–60 days, without residual scarring (Poss et al., 2002). Since then, zebrafish has been introduced as an emerging model organism for the cardiac regeneration field.

Currently, there are three major approaches to induce myocardial damage in adult zebrafish. The earliest established and still most popular model is the surgical method of apical resection, which amputates around 20% cardiac ventricle by removing the apex part and triggers regeneration through robust CM proliferation within 30–60 days (Poss et al., 2002; Raya et al., 2003). Compared with human MI, apical resection showed no/rarer ischemia-induced cell death and necrosis along the amputation plane. Only small collagen depositions were observed in the fiber clot (Poss et al., 2002). An alternative procedure is cryoinjury, which damages the cardiac ventricle without removing any tissues, and induces massive CM death and scar formation within the injured area. This process highly mimics the mammalian ventricular remodeling after MI. However, in contrast to the human heart, the zebrafish heart gradually resolves fibrotic tissues, and eventually replaces them with regenerated myocardial cells (Chablais et al., 2011; González-Rosa et al., 2011; Schnabel et al., 2011). Cryoinjury-initiated zebrafish heart regeneration is much slower than the apical resection model, taking up to 180 days for full recovery (Hein et al., 2015). Another tissue-specific Cre-loxP-based method involves the genetic ablation of over 60% of the ventricular CMs without resulting in any damage to non-CM cells (Wang et al., 2011). Two transgenic lines were used to perform this tissue-specific ablation: the cardiomyocyte-specific promoter driver line with the inducible Cre-recombinase, and the conditional line containing the transgene of cytotoxic diphtheria toxin A (DTA) downstream of a *loxP*-flanked STOP cassette. Upon the Cre-loxP-induced removal of the STOP cassette in CM-specific cells, DTA is expressed, and eventually causes cell death to trigger the regenerative response in zebrafish hearts (Wang et al., 2011). All three injury models have been widely used in cardiac regeneration studies, not only in zebrafish but also in other organisms.

More and more cellular and molecular events during zebrafish heart regeneration have been revealed. Similar to the mammalian heart, the zebrafish heart is composed of three layers, the inside endocardium, the outmost epicardium, and the middle myocardium. In regenerating hearts, the endocardium and epicardium are reactivated, requiring CM proliferation and coronary revascularization. Epicardial cells dynamically re-express several developmental genes, such as *fn1a*, *raldh2*, *tbx18*, and *wt1*, and undergo an FGF signaling-induced epithelial-mesenchymal transition (EMT) (González-Rosa et al., 2011; Kikuchi et al., 2011b; Lepilina et al., 2006; Schnabel et al., 2011; Wang et al., 2013). Epicardial derived cells have been indicated to regulate and contribute to vascularization (Kim et al., 2010; Lepilina et al., 2006; Marín-Juez et al., 2019). They give rise to myofibroblasts and perivascular cells, but not to cardiomyocytes during cardiac regeneration in zebrafish (González-Rosa et al., 2012; Kikuchi et al., 2011a). Furthermore, genetic depletion of the epicardium after injury leads to inhibition of CM proliferation and vascularization, and eventually to the deficit of heart regeneration (Wang et al., 2015). The importance of epicardium in hearts has also been revealed in other animal models. In the mouse model, epicardial C/EBP family members regulate the expression of *raldh2* and *wt1* during heart development and injury (Huang et al., 2012). An intriguing study has shown that only epicardial, but not myocardial Fstl1, can promote regeneration. Human FSTL1 protein, delivered via a bioengineered epicardial patch, stimulates proliferation of pre-existing CMs and improves heart function and survival after MI in mice and swine models (Wei et al., 2015), which implies the therapeutic target potential of the epicardium.

Similar to the epicardium, the endocardium is also activated after cardiac injury. In the regenerating heart, the endocardial cells rapidly respond to injury by undergoing dramatical morphological and transcriptional changes, characterized by a shape-shift from flattened to rounded, and upregulated and highly dynamical expression of *raldh2*, within 24 h after injury. This expression becomes localized to endocardial cells at the border of the wound area, where the circulating CMs awake (Kikuchi et al., 2011b). IGF pathway factor, *Igf2b,* is induced in the endocardium upon injury, and is required for CM proliferation (Huang et al., 2013). As an important developmental signaling pathway, the Notch pathway is specifically activated in endocardium and epicardium in response to apical resection or cryoinjury in zebrafish, required for CM proliferation and heart regeneration (Münch et al., 2017; Zhao et al., 2014). Endocardial Notch signaling attenuates inflammation to promote CM proliferation, via regulating the expression of the *serpine1* gene, which is involved in the endocardium proliferation and maturation (Münch et al., 2017). In a following study, our group demonstrated that endocardial-specific Notch signaling is required for CM proliferation and heart regeneration. Two Wnt signaling antagonists, Wif1 and Notum1b, were identified to associate with the activation of endocardial Notch pathway after injury, and then dampening myocardial Wnt activity to support CM proliferation. This

study reinforces the importance of cross-talking between endocardium and myocardium and highlights the molecular mechanism of Notch and Wnt pathways orchestrating CM proliferation during zebrafish heart regeneration (Zhao et al., 2019b).

Unlike mammalian adults, zebrafish can fully restore lost cardiomyocytes during regeneration. The cellular source of newly regenerated CMs has been revealed using the Cre-loxP lineage tracing technology. Pre-existing CMs undergo dedifferentiation and proliferation in order to generate new cardiac muscle cells (Jopling et al., 2010; Kikuchi et al., 2010). Another study indicated that zebrafish larval atrial CMs undergo trans-differentiation (or reprogramming) to contribute to the regeneration of the injured ventricle. Here, endocardial Notch provides an essential contribution in a non-cell-autonomous manner (Zhang et al., 2013). The naturally diploid mononuclear CMs in adult zebrafish assign their proliferative capacity to cardiac regeneration (González-Rosa et al., 2018). A subset of neural crest (*sox10*$^{+}$) derived CMs was found to contribute to CM proliferation following cardiac injury (Sande-Melón et al., 2019; Tang et al., 2019). Two recent studies showed that AP-1 and Tbx20 could reactivate embryonic gene programs, to promote CM dedifferentiation and proliferation after cardiac injury (Beisaw et al., 2020; Fang et al., 2020). Several other factors have been identified to participate in CM proliferation upon cardiac injury, such as Brg1, Nrg1, PPARδ, vitamin D, and hemodynamic forces (Gálvez-Santisteban et al., 2019; Gemberling et al., 2015; Han et al., 2019; Magadum et al., 2017; Xiao et al., 2016).

Mammals

Adult mammals have extremely limited cardiac regenerative capacity after injury. Consistent with humans, adult mice also have a low rate of CM renewal (around ~1% per year) throughout life (Senyo et al., 2013). However, neonatal mice can fully regenerate cardiac tissues following different injury types, such as the experimental injury approaches aforementioned in zebrafish studies, and left anterior descending coronary ligation (LAD ligation). Porrello and colleagues were the first to demonstrate that following apical resection, one-day-old neonatal mice possess complete cardiac regenerative capacity. Along with a global activation of CM proliferation in the entire heart, regenerated CMs are derived from the pre-existing CMs through cell division (Porrello et al., 2011). However, the window of cardiac regeneration in neonatal mice is closed by postnatal day 7, in both resection and LAD ligation models (Porrello et al., 2011; Porrello et al., 2013). Especially, a rapid decline was reported for this regenerative ability within 48 h after birth (Notari et al., 2018). Similar to zebrafish, epicardial activation was observed in the cryoinjury mouse model (Darehzereshki et al., 2015). To support cardiac regeneration, endocardial IGF2 is required for maintaining a high percentage of mononuclear diploid CMs with a high proliferative rate (Shen et al., 2020).

Not only mice, but also large mammals such as pigs and sheep, have been reported to regenerate heart injury after being subjected to LAD ligation in the neonatal stage (Hodges et al., 2021; Ye et al., 2018; Zhu et al., 2018b). Compared to neonatal mice, the neonatal pig has a narrower window of regeneration within the first two days of life. The proliferating CMs also originate from a pre-existing CM source, like in neonatal mice or zebrafish (Ye et al., 2018; Zhu et al., 2018b). Even in humans, several clinical cases suggested that the newborn may retain a similar regenerative capacity (Haubner et al., 2016; Saker et al., 1997). These clinical observations are consistent with the finding that young humans have a relatively higher ability of CM proliferation (Bergmann et al., 2015; Mollova et al., 2013).

Other organisms

Beyond the widely used model animals, like zebrafish and mouse, cardiac regeneration has been investigated in several other organisms. Medaka is a teleost fish with a remarkable aptitude of fin regeneration. However, it lacks the cardiac regenerative ability, causing lack of activation of CM proliferation or epicardial expression of *raldh2* and a retarded immune response after injury (Ito et al., 2014; Lai et al., 2017). Giant danio and Goldfish, also belonging to teleost fish but with a bigger body size than zebrafish, could restore hearts damage following cardiac injury (Grivas et al., 2014; Lafontant et al., 2012). An “ancient fish”, *Polypterus*, which diverged from teleost fish ~400 million years ago, displays CM proliferation as well as endocardial and epicardial induction of *raldh2* expression in response to cardiac injury (Kikuchi et al., 2011b). Intriguingly, a recent study indicated that the Mexican tetra (or blind cavefish), a single fish species comprising a cave-dwelling population without eyes and a surface population with eyes, displays hugely different cardiac regenerative capacities, even though the equivalent CM proliferations are illustrated at the injury sites (Stockdale et al., 2018).

Salamanders, including newts and axolotls, are excellent model animals for regeneration studies (Joven et al., 2019). About 40 years ago, an early exploratory study demonstrated the capacity of cardiac regeneration in newt (Oberpriller and Oberpriller, 1974). Recent studies further revealed cellular and molecular processes during newt heart regeneration (Laube et al., 2006; Piatkowski et al., 2013; Singh et al., 2018; Witman et al., 2011). Cardiac regeneration in axolotls involves cardiomyocytes reentering the cell cycle, and interactions between macrophages and fibroblasts (Cano-Martinez et al., 2010; Flink, 2002; Godwin et al., 2017). Another amphibian model, *Xenopus*, has also been evaluated for its cardiac regeneration capacity. Interestingly, contradictory results were reported in adult frogs. *Xenopus laevis*

frogs show persistent fibrosis with no activation of CM proliferation and failure to regenerate following injury (Marshall et al., 2017), while *Xenopus tropicalis* frogs are able to completely regenerate damaged hearts without scar tissue deposition (Liao et al., 2017). A follow-up study demonstrated that juvenile *Xenopus laevis* frogs possess full cardiac regeneration ability (Marshall et al., 2019). In birds, there are far fewer studies on cardiac regeneration. Only 2–3 days old chicken embryos were shown to have complete regeneration capacity after cardiac injury. This capacity dramatically declined at the age of 3–5 days old, and totally diminished at the age of 18-day old or newly hatched (Novikov and Khloponin, 1982).

Evolutionary enlightenment for future

There are huge morphological differences among hearts in the animal kingdom, from the simplest tube-formed heart in *Drosophila* to a four-chambered human heart, due to the genetic and environmental adaptations during millions of years of evolution. Other features however, such as the physiological function, organ/tissue structure, cell types, and the underlying molecular basis governing cardiac development, are highly conserved. This makes it feasible to survey the intrinsic cellular and molecular mechanisms of cardiac regeneration from comparative analyses from an evolutionary perspective.

Currently, the knowledge on cardiac regeneration from studies in about a dozen vertebrate species, has illuminated the evolutionary conserved strong correlation between regenerative capacity and several key factors such as cardiac metabolism, oxidation status, and body thermoregulatory regulation (Vivien et al., 2016). For example, zebrafish and salamanders, that possess remarkable cardiac regeneration capacities during adulthood, are ectotherm or cold-blooded species without a body temperature regulatory system and live in an aquatic environment with low oxygen concentration. Similarly, under hypoxic circumstances, the heart of a neonatal mammal is capable of regenerating in the early days after birth but then takes a drastic shift in oxygenation status. This coincides with a loss of regenerative capacity. An apparent fact is that mammals and birds are endotherms or warm-blooded species, while their neonates generally lack a competent thermoregulatory system. Several studies assessing oxygen level and metabolic remodeling have proposed the intrinsic mechanisms (Cardoso et al., 2020b). Increase of oxygen consumption after birth results in CM cell cycle arrest (Puente et al., 2014). This is associated with fatty-acid utilization as a substrate of mitochondrial oxidative phosphorylation as the major energy source, instead of the glucose oxidation, in hearts of postnatal mice (Cardoso et al., 2020a). A recent study indicated that cycling CMs exist in adult mouse hearts in a state of hypoxia and low-metabolic activity (Kimura et al., 2015). Furthermore, chronic hypoxemia exposure of adult mouse hearts demonstrates the induction of CM proliferation and leads to cardiac regeneration following MI, with significant functional recovery (Nakada et al., 2017). In zebrafish, hypoxia is required for CM proliferation and heart regeneration (Jopling et al., 2012). As a relevant result, therefore the metabolic switch from mitochondrial oxidative phosphorylation to glycolysis promotes CM proliferation after cardiac injury (Fukuda et al., 2020; Honkoop et al., 2019). Taken together, it seems that the cardiac regenerative capacity has a bias toward low-metabolic ectotherms.

However, the intrinsic mechanisms are still hardly known in detail. In the current circumstances, evolutionary insights into natural cardiac regeneration are critical for our perspective. Considering that there are more than 50,000 living species of vertebrates, it is not enough that only a small number of organisms have been investigated for the capacity of cardiac regeneration. Therefore, large-scale exploration of cardiac regeneration, based on comparative analyses, is required to illuminate the underlying mechanisms. The "large-scale exploration" does not mean to check every single species of the entire phylogeny. However, two relatively small groups of representative species could be used for the investigation of cardiac regenerative capacity instead. The first group is the key species of a phylogeny with adaptations, or an evolutionary intermediate species. For example, the lungfish, representing a type of essential transition from aquatic to terrestrial vertebrates, can complete fin and tail regeneration (Conant, 1973; Verissimo et al., 2020), but whether it has a similar cardiac regenerative capacity following injury is unknown. Recently, an elegant study using systematic comparison of African killifish and zebrafish, demonstrated that evolutionary conserved regeneration-responsive enhancer elements exist, and tightly modulate regenerative capacities in vertebrates (Wang et al., 2020a). The second group includes the species in a unique geographic environment, such as Tibetan Plateau, where the biodiversity is plentiful, especially for fish. For example, the clade of *Schizothoracinae* comprises more than 100 species, and the *Triplophysa* includes more than 140 species (Deng et al., 2020), which live at an altitude from 1,250 m to above 5,600 m, providing abundant material for elucidating the mechanisms of fine-tuning cardiac regeneration.

Understanding the evolutionary context via large-scale comparative analyses, and deciphering cellular and molecular mechanisms of natural regenerative capacity among vertebrates, particularly, in mammals, would shed light on developing therapeutic strategies for cardiac diseases.

Limb regeneration in salamanders (Figure 8)

Regeneration is a process during which organisms restore damaged or lost tissues, organs, and even the whole body.

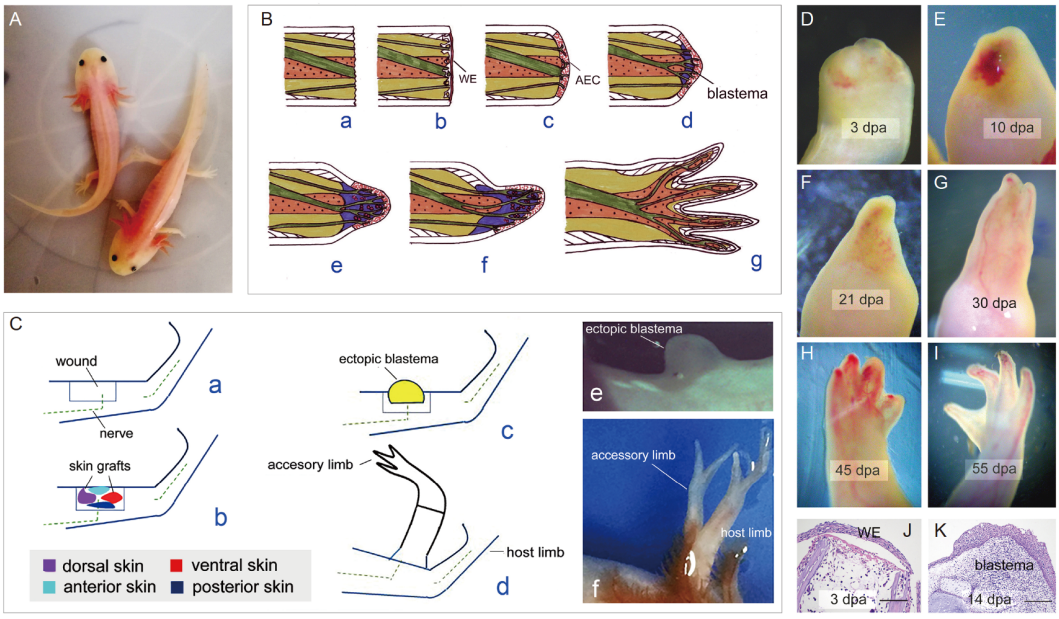

Figure 8 Limb regeneration of axolotl (*Ambystoma mexicanum*). A, Axolotls. B, Diagrams of limb regeneration process: (a–c) wound healing after amputation, (d and e) blastema formation and expansion, (f and g) cell differentiation and morphogenesis. C, Induction of accessory limb: (a–d) strategy of limb induction, (e) ectopic limb bud, (f) accessory limb. D–I, Morphological progress of limb regeneration. J and K, Representative longitudinal sections of regenerating limbs at 3 and 14 dpa, respectively. WE, wound epidermis; AEC, apical epithelial cap; dpa, days post-amputation. Scale bar represents 200 μm.

This phenomenon has been observed among numerous animal phyla and is achieved in diverse modes, as animals adapted various regenerative strategies. Salamanders exhibit a powerful capacity for regeneration, regrowing multiple tissues and organs after injury. Since the salamander limbs are anatomically similar to their human counterparts, their mode of regeneration could provide important insights into the regenerative medicine studies.

For many years, scientists wondered why salamanders possess such amazing regenerative capabilities, while other species do not. Although several theories have been proposed, it seems that the most explanatory is the theory of neoteny, which means that the salamanders never complete metamorphosis, therefore certain cells maintain embryonic-like characteristics throughout life. Additionally, the adaptive immune system of salamanders is relatively simple compared to that of amniotes, thus weak inflammatory response after injury initiates regeneration (Mescher and Neff, 2005). Limb regeneration in salamanders occurs via epimorphosis, which involves the dedifferentiation of adult tissues upon damaging, formation of the blastema, and the subsequent re-specification. Injury, like amputation, initiates a healing process, in which a plasma clot forms at the wound area, then within 6–12 h, nearby epidermal cells, migrate alongside, and finally cover the entire injured surface to form an epidermic structure called wound epidermis (WE). In the following few days, the WE keeps proliferating to reconstruct the anatomy, apical epithelial cap (AEC), under the guidance of nervous signals. Meanwhile, beneath the developing AEC, a group of cells, named "blastema", derived from the de-differentiated cells located at the injury border of the stump, lost their differentiated characteristics, and became detached from each other, associating with dramatic alteration of the transcriptomic profile. The cells in the blastema continually proliferate and differentiate to complete regeneration of a new limb.

Here, we focus on the current progress on limb regeneration in salamanders, discussing several aspects including formation of blastema, morphogenesis/patterning, and the role of nerve cells during the regenerative process.

Formation of blastema

The establishment of the blastema is crucial for successful limb regeneration. It has been demonstrated by the accessory limb model (ALM) that in order for the blastema to be formed, several conditions must be met (Endo et al., 2004). One of the most critical conditions is the presence of nerves and wound epithelium. In case when nerves have not deviated, the wound will heal. However, blastema will not be formed. That proves the demand for nerve signaling, which will be discussed further. Furthermore, dermal cells and the ECM are also essential for blastema formation (McCusker and Gardiner, 2013). Interestingly, inflammatory signals from macrophages also seem to be necessary for limb regeneration (Godwin et al., 2013). Hence, in order to induce blastema formation, signals from nerves and inflammatory cells seem to be required. Interactions between nerves and WE leading to the formation of an AEC, are influenced by

numerous factors.

Regeneration blastema is formed as a result of the following processes: formation of a WE that closes the wound; formation of progenitor cells by histolysis and release of dedifferentiated cells; blastema cell migration and aggregation under the apical epidermal cap.

Just after amputation, the wound is sealed by a blood clot. Fibronectin in the clot constitutes a substrate for the epithelial cells. Then, accumulation blastema forms, and the WE thicken to form the AEC. The wound epidermis expresses antigens (WE3, WE6) that are not expressed in the uninjured epidermis, indicating that they are explicit to regeneration—they might be involved in AEC formation (Satoh et al., 2010). During histolysis, fibroblasts are released from the dermis, connective tissue, periosteum, and nerve sheath. Myofibers fragment and break up into mononucleate cells, while releasing stem cells (Santosh et al., 2011). Enzymes, known as matrix metalloproteinases (MMPs), have been proven to be required for histolysis, as various experiments indicated that without these, blastema will not be formed. The main sources of MMPs are the WE and the AEC. Histolysis progresses until the medium bud stage, when it is stopped by tissue inhibitors of metalloproteinases (TIMPS), which are further upregulated when the MMP level reaches the maximum (Santosh et al., 2011).

Another mechanism that leads to blastema formation is dedifferentiation. Dedifferentiation is a process where cells are being reprogrammed to an embryonic-like state, to obtain increased developmental potential. Induction of dedifferentiation requires nerve/WE/AEC signaling, and involves FGF signaling (Satoh et al., 2010). Cells released during histolysis are a mixture of stem/progenitor cells and dedifferentiated cells. During dedifferentiation, transcription of differentiation genes is inhibited, while proteins associated with stemness, cell stress reduction, and remodeling of internal structure, are activated. Suppression of differentiation genes does not influence histolysis. An important aspect of dedifferentiation is the dedifferentiation of myofibers. Unfortunately, molecular details of this process are still poorly understood. Muscle dedifferentiation is dependent on a programmed cell death response. Programmed cell death response-induced fragmentation produces intermediate cells with a capacity of resuming proliferation and contributing to muscle regeneration. Although the blastema cells look quite similar, these cells are heterogeneous, which is due to their heterogeneous origins and consequently their different fates (Kragl et al., 2009). This cellular heterogeneity was recently confirmed by transcriptome analysis of regeneration blastema at the single-cell resolution (Leigh et al., 2018). Combining genetic tracing with the single-cell sequencing techniques proves that connective tissue is a major source of the blastema (Gerber et al., 2018). Another contribution comes from activated muscular stem cells known as satellite cells (Fei et al., 2017).

Many genes are upregulated during blastema formation. Some of them were identified by subtractive hybridization, microarray, and RNA-Seq analysis. These genes are mainly related to metabolism, cell physiology, and cell cycle regulation. Although there could be a separate chapter on this topic, we provide several examples and shortly summarize their functions. Genes related to progenitor status involve several genes, including *msx*1, *msx*2, *nrad*, *rfrng*, *notch*. *Msx1* inhibits myogenesis; *nrad* expression is correlated with muscle dedifferentiation, while *notch* is a mediator of stem cell self-renewal. An axolotl transcriptome study revealed *cirbp*, the RNA binding protein gene (it has a cytoprotective role in limb regeneration), and *kazald*1, the serine protease inhibitor (which impairs regeneration) (Bryant et al., 2017). The proteomic analysis enabled detection of proteins involved in canonical or non-canonical Wnt signaling during axolotl limb blastema formation. Wnt8, APC, and DIXDC1 are components of the canonical Wnt pathway and are strongly upregulated, while inversin and CCDC88c are part of the non-canonical pathway. Both canonical and non-canonical Wnt pathways control blastema formation.

Summarizing, prior to blastema formation, WE/AEC is formed in response to nerve signals. Additionally, the AEC also provides a lot of important signals, like FGFs, BMPs, Wnts, and enzymes that degrade ECM in the adjacent tissues. One of the early steps is the proliferation of myoprogenitor cells, followed by the reentry into the cell cycle of blastema progenitor cells from the connective tissues. After several days, cells from the dermis migrate along with the connective tissue fibroblasts and accumulate in the center of the wound area, underneath the AEC.

Pattern formation/morphogenesis of limb regeneration

Morphogenesis is a process that causes particular tissues to develop their shape by controlling the spatial distribution of cells during development. Tissues and organs acquire the shape that is critical for their functions. This process also occurs during regeneration. Understanding the morphogenetic mechanism involved in the re-creation of missing limb parts, is a fascinating and central problem of regeneration. It seems that that the early pattern information is contained in the limb skin, and is asymmetrically distributed around the circumference of the limb. For example, when making a wound on the limb's anterior side in newt and re-direction of the nerve to the wound site, then a blastema-like structure can be induced. Blastema formed in that way cannot grow further and finally regresses. On the contrary, if a piece of full skin from the opposite side (posterior side) of the limb is grafted into the nerve-deviated wound site, then induced blastema is induced and undergoes the subsequent pattern formation process and an accessory limb recreates.

In addition to the skin around the cuff of the limb, the

blastema itself also contains position information. The positional information in the early and late blastema is acquired through the expression of *HoxA* genes. New positional information is initially elastic and becomes preserved as blastema differentiates. Hence, the positional information can be reprogrammed through time. An exception to this are cells in the stump tissue and the basal region of the late bud blastema, which cannot be reprogrammed (McCusker and Gardiner, 2014). One factor contributing to positional reprogramming is an activated receptor; however, it might not be enough. Another possibility is the "flexible" state of undifferentiated blastema cells due to the chromatin state (McCusker and Gardiner, 2014). There is more evidence for plasticity of the positional information in undifferentiated blastema cells, since grafts of early bud (EB) and the apical region of late bud tissues into the new host location do not cause the formation of accessory structures on either PD or AP axes of the limb. On the contrary, grafts of differentiated blastema cells and stump tissue result in the formation of supernumerary structures. What is more, grafted EB blastema cells do not maintain the expression of a marker from the original location, but start the expression of a marker that corresponds to the new host location (McCusker and Gardiner, 2013). These data confirm that positional information is gradually stabilized in the blastema.

The key roles of nerve cells in limb regeneration

The role of nerve signaling in the regeneration process aroused interest in scientists already a long time ago. Up to date, various studies have described the importance of nerve cells in the regeneration process, and indicated that presence of nerves controls the initiation of limb regeneration (Stocum, 2011). As mentioned before, nerve deviation induces the formation of an ectopic blastema. Nerve signaling may also occur when nerves are not deviated; however, this occurs on a significantly lower level. Thus, the threshold for blastema formation might not be reached. Additionally, this threshold is different at distinct PD levels of the limb (Stocum, 2011). Importantly, nerve signaling is required not only for blastema formation but also for its further growth and development. AEC can be formed in the absence of nerves; however it will not be maintained, and formation of the blastema will fail (Stocum, 2011).

In order to induce scar-free healing—leading to blastema formation—there must be an interaction between WE and AEC, which leads to changes in gene expression. An example of such an interaction is the induction of dedifferentiation of WE keratinocytes by nerve signaling, which keeps these cells undifferentiated in the blastema. These processes are regulated by the nerve-dependent expression of zinc-finger transcription factor *Sp9* (Satoh et al., 2008).

Another aspect that has attracted scientists' interest is related to regeneration signaling pathways responsible for migration, proliferation, and differentiation of limb bud cells. It has been speculated that FGFs can constitute a substitute for the nerve in the ALM. Although scientists were able to induce the growth of a blastema-like structure, it did not have the features of a blastema. However, it turned out that the combination of FGF2, FGF8, and GDF5 together led to blastema formation and further limb regeneration. Although denervated growth results in a full proximo-distal array of skeletal elements, these are smaller than regular skeletal parts (Stocum, 2011). Another example is the anterior gradient protein (nAG) occurring in newts, which can support regeneration in partially innervated limbs (Kumar et al., 2007).

Nerves also play an essential role in the recruitment of blastema cells. Interaction of the nerve and WE/AEC determines the direction of cell migration, i.e., where the blastema forms. This is supported by the fact that FGFs produced as a result of the aforementioned interaction serve as early pro-regenerative signals. Distal migration of limb bud cells can be redirected toward implanted beads soaked in FGF. Only after cells have migrated into the center of the wound, reentry into the cell cycle of the blastema progenitor cells may occur.

Environmental stress, adaptation and evolution

Horizontal gene transfer in genomes (Figure 9)

Genetic materials underlie the basis of ontogenesis and development of organism. Genes in a genome gradually perform the processes of life, under precise regulation, within organisms and corresponds to all possible phenotypes, including both the group-common and species-specific. Accordingly, "core" and "accessory" (or "flexible") functional gene groups are designated as a response to varying gene content of these two distinct functions of a genome. Core genes, shared by all members of a predefined group, play their roles as constraints via encoding the fundamental and indispensable functions. Accessory genes, present in only a subset of members, usually encode the specialized characters and result in the phenotypic divergence within this predefined group (Sugawara et al., 2013). Accessory genes are important for adaptive evolution and diversity formation of species, by assisting organisms to obtain the selective advantages, especially for extremophile clades, such as Cyanidiales, which thrive in acidic and thermal habitats worldwide (Rossoni et al., 2019). From the ecological perspective, the existence of a single accessory gene with the processes of duplication and substitution can lead to the formation of new community interactions. It might thereby hold great potential to cause clade-specific niche expansion and could even change the worldwide ecological patterns. *Thalassiosira pseudonana* is a diatom model species for

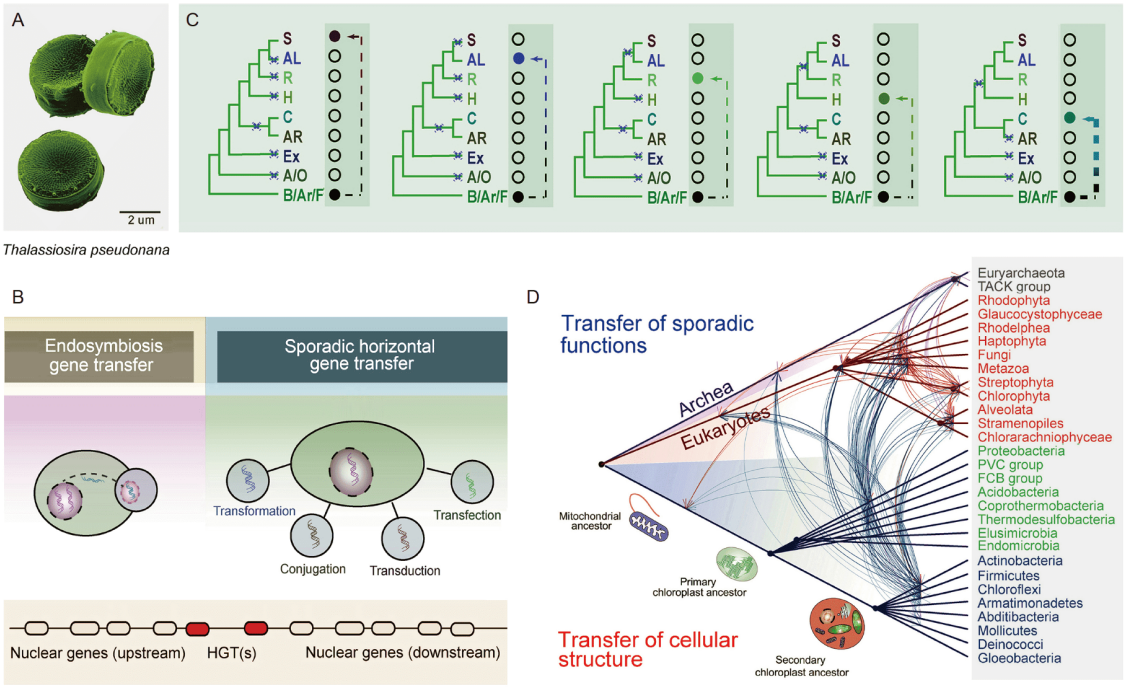

Figure 9 Horizontal gene transfer (HGT). A, A SEM (scanning electron microscope) figure of model phytoplankton species for HGT study, *Thalassiosira pseudonana*. B, Two main styles of HGT, EGT via engulfing organism as endosymbionts and sporadic horizontal gene transfer via transformation, conjugation, transduction and transfection. Successfully transferred genes (red ellipses) located in genome flanking by host genes. C, The phylogeny strategy to infer HGT events via balancing the hypotheses of DL and HGT. For the abnormal clustering of two distant groups (solid circles) in a tree, the purple crosses stand for the hypothetical reduced groups (blank circles) by DL theory while the arrows stand for the direct gene transfer by HGT theory. The probability of four loss events in a gene family is extremely low, so all these five cases are considered as HGT. D, Recent studies that state the importance of HGT to life history. Of which, some EGT events were looked as milestones in life history.

studying horizontal gene transfer from the perspective of biology and ecology. It derived large amounts of genes from photosynthetic endosymbionts and sporadic genes from bacteria, enabling it to dominate the marine phytoplankton (Moustafa et al., 2009; Deschamps and Moreira, 2012; Dorrell et al., 2017). The contribution of accessory genes to adaptive evolution and niche adaptation in eukaryotes, which is significantly different from prokaryotes, is hotly disputed. This directly influences our understanding of the origin of metabolic processes in cellular evolution.

Regarding the origins of these accessory genes, two dominant evolutionary hypotheses, the differential loss hypothesis (DL) and horizontal gene transfer (HGT), have been proposed. The DL hypothesis favors a "pristine" view of eukaryotic genome evolution, with the current sporadic distribution of many HGT-derived gene families explained by DL since the origin of the last eukaryotic ancestor. The main claim of this hypothesis is that many genes shared by the eukaryotic common ancestor have been lost in some lineages. In contrast, the HGT or lateral gene transfer hypothesis is commonly defined as the exchange of genetic material between two "non-genealogical" species. It allows for the dynamic acquisition and fixation (e.g., due to local selection) of novel gene functions by HGT from prokaryotes over during evolution. HGT mainly happens in two ways: the sporadic horizontal gene transfer, where one species actively acquires or passively receives a single fragment of DNA from another; and the endosymbiotic gene transfer (EGT), a gradual genetic material communication between the donor and host that maintain a stable endosymbiotic relationship.

Methodology advances in HGT identification

Transfer genes form a special group of genes in the recipient genome, because of their difference with core DNA in GC content, codon usage, the presence or absence of introns, transcriptional promoters, and unequal selective pressure (Derelle et al., 2006; Koutsovoulos et al., 2014; Choi et al., 2015; Fan et al., 2020). This leads to different genes in the same genome, exhibiting different evolutionary histories (Husnik and McCutcheon, 2017). These differences in retained characteristics in gene content make "sequence similarity-based strategy" underlie the methodological basis for the identification of HGT genes. In earlier days, HGT genes were generally isolated by means of the GC content, the codon usage bias, and intron number among species (Derelle et al., 2006). Most outcomes of these methods are prone to false positives, given their simple and crude nature. However, none of these applications should be arbitrarily excluded. Then the homologous strategy was used to search for the incompatible families, made up by genes from geneti-

cally distant species (Ku et al., 2015). In recent years, the phylogeny method is being used to find taxonomic conflict on a gene tree. Specific phenotype sharing between genetically distant organisms is basically driven by the overlap of their genomes, which can manifest as a monophyletic relationship in a gene tree. The absence of the genes in other branches among the animal kingdom can be explained by large-scale loss, or more likely, by acquisition through HGT (Salzberg et al., 2001). That is, if a nesting relation of two taxonomically distant genes in a tree (taxonomic conflict) needs to be interpreted by more gene loss events, the more likely it is caused by HGT, because HGT can in principle occur between any two distant organisms that contain DNA genomes. The phylogeny strategy, with a reasonable estimation of the evolutionary model, is the key step in HGT identification, given its wide application of statistics and thorough consideration of evolution. It forms the main battleground between the "DL" and "HGT" hypotheses and eventually brings them to a compromise. Recent HGT studies reported so far, use the systematic method mainly based on homologous classification+phylogeny, with the auxiliary validation of gene similarities comparison (Fan et al., 2020; Curtis et al., 2012). With the development of technology, a variety of databases and a pipeline have been developed to largely automate the identification process of HGT, include Pfam (Finn et al., 2016), COG (Tatusov et al.,2003), TIGRfam (Haft et al.,2003), RAST (Aziz et al., 2008), HGTree (Jeong et al.,2016), GOLD (Pagani et al., 2012), fusionDB (Zhu et al., 2018a). Additionally, recent expansion of sequenced genomic data has enabled the construction of genome-wide phylogenies to define taxonomy. This would be helpful in order to address an important aspect of the species-sampling effect, namely the phylogenetic bias in the data sets that are being analyzed. More comprehensive tests are needed to assess past hypotheses and observations that were seemingly at odds in explaining HGTs.

Contributions of HGTs to life history

HGT events occurred continuously during the history of life. Large-scale HGT events have been studied till now and some of them have been acknowledged as milestones in the evolutionary history; there is general consensus about the formation of eukaryotic mitochondria and photosynthetic chloroplasts. (Bhattacharya and Price, 2020). The evolutionary history of the latter is particularly fascinating, since photosynthetic endosymbionts were engulfed more than once and at multiple levels. The hypotheses of key points in chloroplast spreading still remain controversial. The story began with an occasional engulfment event of a photosynthetic cyanobacterium-like organism by a non-photosynthetic single-celled eukaryote, ca. 1 Gya–1.6 Gya (10^9 years ago). This created an opportunity to formation of the circulation system of energy and matters that enabled the host and endosymbiont to permanently maintain a mutually beneficial relationship (Kurahashi, 2016). The probability was thought to be extremely low, but it did happen. Three extant photosynthetic clades, the Glaucophyta, the Rhodophyta, and the Viridiplantae, were derived from this event and stand as evidence (Cavalier-Smith, 2017; Bhattacharya and Price, 2020). This event was later dubbed the Primary Endosymbiosis. Subsequently, genes of the primary cyanobacteria endosymbiont were transferred continuously to the host nucleus or lost due to their non-essential functionalities or inefficient transcription. This led to generation of the current degraded plasmid with a very genome, the chloroplasts. After this, it has been known that two of those three groups were independently engulfed by heterotroph groups during the long course (termed as secondary endosymbiosis) with, yet again, subsequent large-scale EGTs to hosts. These independent events give rise to a series of groups with great importance to the earth's ecology, such as diatoms and kelps. The series of large-scale EGT of both primary and secondary endosymbiosis spread the effects of photosynthesis in the eukaryotic world. It had special significance for the evolution of life on earth: the limitless solar energy is converted to chemical energy that flows within the organisms, and thus increases the energy level of biochemical reactions. The carbon-oxygen cycle rapidly changed the atmosphere content that gave rise to the current terrestrial plants and animals (Ball et al., 2016). Unlike EGTs that continuously transfer genes from a single donor to a single receptor, giving the possibility of transferring genes in the same metabolic pathways, the sporadic HGT help the host to suddenly obtain advantageous traits which are a key factor for its survival in extreme environments. A few successful examples include the obtaining of GH in plants, virus genes found in the human genome (Magiorkinis et al., 2013), gene gains in the thermophilic red algae *Galdieria sulphuraria* (Rossoni et al., 2019). By incorporating foreign DNA with high efficiency, both HGTs and EGTs help to obtain novel function and contribute to species divergence and adaptation (Andersson, 2009; Cooper, 2014). They largely influence the evolutionary processvia combination and selection and have a profound impact on the current biological pattern.

HGT by fusing genetic materials among genetic distant groups challenged the classical evolutionary theory and are thereby important types of evolution. While HGT is widely accepted as one of the main driving forces in prokaryote evolution, the relevance of HGT in eukaryotic evolution remained controversial for a long time. The extent of influence of HGT is difficult to measure accurately and has often been over-estimated in eukaryotes (Keeling and Palmer, 2008). We highlight here the significance of recent studies reporting a HGT study via phylomes in chromalveolata (CRASH group). Recent collaborative work provided strong

evidence for the HGT hypothesis through analysis of the most diverse and ecologically important groups of eukaryotes on our planet, the CRASH taxa (cryptophytes, rhizarians, alveolates, stramenopiles, and haptophytes) This group includes taxonomically diverse diatoms and dinoflagellates as well as kelps, heterotrophs, saprobes, and the malaria parasite (Fan et al., 2020). Other strong evidence for the HGT hypothesis was provided through analysis of 10 novel genomes from the extremophilic red algae (Cyanidiales) (Rossoni et al., 2019). Recent work investigated the HGT instances among protists, algae and yeasts, and HGT appears small in sizes but significant in functions (Van Etten and Bhattacharya, 2020). These results demonstrate that HGT impacts only about 1% of the gene inventory, the "1% rule". Despite this small number, many novel functions arose that likely played a key role in remarkable success, e.g., adaptation by Cyanidiales to hot springs habitats, and diversification of phenotypes in phytoplankton to differing environments.

In contrast to the vertically inherited genetic information from parents, that underlies the conservation of biological heritage in eukaryotes and ensure the stability of the tree of life (Husnik and McCutcheon, 2017), HGT drives the diversification of evolution of eukaryotic species, yet representing a significant force in adaptation to various environments (Eyres et al., 2015). Whereas HGT as a major force driving prokaryote evolution is well accepted (Wagner et al., 2017), its role in eukaryote evolution is highly disputed, due to the complex nature of eukaryotes and the sequence contamination from microorganisms. More work needs to be done in this field.

Spontaneous and environment-dependent mutations in organisms (Figure 10)

Mutations are the fuel for evolution, and the causes of numerous diseases (Knudson Jr, 1971; Odagiri et al., 1998). They are usually caused by various endogenous and exogenous factors, such as replication errors, deamination, radiation, oxidation, mutagenic chemicals, stress, and other physicochemical factors (Duncan and Miller, 1980). Here, we define mutations as changes in DNA, from single nucleotide substitutions to large-scale structural variants. Depending on effect of the mutations on the fitness of the focal organisms, they are canonically categorized into deleterious, neutral, and beneficial mutations. Recent technological advances, such as genomics and bioinformatics, facilitated research on spontaneous and environmental mutagenesis, mutation repair, and mutation rate evolution, especially for model microorganisms.

Spontaneous mutagenesis bias

Different types of pre-mutations (mutations before repair) do not usually occur at similar frequencies. DNA mismatch repair systems (MMR) are most powerful for repairing pre-mutations. MMR-deficient organisms reveal true mutational patterns that are untouched by the repair system. Mutation accumulation experiments combined with whole-genome sequencing—the most accurate technique for deciphering both genomic mutation rate and spectrum, though laborious and time-consuming—reveal that transitions usually occur tens to hundreds of times more frequently than transversions. This might be a consequence of the structural similarity of pyrimidine or purine molecules, i.e., pyrimidine is more easily substituted by another pyrimidine, not a purine, since pyrimidines and purines differ dramatically in molecular structures. It might also be due to selection caused by the weaker effects of transitions on coded proteins. Spontaneous deamination or depurination occurs at higher frequency in methylated nucleotides than in non-methylated ones, which causes a higher base substitution mutation rate. Oxidized nucleotides, especially 8-oxo-guanines either in DNA strands or in the nucleotide pool, cause mostly transversion mutations. Small indels, usually caused by replication slippage, are also prone to occur in simple sequence repeats.

Recent mutational studies revealed that mutations do not occur randomly along the chromosomes, so do mutation repair systems (Foster et al., 2013; Long et al., 2015). Base composition of nucleotides flanking a focal nucleotide, heavily influences its mutation rate. For example, mutation rate of a nucleotide flanked by upstream and downstream G:C could be 67.4 times higher in mutation rate than when flanked by A:T (Long et al., 2015). This might be caused by base-stacking and/or different Von der Waal forces, while no empirical test has been conducted yet. In addition to this local non-randomness, it was also observed that mutation rate in bacteria is distributed in a wave-like pattern, with peak mutation rate around the replication terminus and lowest mutation rate near the origin of the replication. Such observations have been confirmed in several bacteria species. This pattern is believed to be shaped by various factors, such as histone(-like) protein distribution, G/C content (Foster et al., 2013).

Because organisms differ dramatically in nucleotide composition, and because it was previously thought that all mutations are biased to the A/T direction, mutation bias was thus believed to be minor in determining the genomic nucleotide composition. However, recent studies on GC-rich bacteria, such as *Deinococcus radiodurans* and *Burkholderia cenocepacia*, demonstrated that some bacteria may be biased to the G/C direction, and that the A/T bias is not universal. Further, using high-power whole-genome mutation datasets especially from microbes, (Long et al., 2015) showed that mutation bias, together with natural selection and/or biased gene conversion, heavily influences the nucleotide composition of genomes. This refutes previous assertions that

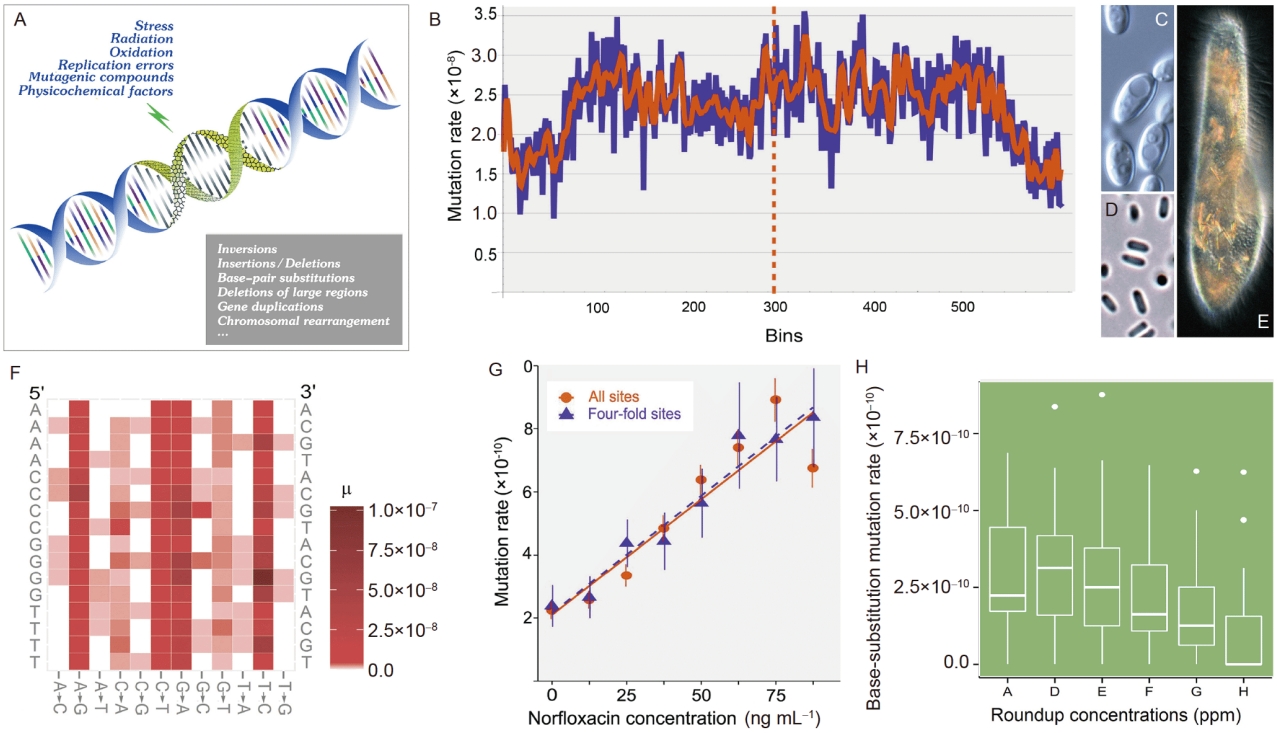

Figure 10 Spontaneous and environment-dependent mutations in organisms. A, Physiochemical factors causing mutations. B, Different mutation rate along genome (Long et al., 2015). C, The oil-producing yeast *Rhodotorula toruloides*. D, *E. coli*. E, *Paramecium biaurelia*. F, Mutation rate of nucleotides with different flanking nucleotides (Long et al., 2015). G, Norfloxacin elevates genome-wide mutation rate of *E. coli* (Long et al., 2016). H, The glyphosate-based herbicide Roundup does not elevate genomic mutation rate of *E. coli* (Tincher et al., 2017).

mutation is not important in the evolution of genome composition.

Environmentally induced mutations

We here define "environmental" as extracellular physiochemical conditions. Recent studies revealed genomic mutational response to some environmental changes: (i) as a result of global warming, increased atmospheric CO_2 makes seawater more and more acidic. Could this have any effect on the genomic stability of microbes in the sea? If so, how? In order to answer this question, (Strauss et al., 2017) designed a mutation accumulation experiment using *Vibrio shilonii*—a pathogen causing coral reef bleaching—cultured on agar plates with gradients of pH. The results showed a positive relationship between pH value and mutation rate, as well as decreased A/T mutation bias at lower pH. Increased DNA polymerase replication fidelity, and decreased cytosine deamination as pH drops, could account for these. (ii) Glyphosate-containing herbicide is one of the most popular herbicides in the world, although it has been speculated to be carcinogenic, drawing support from a previous claim that glyphosate is possibly mutagenic to microbial DNA. (Tincher et al., 2017) explored the mutagenic effect of the glyphosate-based herbicide Roundup on the model bacterium *Escherichia coli*. They did not find any mutation rate increase, even in cell lines treated with extremely high concentrations of Roundup, which thus casts doubts on WHO's premature conclusion of this most popular herbicide around the world. (iii) Influence of temperature on mutation rate is unresolved, with different conclusions from studies on different organisms (Ryan and Kiritani, 1959; Lindgren, 1972; Chu et al., 2018). (iv) Misuse or abuse of antibiotics causes resistance in pathogenic bacteria, and thus poses a great threat to human health. Spontaneous resistance mutations are known to be selected by antibiotic use. Could mutations also be induced by antibiotic use, and thus elevate resistance mutations? One study, using hundreds of *E. coli* mutation accumulation lines treated with the antibiotic norfloxacin, confirmed this speculation (Long et al., 2016). Antibiotic treatment elevated the genomic mutation rate, which was associated with low fidelity DNA polymerases expressed during stress response and reduced DNA mismatch repair efficiency. (v) Many metabolites may cause mutations, especially those oxidizing DNA strands or nucleotides, and they are strongly associated with culturing media. Media with stressors, such as missing certain nutrients, oxygen levels, can cause large variation in mutation rate, type, and/or spectrum of cultured microbes (Maharjan and Ferenci, 2017; Shewaramani et al., 2017). (vi) Ionizing or UV radiations could break DNA strands and elevate mutation rate of various types of mutations at whole-genome level (Adewoye et al., 2015; Shibai et al., 2017).

Unresolved questions about mutations

Recent studies have revealed interesting patterns based on directly accumulated mutations. However, some of the patterns do not have a clear explanation yet: (i) for mutation patterns, more information on quantifiable mutagenesis mechanisms is needed, such as G:C→A:T transitions of most A/T-biased organisms show higher mutation rate than A:T→G:C transitions. How are such uncommon structural variants generated, while the exact mechanisms accounting for these observations are scarce? (ii) Most previous mutation experiments were performed in lab environments. Do the results reflect mutational features of organisms in nature, where most physicochemical factors fluctuate? Also, most mutational studies used a limited number of strains, while a true mutation pattern of one species should include multiple strains to capture variation. (iii) New techniques for estimating mutation rate and spectrum need to be introduced, especially for rare and/or structural variant mutation detection. Current methods such as mutation accumulation experiments combined with whole-genome sequencing, require a tremendous amount of research resources, while most SV programs based on Illumina sequencing have high false positive rates, and so on. (iv) Mutagenic effects of temperature and biotic factors, such as competition and predation, should be further explored.

A newly developed ciliate model system: its life cycle, genome-wide rearrangement and stop codon reassignment (Figure 11)

Ciliated protists (ciliates) are the most morphologically complex and highly differentiated group among the unicellular eukaryotes (Gao et al., 2016; Song and Shao, 2017). They have emerged approximately one billion years ago, and are distributed in diverse habitats across the globe, even in extreme environments (Hu, 2014). Therefore, ciliates have evolved a wide variety of biological mechanisms to survive in different environments during their deep evolutionary history. Their distinguishing characteristics, e.g., high morphological diversity, unique nuclear dimorphism (containing both the germline and somatic nuclei within the single cell), multiple mating types during sexual reproduction (conjugation), and extensive genome rearrangement, have made ciliates excellent model organisms for studies on taxonomy, cytology, ecology, evolution, genomics, epigenetics, etc. (Chen et al., 2019; Gao et al., 2016; Hu et al., 2019; Song and Shao, 2017; Sheng et al., 2020; Wang et al., 2019; Xu et al., 2019).

Compared to the high diversity of ciliate species, our knowledge about ciliate biology is mostly limited to the studies using the model organisms, e.g., *Tetrahymena* and *Paramecium*, which are freshwater and less differentiated species. In fact, many more important and interesting phenomena and biological mechanisms are still unknown for other ciliates, especially for the large number of marine ciliates with high diversity and complexity (Hu et al., 2019). For example, euplotid ciliates (represented by *Euplotes* species) are the most highly differentiated and cosmopolitan group (Hu et al., 2019). They have extensively fragmented somatic genomes (Chen et al., 2019), the conventional stop codon UGA reassigned as cysteine (Meyer et al., 1991), high frequency of +1 programmed ribosomal frameshifting at stop codons (Wang et al., 2016), high-multiple mating type systems (Luporini et al., 2016), and strong resistance to environmental stressors (Trielli et al., 2007). However, the molecular mechanisms that account for these remarkable traits remain largely unknown. Therefore, it is necessary and significant to develop these biologically and ecologically important marine ciliates into model systems.

Recently, we developed the cosmopolitan marine ciliate *Euplotes vannus* into a model system, including isolation and culturing of different mating types, life cycle characterization, construction of a genome database, establishment of gene expression profile at different life stages and under varying conditions, exploration of genetic manipulation tools, etc. (Chen et al., 2019; Gao et al., 2020; Jiang et al., 2010; Jiang et al., 2019; Tang et al., 2020). This provides an important platform to explore the molecular mechanisms for a wide range of key biological phenomena. Here, we review some important features of *Euplotes* and compare these processes with those in other species.

Nucleus and cortical structure development during life cycles

Ciliates possess two structurally and functionally distinct nuclei within a single cell: the germline MIC, which is transcriptionally silent during vegetative growth, and the somatic MAC, which is transcriptionally active and controls the cell phenotype (Prescott, 1994). Ciliates can reproduce both asexually and sexually, and the two distinct nuclei function differently during reproduction. During the asexual reproduction, MIC undergoes mitosis while MAC divides by amitosis (except in the class Karyorelictea, in which macronuclei are unable to divide) (Song and Shao, 2017). During the sexual process, MIC undergoes meiosis and generates the gametic pronuclei, which are exchanged between the two mating partners. After mutual fertilization, the zygotic nucleus undergoes mitosis and the mitotic products develop into the new MIC and MAC, while the parental MAC degenerates (Raikov, 1982).

Details of the nuclear events during conjugation vary dramatically among ciliate species, with the differences mainly in (i) patterns of prezygotic and postzygotic nuclear divisions, and (ii) activities of the parental MAC during development of the new MAC (Raikov, 1982). For example, the conjugation process of *E. vannus* lasts about 75 h, in-

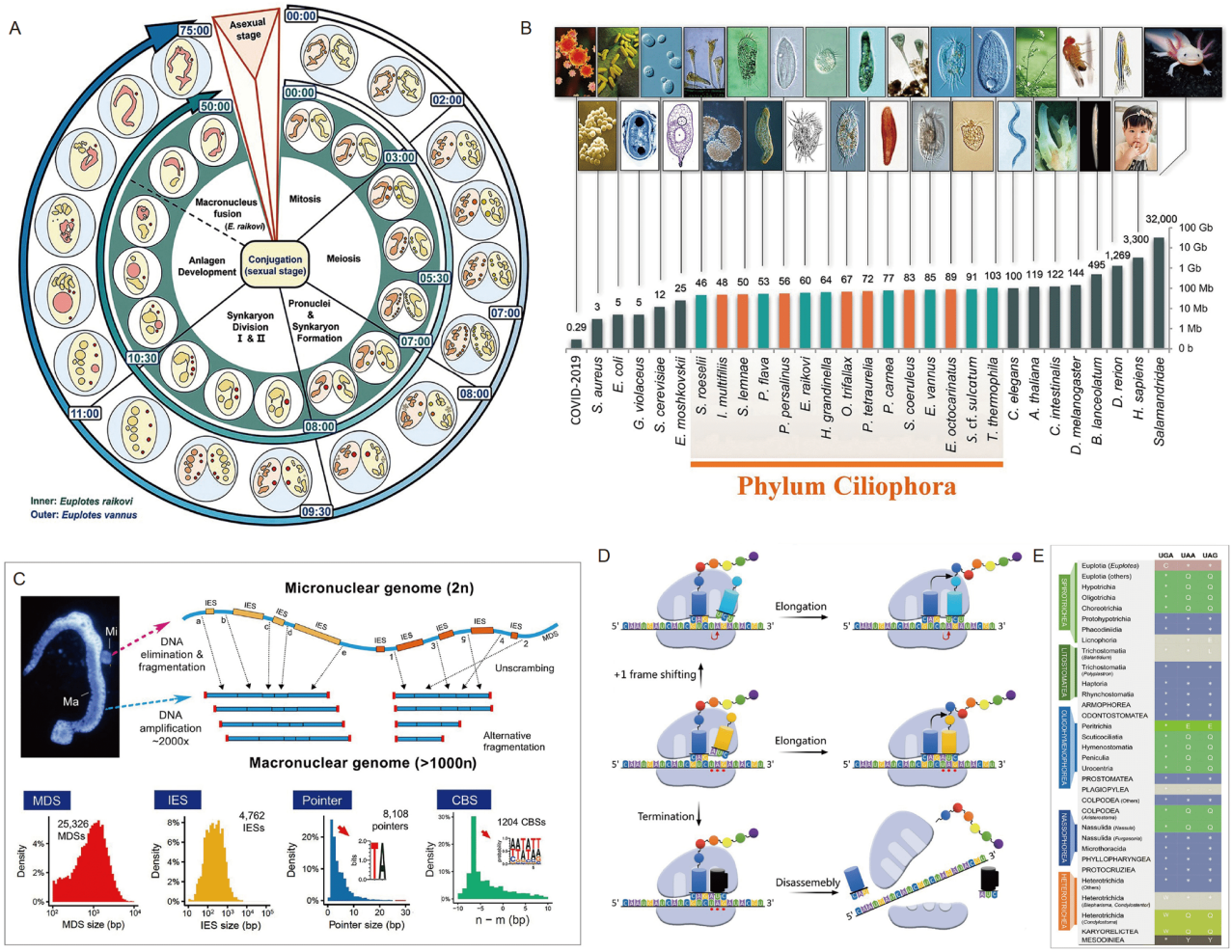

Figure 11 Some remarkable traits in the newly developed model system of ciliates. A, The life cycle of two *Euplotes* species focusing on timing of nuclear events. B, The genome size of some representative species. The data is mainly from GenBank. The genome of ciliates is indicated by their somatic macronuclear genome, with some unpublished data from Laboratory of Protozoology, OUC. C, Development of the *Euplotes* somatic macronuclear genome from the germline micronuclear genome, including chromosome fragmentation, DNA elimination, and DNA amplification. The size distribution of macronuclear destined sequences (MDS), internally eliminated sequences (IES), direct repeat at IESs boundaries (pointer) and chromosome breakage sites (CBS) of *Euplotes vannus* are provided. D, Schemes of translation process when the ribosome meets the stop codon UAG, it would be terminated in most organisms (bottom row), reassigned to amino acids in some ciliates (middle row) or +1 frameshift in *Euplotes* (top row). E, Stop codon usage among different ciliate groups shows high diversity and flexible patterns.

cluding three prezygotic MIC divisions (mitosis and meiosis I and II), and two postzygotic synkaryon divisions (Jiang et al., 2019). Three prezygotic divisions result in eight nuclei, two of which become gametic nuclei. After the exchange and fusion of the gametic nuclei, two of the four products of the postzygotic divisions differentiate into the new MIC and MAC, respectively. The parental MAC degenerates completely. In comparison, there could be four prezygotic divisions while the number of postzygotic divisions is highly variable in other ciliates (as reviewed in Jiang et al., 2019; Raikov, 1982). More interestingly, instead of being degenerated completely, in some ciliates some fragments of the parental MAC may regenerate and fuse with the developing new MAC (Gong et al., 2020). This indicates that the residual parental MAC plays important roles in the development of the new MAC, although the detailed molecular mechanisms are still unclear. More importantly, it has not been fully clarified how the same products of the last postzygotic division differentiate into the distinct germline and somatic nuclei within a single cell, though recent studies indicate that nucleus differentiation requires a biased assembly of the nuclear pore complex (Iwamoto et al., 2015).

The cortical structures are also regenerated dramatically in cells undergoing both asexual and sexual reproduction, which require complex mechanisms of gene expression and organelle differentiation. During asexual reproduction in *E. vannus*, the oral primordium of the proter is inherited from the parent, while that of the opisthe develops *de novo*. The frontal, ventral, and transverse cirri develop separately in both progenies; the marginal cirri are formed *de novo*. The

dorsal kinety anlagen occur within the parental structures at mid-body, and the caudal cirri are generated from the rightmost two to four old dorsal kineties (Jiang et al., 2010). The morphogenetic process during conjugation is even more complex, since the cortical structures in the ventral side reorganize twice. The first round of morphogenesis generates an incomplete ventral structure (missing the posterior part of the adoral zone of membranelles, the leftmost frontal cirrus and paroral membrane), which will be then completed by the second reorganization (Gao et al., 2020). A limited number of studies reveal that the patterns of morphogenesis during sexual reproduction, vary dramatically among ciliates (as reviewed in Gao et al., 2020). Molecular mechanisms underlying this complex process are still waiting for further investigations.

Genome-wide rearrangements from germline to somatic genome during conjugation

As mentioned above, ciliates possess two distinct nuclei in each cell, whose genome structures are significantly different. Up to now, the somatic MAC genome of more than 20 species and the germline MIC genome of only three species have been well sequenced (Chen et al., 2014; Sheng et al., 2020). The MAC genome size of the available ciliates varies from 46 to 103 Mb, while the MIC genome size varies from 100 to 500 Mb. The significant difference between MAC and MIC genomes results from the extensive DNA rearrangements during MAC development after conjugation, including chromosome fragmentation, DNA elimination, and DNA amplification (Allen and Nowacki, 2017; Noto and Mochizuki, 2017; Gao et al., 2015).

Euplotes vannus is one of the ciliates that perform the most exaggerated DNA rearrangements (Chen et al., 2019). Its MAC genome is extensively fragmented, containing more than 25,000 complete "gene-sized" nanochromosomes (~85 Mb haploid genome size) with an average size around 1.5 kb and telomeric repeats of C_4A_4. Only a small proportion of chromosomes (744 out of the 25,519) were found to contain more than one gene. Moreover, the introns (mostly 25 bp in length) and untranscribed regions (average 27 bp of 5′ untranscribed region (UTR) and 242 bp of 3′ UTR) are noticeably short, indicating a streamlined and efficient MAC genome. The chromosome breakage sites (CBSs), where fragmentation generally occurs, are 6 bp long and AT-rich. Their flanking regions are in an overall palindrome structure with a more conserved sequence element of 5′-TTGAA-3′ beginning at 12 bp from the CBSs. Chromosome breakage involves a 6 bp staggered cut at the CBSs, which are filled-in prior to, or during the process of telomere addition, resulting in the duplication and retention of the CBSs in the MAC genome (Chen et al., 2019; Klobutcher et al., 1998). The extensive fragmentation (with "gene-sized" nanochromosomes) has been found to occur in members of three separate ciliate classes, Spirotrichea (including *Euplotes*, *Oxytricha*, *Stylonychia*, *Uroleptopsis*), Phyllopharyngea (e.g., *Chilodonella*), and Armophorea (e.g., *Metopus*). This demonstrates multiple origins within ciliates (Riley and Katz, 2001).

Besides chromosome fragmentation, another important event during MAC development is DNA elimination, which involves the excision of thousands of interstitial DNA segments (internally eliminated sequences, IESs). The types of DNA elimination during macronuclear development are quite diverse, both within a given ciliate species and among different ciliates. In *Euplotes*, IESs consist of both short (<600 bp) unique DNA sequences and large families of transposable elements (Tec elements) (Jacobs and Klobutcher, 1996). The sequence motif 5′-TA-3′ is highly conserved at nearly all IESs boundaries in the MIC genome. A number of IESs reside within coding regions, therefore IESs excision is precise. After excision, a single TA direct repeat is retained in the MAC DNA molecules, which is similar to the process of chromosome fragmentation (Chen et al., 2019).

The genome-wide DNA rearrangement during macronuclear development has been observed in all the ciliates examined. However, the rearrangement patterns and mechanisms are highly diversified among different ciliates, e.g., the extent of chromosomal fragmentation varying from limited to extensive, the percentage of IESs ranging from 30%–95%, precise or imprecise excision, etc. (Allen and Nowacki, 2017; Chen et al., 2014; Noto and Mochizuki, 2017). The mechanisms underlying the genome rearrangement have been studied in three ciliate species (*Paramecium*, *Tetrahymena* and *Oxytricha*). Though these mechanisms are all mediated by trans-generational comparison between the MIC and the maternal MAC genome through an RNA-mediated epigenetic mechanism, the pathways differ a lot from each other. The mechanism in *Euplotes* is still unknown. Considering that the chromosomal fragmentation in *Euplotes* is similar to that in *Oxytricha* while its DNA elimination resembles *Paramecium*, we believe that the mechanism in *Euplotes* would be distinctive. Revealing this mechanism would enhance understanding of the dynamic nature of genomes, and provide new insights into the complex process of trans-generational programming of chromosomal rearrangements.

Stop codon reassignment and high frequency of programed ribosome frameshifting

The eukaryotic nuclear genetic code was previously thought to be largely frozen and unambiguous, with 61 codons encoding 20 amino acids, and the remaining three codons (UAA, UAG and UGA) as termination signals for translation. The exceptions to the universal usage of nuclear genetic codes were first reported in ciliates, where the standard stop codons UAA and UAG are reassigned to glutamine while

only UGA is used as stop codon (Caron and Meyer, 1985). Subsequently, additional stop codon reassignments were discovered in other ciliates, showing high diversity and flexible patterns: (i) UAR encodes glutamine (Caron and Meyer, 1985), glutamate (Heaphy et al., 2016), or tyrosine (Johnson et al., 2004) while UGA is the stop codon; (ii) UGA encodes cysteine (Meyer et al., 1991) or tryptophan (Lozupone et al., 2001), while UAR is stop codons; (iii) UAG and UGA encode glutamine, while UAA is stop codon (Yan et al., 2019); (iv) all three standard stop codons can either code for amino acids, or terminate translation in a context-dependent manner (Swart et al., 2016). This indicates that the standard stop codons have been reassigned independently many times in different ciliate lineages.

Euplotes species are the only linage reported to translate UGA as cysteine while they use UAA and UAG for termination (Meyer et al., 1991; Chen et al., 2019). As *Euplotes* is one of the spirotrichous groups that mainly use UAR to encode glutamine and UGA as stop codon, the evolution of the *Euplotes* code is from an ancestor that either used UAR to encode glutamine or used a standard code. The former scenario requires loss of extra glutamine tRNAs, eukaryotic release factor 1 (eRF1) mutations that decrease UAR readthrough and increase UGA readthrough, and mutations enabling a $tRNA^{Cys}$ to read UGA. The latter scenario requires eRF1 mutations to increase UGA readthrough, and mutations enabling a $tRNA^{Cys}$ to read UGA. It is reported that *Euplotes octocarinatus* only has one type of $tRNA^{Cys}$ with a GCA anticodon, which requires a G:A mispairing in the first anticodon position to translate UGA (Grimm et al., 1998). Therefore, the latter scenario seems more likely to occur.

In addition to *Euplotes* terminating translation with UAA and UAG, they also evolve programmed ribosomal frameshifting (PRF)-reading through the stop codons UAA and UAG residing in the coding regions (Klobutcher and Farabaugh, 2002). PRF is an important recoding mechanism to regulate the expression of many genes, with the most common type of −1 and +1 frameshift. The highest frequency of +1 PRF events are detected in *Euplotes* species, occurring at the sites with a canonical motif of 5′-AAA-UAR-3′ (Chen et al., 2019; Lobanov et al., 2017; Wang et al., 2016). Some +2 and −1 PRF events were also found in *Euplotes* (Chen et al., 2019). A putative suppressor tRNA of UAA was reported in *E. octocarinatus*, which was proposed to decode four nucleotides when the ribosome meets the slippery stop codon, and plays an important role in +1 frameshifting (Wang et al., 2016). No strong evidence of the presence of "suppressor" tRNAs was found in other *Euplotes* species (Chen et al., 2019). The mechanism underlying +1 PRF is still largely unknown.

However, *Euplotes* is the only ciliate group in which frameshifting was detected, though ciliates evolved a diversified and flexible nuclear genetic code from their ancestors. For most ciliates, UGA remains as a stop codon while UAR is reassigned to code amino acids, which is opposite in *Euplotes*. Instead of reassigning UAR to amino acids, *Euplotes* utilizes PRF to avoid the premature stops. It is also proposed that the default function of stop codons in *Euplotes* is ribosomal frameshifting, and its function for termination is determined by its proximity to poly(A) tails (Lobanov et al., 2017). This would be much more robust when the MAC genome is extensively fragmented to nanochromosomes with a short 3′ UTR, where stop codons might even be unnecessary.

Evo-Devo and adaptation to the global climate change in marine model nematode (Figure 12)

Nematodes represent about 80% of the number of multicellular animals in numbers on the earth, and are distributed in almost all ecological niches, from terrestrial soil to the ocean (Cao and Zhang, 2018; Eisenhauer and Guerra, 2019; van den Hoogen et al., 2019; Xie et al., 2020). The phylum Nematoda comprises more than 25,000 described species, and as many as one million species still need to be described (Hugot et al., 2001; Abad et al., 2008). More than half of the described species are free-living and feed on bacteria, fungi, or algae, but there are also many species that parasitize animals or plants (Kikuchi et al., 2017). More than 4,100 and 5,000 species of plant and animal-parasitic nematodes, respectively, have been documented to date (Kikuchi et al., 2017). Over two billion humans are infected with parasitic nematodes (International Helminth Genomes Consortium, 2019; Else et al., 2020), and parasitic nematodes also cause diseases in domesticated animals, marine fishes, and crop plants, resulting in hundreds of billions of dollars economic loss every year (Abad et al., 2008; Cao and Zhang, 2018). Collectively, nematodes not only play major roles in terrestrial and ocean ecosystems, but also cause significant parasitic infections in humans, animals, and plants.

Establishment of a terrestrial-marine relative nematodes pair model for developmental evolution and environmental adaptation

C. elegans is widely used as a biomedical model organism. Its short life span, ease of handling and maintenance, clear genetic background and advanced genetic and molecular biology tools together, make *C. elegans* a powerful model to study development, neurobiology, longevity, and stress responses (Zhang et al., 2015b; Cong et al., 2020b). During the 20th century, the transition in biology from description to mechanistic understanding was largely due to widely employed model organisms (Russell et al., 2017). Therefore, the terrestrial soil nematode *C. elegans* became one of the most successful model animals from the 1970s (Zhang et al., 2015b). However, there are no marine nematode models

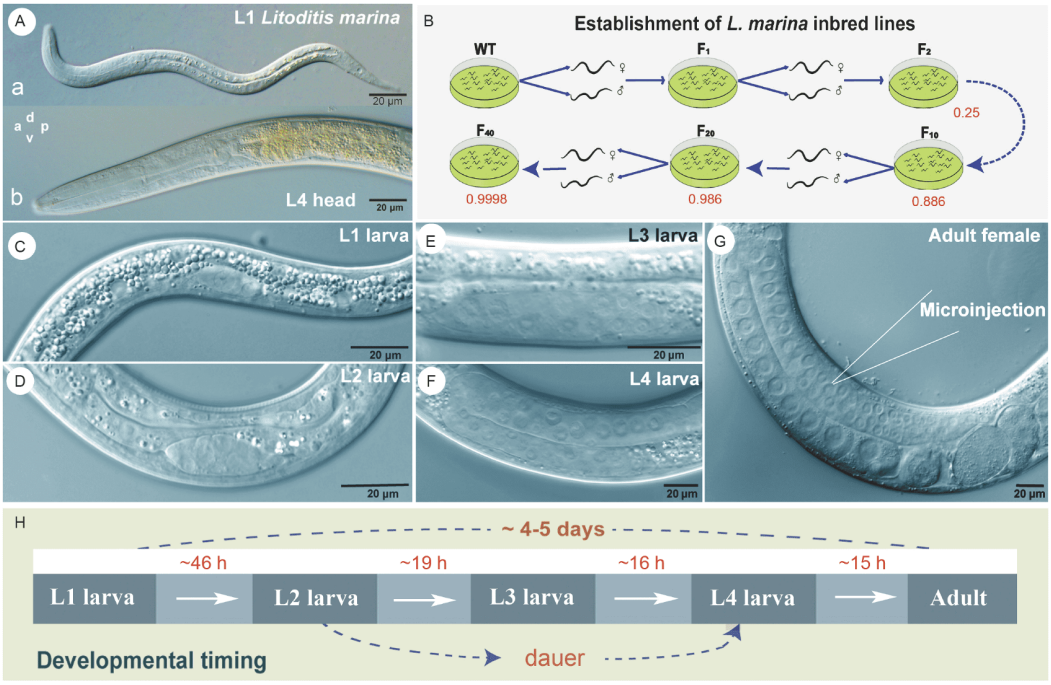

Figure 12 Morphology, inbred lines and developmental characteristics of marine nematode *Litoditis marina*. A, Differential interference contrast (DIC) images of *L. marina* L1 developmental stage larva and head of L4 larva. B, Carton illustration of construction of the first marine nematode inbred lines. C–G, Gonad development of *L. marina*. C, L1 larva developmental stage. D, L2 larva developmental stage. E, L3 larva developmental stage. F, L4 larva developmental stage. G, Adult female and the microinjection site illustration. H, *L. marina* developmental timing. A, anterior; D, dorsal; P, posterior; V, ventral.

available, and all the major, widely used, advanced model organisms are almost all from the terrestrial niche (Arendt and Extavour, 2016; Russell et al., 2017; Xie et al., 2020).

Oceans cover about 71% of the Earth's surface and represent almost 99% of available habitats. Major physical and chemical differences between terrestrial soil and marine sediments include salinity, temperature variation, oxygen concentration, and pH (Peng et al., 2020a). How close relatives from the same animal phylum, or even the same family, adapt to their respectively marine and terrestrial physical and chemical environments, is a key question in life science. However, the underlying mechanisms are largely unknown. In marine sediments, free-living nematodes contribute about 70%–90% to the abundance of meiofauna (Higgins and Thiel, 1988), playing key roles in the benthic ecosystems. There are about 6,900 described free-living nematode species in the ocean, and the number of parasitic marine nematode species is about 4,500 (Appeltans et al., 2012). Molecular mechanisms underlying their developmental regulation and environmental adaptation remain poorly understood. The first emerging marine model nematode, *Litoditis marina*, has recently been developed in our research group (Xie et al., 2020).

The bacterivorous marine nematode *L. marina* (Bastian, 1865) is widely distributed on coasts all over the world (Derycke et al., 2016). Our research group constructed the first inbred lines of the free-living marine nematode *L. marina*, sequenced and assembled its genome, and successfully applied CRISPR/Cas9 genome editing in *L. marina* (Xie et al., 2020). In addition, we characterized full-length transcriptomes of different developmental stages in *L. marina*. With a short generation time (4–5 days), highly inbred lines, and the comprehensive genetic and genomic resources developed in our group, *L. marina* is now a promising marine animal model, and a unique satellite model to the well-known biomedical nematode *C. elegans* (Xie et al., 2020).

Nematode developmental evolution and response to global climate and environment change

Life on our planet originated in oceans about 4 billion years ago, and nematodes originated from a marine habitat during the Cambrian Explosion (van Megen et al., 2009). They colonized land about 100 million years later (Rota-Stabelli et al., 2013). *L. marina* and *C. elegans* belong to the same family, *Rhabditidae*, and they are morphologically quite similar (Figure 12A, Xie et al., 2020). We found that *C. elegans* could not survive in 30‰ salinity conditions, which is equivalent to the medium sea water salinity, while the marine nematode *L. marina* could survive in a 60‰ salinity environment. Ninety-two conserved genes appear to be positively selected in *L. marina* compared to terrestrial nematodes, which may underpin the osmotic and other environmental changes in the marine nematode (Xie et al., 2020). Surprisingly, ecdysone receptor (EcR) and Retinoid X

receptor (RXR), which are reported in insects and filarial parasitic nematodes as major players in molting and development, are found in *L. marina*, while absent in most free-living nematodes (Xie et al., 2020). As nematodes and farmed shrimp and prawns belong to Ecdysozoa, *L. marina* is therefore a promising model for gene function verification in marine shrimps and crabs. It is also a unique model to develop economic traits, such as resistance to infections and a faster growth rate in shrimp and prawn breeding programs, boosting seafood production (Xie et al., 2020). Therefore, our work will provide a strong platform to facilitate ongoing work on animal development, environmental adaptation, utilization of marine biological resources, as well as mechanisms underlying evolution from the ocean to land or *vice versa*.

Global climate change leads to major variations in the ocean, such as temperature increase, ocean acidification and hypoxia; causing severe negative impacts on marine organisms and ecosystems. How animals respond and adapt to the acidic pH and other stresses, is a key question in marine life science and ecology. However, the underlying mechanisms are largely unexplored. Recently, we employed RNA-Seq (RNA Sequencing) to ask how the terrestrial nematode *C. elegans* and the marine nematode *L. marina* respond to the acidic pH stresses, respectively (Cong et al., 2020b; Cong et al., 2020a). Two major response strategies to the reduced pH were found in *C. elegans*. First, cuticle structure and integrity genes were significantly upregulated when the pH decreased from 6.33 to 4.33, where 6.33 is the optimal culture pH for *C. elegans*. Second, to deal with even lower acidic pH stress, *C. elegans* accelerated their xenobiotics metabolism by a large number of cytochrome P450 pathway genes (Cong et al., 2020b). *C. elegans* is able to grow into an adult and lay eggs at pH 3.13, while *L. marina* is unable to develop into adulthood at pH 4.33, appearing to be more vulnerable to acidic stress, and the number of increased P450 pathway genes in acidic pH is much lower than in *C. elegans* (Cong et al., 2020a; Cong et al., 2020b). Consistent with our comparative genomics analysis, the detoxification of the xenobiotics P450 pathway genes is significantly contracted in the marine nematode *L. marina* compared to its land relatives (Xie et al., 2020). Therefore, we speculate that the cytochrome P450 pathway gene contraction in *L. marina* might explain its lower tolerance to acidic environments. CRISPR/Cas9 genome editing and overexpressing of candidate P450 genes are employed in our laboratory, to identify the master gene(s) responding and adapting to acidic pH stress in nematodes. If the master gene identified in nematodes is conserved in severely damaged invertebrate species such as coral, it might provide solutions to generate novel genotypes via genome editing, in order to restore coral bleaching and coral reef ecosystems in the context of acidic and thermal stresses from natural and anthropogenic climate and environmental changes.

"Simple" model organisms such as *L. marina* are an extraordinary test case to determine the following scientific questions in the field of marine life science. What is the cell lineage from a fertilized egg to an adult with about 1,000 somatic cells in a marine invertebrate? How are neurons structurally and functionally connected in a marine nematode with about 300 neurons? Are cell lineage and connectome characteristics determining factors of adaptation of the animal to a marine environment? How are marine nematodes developmentally regulated in the context of global climate change? What are the molecular mechanisms underlying Eco-Evo-Devo between nematodes and their survival in dynamic environments? We believe that the relations between the marine and terrestrial nematode model system will provide novel solutions to the above questions.

Perspectives for future biodiversity-based Evo-Devo studies

So far, the majority of our knowledge of natural embryonic development is based on studies using classical model organisms. Increasing evidence, however, has indicated that the developmentally regulatory mechanisms are not always consistent across the animal kingdom. The entire blueprint of organismal embryogenesis mechanisms is far beyond the outcomes of studying a few model systems. The necessity of studies in non-model organisms is noticeably clear. Applying the new methods on non-model organisms makes it possible to resolve the contradiction between limited regulatory mechanisms from model organisms and the vivid biodiversity on the planet. For example, rapid developing and updated single-cell sequencing techniques provide the possibility to perform linage-tracing at the single-cell resolution, and thus clarify evolutionary relationships of various cells in a developing embryo. CRISPR/Cas9 systems make gene editing and transgenesis feasible, improving the availability of microscopic imaging and optogenetics applications in non-model organisms. In addition, biomechanics is becoming an emerging research paradigm on approaching morphogenesis, and this high -yielding field added a new dimension to understanding developmental processes. New techniques, such as laser cutting, aspiration by pipetting, tissue deformation by magnetic fields and optical tweezers, offer reliable ways to probe the tissue material properties and mechanical status. Combined with biophysical theory, biomechanics will deepen our insight on how an embryo organizes itself.

Regarding regeneration and genetically regulatory signaling and considering the high complexity of biological events including organ regeneration, construction of a dynamic network of genetic regulations could be an efficient and necessary approach to decipher phenotypes from cell/tissue

levels to whole organ/organism levels. This network includes, but is not limited to, epigenetic modifications, signaling pathways, transduction cascade and crosstalk, control of downstream transcriptional activity, and subcellular structure changes. Actually, studies of regeneration and genetic regulation to date are mainly conducted using well-established model systems, such as *Drosophila*, zebrafish, and mouse, which offer unique advantages with plentiful availability of genetic tools and massive knowledge generated from many years of investigation. However, to fully address how these biological processes occur and diversify among species during evolution, a wide variety of non-model organisms needs to be explored. Gathering information from non-model organisms based on the robust developed approaches of multi-omics, analyzing the massive data relying on advanced techniques of "Big Data Analytics" and "Machine Learning", and developing new genetic tools are the crucial steps. Cross-species analysis to discover conserved key components and effective factors, therefore, will be an important step toward unraveling these complicated biological processes. In general, a feasible strategy would be to perform functional validation using model organisms to identify pivotal determinators predicted from the exploration of non-model organisms. To the community, studies integrating the model and non-model organisms will empower researchers to understand the breadth of regeneration and the depth of the genetic regulation mechanisms across the animal kingdom, and to develop possible clinical methods for recapitulating the regenerative capacities in humans.

On the aspects of environmental adaptation and evolutionary studies, we have shown that various marine organisms provide deep insights into several evolutionary mechanisms, including mutation, HGT, genome rearrangement, adaptation to a changing environment, etc. Future evolutionary studies would never be limited to these topics since new techniques and findings are being reported in these emerging non-model organisms. Further topics could be broader, more systematic, and mathematic, for an example, population genetics-based evolution, which would utilize computational models taking multiple forces into account, such as mutation, selection, genetic drift, migration, recombination, etcetera. With more and more genomic and bioinformatic tools developed, and most marine organisms being truly cosmopolitan, population genetic models combined with big data could precisely reveal gene flow, population connectivity, introgression, speciation, and other forces that shape the genetic diversity of marine life.

There is little debate that life originates from the ocean, and it is widely accepted that marine eukaryotes exhibit amazing diversity. However, it is clear that research on marine organisms is far behind research using model organisms such as mouse, fruit fly, zebrafish, yeast, and so on, while policymakers, especially those in China, have fully realized the importance of the ocean in economy, ecology, international relationships, etc. Thus, more resources have been invested into scientific research, which provides great opportunities to explore large-scale evolutionary questions. By taking advantage of this, the investigation of non-model organisms, including the introduction of marine model organisms, would reach a golden age and make more contributions to evolutionary studies.

Compliance and ethics *The author(s) declare that they have no conflict of interest.*

Acknowledgements *This work was supported by the National Natural Science Foundation of China (31771649, 32030015, 31772442, 31970506, 31922013, 32070437, 31872228, 31970475, and 31991194), the National Key Research and Development Program of China (2019YFE0190900), the Young Taishan Scholar, and Taishan Scholar Program of Shandong Province, China. Thanks are given to Ms. Tian Gan, graduate student of IEMB, Ocean University of China, for some line drawings in Figure 7. We apologize to all our colleagues whose original studies could not be cited due to space limitations.*

References

Abad, P., Gouzy, J., Aury, J.M., Castagnone-Sereno, P., Danchin, E.G.J., Deleury, E., Perfus-Barbeoch, L., Anthouard, V., Artiguenave, F., Blok, V.C., et al. (2008). Genome sequence of the metazoan plant-parasitic nematode *Meloidogyne incognita*. Nat Biotechnol 26, 909–915.

Abitua, P.B., Wagner, E., Navarrete, I.A., and Levine, M. (2012). Identification of a rudimentary neural crest in a non-vertebrate chordate. Nature 492, 104–107.

Adewoye, A.B., Lindsay, S.J., Dubrova, Y.E., and Hurles, M.E. (2015). The genome-wide effects of ionizing radiation on mutation induction in the mammalian germline. Nat Commun 6, 6684.

Allen, S.E., and Nowacki, M. (2017). Necessity is the mother of invention: ciliates, transposons, and transgenerational inheritance. Trends Genet 33, 197–207.

Alvers, A.L., Ryan, S., Scherz, P.J., Huisken, J., and Bagnat, M. (2014). Single continuous lumen formation in the zebrafish gut is mediated by smoothened-dependent tissue remodeling. Development 141, 1110–1119.

Ammermann, D., Steinbrück, G., Baur, R., and Wohlert, H. (1981). Methylated bases in the DNA of the ciliate *Stylonychia mytilus*. Eur J Cell Biol 24, 154–156.

Amores, A., Force, A., Yan, Y.L., Joly, L., Amemiya, C., Fritz, A., Ho, R. K., Langeland, J., Prince, V., Wang, Y.L., et al. (1998). Zebrafish hox clusters and vertebrate genome evolution. Science 282, 1711–1714.

Andersson, J.O. (2009). Gene transfer and diversification of microbial eukaryotes. Annu Rev Microbiol 63, 177–193.

Appeltans, W., Ahyong, S.T., Anderson, G., Angel, M.V., Artois, T., Bailly, N., Bamber, R., Barber, A., Bartsch, I., Berta, A., et al. (2012). The magnitude of global marine species diversity. Curr Biol 22, 2189–2202.

Arendt, D., and Extavour, C. (2016). Editorial overview: developmental mechanisms, patterning and evolution: new models for genetics and development—diversity at last. Curr Opin Genet Dev 39, iv–vi.

Aziz, R.K., Bartels, D., Best, A.A., DeJongh, M., Disz, T., Edwards, R.A., Formsma, K., Gerdes, S., Glass, E.M., Kubal, M., et al. (2008). The RAST server: rapid annotations using subsystems technology. BMC Genomics 9, 75.

Baer, M.M., Chanut-Delalande, H., and Affolter, M. (2009). Cellular and molecular mechanisms underlying the formation of biological tubes. Curr Top Dev Biol 89, 137–162.

Ball, S.G., Bhattacharya, D., and Weber, A.P.M. (2016). Pathogen to

powerhouse. Science 351, 659–660.
Barrio, L., and Milán, M. (2020). Regulation of anisotropic tissue growth by two orthogonal signaling centers. Dev Cell 52, 659–672.e3.
Basler, K., and Struhl, G. (1994). Compartment boundaries and the control of *Drosopfiffa* limb pattern by *hedgehog* protein. Nature 368, 208–214.
Beh, L.Y., Debelouchina, G.T., Clay, D.M., Thompson, R.E., Lindblad, K. A., Hutton, E.R., Bracht, J.R., Sebra, R.P., Muir, T.W., and Landweber, L.F. (2019). Identification of a DNA N^6-adenine methyltransferase complex and its impact on chromatin organization. Cell 177, 1781–1796.e25.
Beisaw, A., Kuenne, C., Guenther, S., Dallmann, J., Wu, C.C., Bentsen, M., Looso, M., and Stainier, D.Y.R. (2020). AP-1 contributes to chromatin accessibility to promote sarcomere disassembly and cardiomyocyte protrusion during zebrafish heart regeneration. Circ Res 126, 1760–1778.
Bejsovec, A. (2018). Wingless signaling: a genetic journey from morphogenesis to metastasis. Genetics 208, 1311–1336.
Ben-Zvi, D., Pyrowolakis, G., Barkai, N., and Shilo, B.Z. (2011). Expansion-repression mechanism for scaling the Dpp activation gradient in *Drosophila* wing imaginal discs. Curr Biol 21, 1391–1396.
Bergmann, O., Bhardwaj, R.D., Bernard, S., Zdunek, S., Barnabé-Heider, F., Walsh, S., Zupicich, J., Alkass, K., Buchholz, B.A., Druid, H., et al. (2009). Evidence for cardiomyocyte renewal in humans. Science 324, 98–102.
Bergmann, O., Zdunek, S., Felker, A., Salehpour, M., Alkass, K., Bernard, S., Sjostrom, S.L., Szewczykowska, M., Jackowska, T., Dos Remedios, C., et al. (2015). Dynamics of cell generation and turnover in the human heart. Cell 161, 1566–1575.
Bhattachan, P., Rae, J., Yu, H., Jung, W.R., Wei, J., Parton, R.G., and Dong, B. (2020). Ascidian caveolin induces membrane curvature and protects tissue integrity and morphology during embryogenesis. FASEB J 34, 1345–1361.
Bhattacharya, D., and Price, D.C. (2020). The algal tree of life from a genomics perspective. In: Larkum, A.W.D., Grossmann, A.R., and Raven, J.A., eds. Photosynthesis in Algae: Biochemical and Physiological Mechanisms. Heidelberg: Springer International Publishing. 11–24.
Billon, P., and Côté, J. (2012). Precise deposition of histone H2A.Z in chromatin for genome expression and maintenance. Biochim Biophys Acta 1819, 290–302.
Bird, A. (1992). The essentials of DNA methylation. Cell 70, 5–8.
Bird, A. (2002). DNA methylation patterns and epigenetic memory. Genes Dev 16, 6–21.
Boswell, C.W., and Ciruna, B. (2017). Understanding idiopathic scoliosis: a new zebrafish school of thought. Trends Genet 33, 183–196.
Boulan, L., Milán, M., and Léopold, P. (2015). The systemic control of growth. Cold Spring Harb Perspect Biol 7, a019117.
Bourlat, S.J., Juliusdottir, T., Lowe, C.J., Freeman, R., Aronowicz, J., Kirschner, M., Lander, E.S., Thorndyke, M., Nakano, H., Kohn, A.B., et al. (2006). Deuterostome phylogeny reveals monophyletic chordates and the new phylum Xenoturbellida. Nature 444, 85–88.
Bracht, J.R., Perlman, D.H., and Landweber, L.F. (2012). Cytosine methylation and hydroxymethylation mark DNA for elimination in *Oxytricha trifallax*. Genome Biol 13, R99.
Bray, S.J. (2006). Notch signalling: a simple pathway becomes complex. Nat Rev Mol Cell Biol 7, 678–689.
Breiling, A., and Lyko, F. (2015). Epigenetic regulatory functions of DNA modifications: 5-methylcytosine and beyond. Epigenet Chromatin 8, 24.
Bryant, D.M., Johnson, K., DiTommaso, T., Tickle, T., Couger, M.B., Payzin-Dogru, D., Lee, T.J., Leigh, N.D., Kuo, T.H., Davis, F.G., et al. (2017). A tissue-mapped axolotl de novo transcriptome enables identification of limb regeneration factors. Cell Rep 18, 762–776.
Burke, R., and Basler, K. (1996). Dpp receptors are autonomously required for cell proliferation in the entire developing *Drosophila* wing. Development 122, 2261–2269.
Cano-Martinez, A., Vargas-Gonzalez, A., Guarner-Lans, V., Prado-Zayago, E., Leon-Oleda, M., and Nieto-Lima, B. (2010). Functional and structural regeneration in the axolotl heart (*Ambystoma mexicanum*) after partial ventricular amputation. Arch Cardiol Mex 80, 79–86.
Cao, C., Lemaire, L.A., Wang, W., Yoon, P.H., Choi, Y.A., Parsons, L.R., Matese, J.C., Wang, W., Levine, M., and Chen, K. (2019). Comprehensive single-cell transcriptome lineages of a proto-vertebrate. Nature 571, 349–354.
Cao, X.W., and Zhang, L.S. (2018). Application advances and prospects of CRISPR/Cas9 genome editing in nematodes (in Chinese). Sci Sin Vitae 48, 513–520.
Caprile, T., Hein, S., Rodrıguez, S., Montecinos, H., and Rodrıguez, E. (2003). Reissner fiber binds and transports away monoamines present in the cerebrospinal fluid. Mol Brain Res 110, 177–192.
Cardoso, A.C., Lam, N.T., Savla, J.J., Nakada, Y., Pereira, A.H.M., Elnwasany, A., Menendez-Montes, I., Ensley, E.L., Bezan Petric, U., Sharma, G., et al. (2020a). Mitochondrial substrate utilization regulates cardiomyocyte cell-cycle progression. Nat Metab 2, 167–178.
Cardoso, A.C., Pereira, A.H.M., and Sadek, H.A. (2020b). Mechanisms of neonatal heart regeneration. Curr Cardiol Rep 22, 33.
Caron, F., and Meyer, E. (1985). Does *Paramecium primaurelia* use a different genetic code in its macronucleus? Nature 314, 185–188.
Cavalier-Smith, T. (2017). Kingdom Chromista and its eight phyla: a new synthesis emphasising periplastid protein targeting, cytoskeletal and periplastid evolution, and ancient divergences. Protoplasma 255, 297–357.
Chablais, F., Veit, J., Rainer, G., and Jaźwińska, A. (2011). The zebrafish heart regenerates after cryoinjury-induced myocardial infarction. BMC Dev Biol 11, 21.
Chalker, D.L., and Yao, M.C. (2001). Nongenic, bidirectional transcription precedes and may promote developmental DNA deletion in *Tetrahymena thermophila*. Genes Dev 15, 1287–1298.
Chan, S.J., Cao, Q.P., and Steiner, D.F. (1990). Evolution of the insulin superfamily: cloning of a hybrid insulin/insulin-like growth factor cDNA from amphioxus. Proc Natl Acad Sci USA 87, 9319–9323.
Chaudhary, V., Hingole, S., Frei, J., Port, F., Strutt, D., and Boutros, M. (2019). Robust Wnt signaling is maintained by a Wg protein gradient and Fz2 receptor activity in the developing *Drosophila* wing. Development 146, dev174789.
Chen, X., Bracht, J.R., Goldman, A.D., Dolzhenko, E., Clay, D.M., Swart, E.C., Perlman, D.H., Doak, T.G., Stuart, A., Amemiya, C.T., et al. (2014). The architecture of a scrambled genome reveals massive levels of genomic rearrangement during development. Cell 158, 1187–1198.
Chen, X., Jiang, Y., Gao, F., Zheng, W., Krock, T.J., Stover, N.A., Lu, C., Katz, L.A., and Song, W. (2019). Genome analyses of the new model protist *Euplotes vannus* focusing on genome rearrangement and resistance to environmental stressors. Mol Ecol Resour 19, 1292–1308.
Chen, Z. (2019). The formation of the Thickveins (Tkv) gradient in *Drosophila* wing discs: a theoretical study. J Theor Biol 474, 25–41.
Cheng, T., Wang, Y., Huang, J., Chen, X., Zhao, X., Gao, S., and Song, W. (2019). Our recent progress in epigenetic research using the model ciliate, *Tetrahymena thermophila*. Mar Life Sci Technol 1, 4–14.
Chicoine, L.G., and Allis, C.D. (1986). Regulation of histone acetylation during macronuclear differentiation in *Tetrahymena*: evidence for control at the level of acetylation and deacetylation. Dev Biol 116, 477–485.
Cho, E., and Irvine, K.D. (2004). Action of fat, four-jointed, dachsous and dachs in distal-to-proximal wing signaling. Development 131, 4489–4500.
Choi, J.Y., Bubnell, J.E., and Aquadro, C.F. (2015). Population genomics of infectious and integrated *Wolbachia pipientis* genomes in *Drosophila ananassae*. Genome Biol Evol 7, 2362–2382.
Chu, X.L., Zhang, B.W., Zhang, Q.G., Zhu, B.R., Lin, K., and Zhang, D.Y. (2018). Temperature responses of mutation rate and mutational spectrum in an *Escherichia coli* strain and the correlation with metabolic rate. BMC Evol Biol 18, 126.
Cloney, R.A. (1982). Ascidian larvae and the events of metamorphosis. Am Zool 22, 817–826.
Conant, E.B. (1973). Regeneration in the African lungfish, *Protopterus*. III.

Regeneration during fasting and estivation. Biol Bull 144, 248–261.
Cong, Y., Xie, Y., and Zhang, L. (2020a). Transcriptome analysis of the response of marine nematode *Litoditis marina* to acidic stress (in Chinese). Oceanol Limnol Sin 51, 1472–1482.
Cong, Y., Yang, H., Zhang, P., Xie, Y., Cao, X., and Zhang, L. (2020b). Transcriptome analysis of the nematode *Caenorhabditis elegans* in acidic stress environments. Front Physiol 11, 1107.
Cooper, E.D. (2014). Horizontal gene transfer: accidental inheritance drives adaptation. Curr Biol 24, R562–R564.
Corallo, D., Trapani, V., and Bonaldo, P. (2015). The notochord: structure and functions. Cell Mol Life Sci 72, 2989–3008.
Cummings, D.J., Tait, A., and Goddard, J.M. (1974). Methylated bases in DNA from *Parameciumaurelia*. Biochim Biophys Acta 374, 1–11.
Curtis, B.A., Tanifuji, G., Burki, F., Gruber, A., Irimia, M., Maruyama, S., Arias, M.C., Ball, S.G., Gile, G.H., Hirakawa, Y., et al. (2012). Algal genomes reveal evolutionary mosaicism and the fate of nucleomorphs. Nature 492, 59–65.
Darehzereshki, A., Rubin, N., Gamba, L., Kim, J., Fraser, J., Huang, Y., Billings, J., Mohammadzadeh, R., Wood, J., Warburton, D., et al. (2015). Differential regenerative capacity of neonatal mouse hearts after cryoinjury. Dev Biol 399, 91–99.
Datta, A., Bryant, D.M., and Mostov, K.E. (2011). Molecular regulation of lumen morphogenesis. Curr Biol 21, R126–R136.
De Celis, J.F. (2003). Pattern formation in the *Drosophila* wing: The development of the veins. BioEssays 25, 443–451.
De Celis, J.F., and Diaz-Benjumea, F.J. (2003). Developmental basis for vein pattern variations in insect wings. Inter J Dev Biol 47, 653–663.
Dehal, P., Satou, Y., Campbell, R.K., Chapman, J., Degnan, B., De Tomaso, A., Davidson, B., Di Gregorio, A., Gelpke, M., Goodstein, D.M., et al. (2002). The draft genome of *Ciona intestinalis*: insights into chordate and vertebrate origins. Science 298, 2157–2167.
Delsuc, F., Brinkmann, H., Chourrout, D., and Philippe, H. (2006). Tunicates and not cephalochordates are the closest living relatives of vertebrates. Nature 439, 965–968.
Deneke, V.E., Melbinger, A., Vergassola, M., and Di Talia, S. (2016). Waves of Cdk1 activity in s phase synchronize the cell cycle in *Drosophila* embryos. Dev Cell 38, 399–412.
Deng, T., Wu, F., Zhou, Z., and Su, T. (2020). Tibetan Plateau: an evolutionary junction for the history of modern biodiversity. Sci China Earth Sci 63, 172–187.
Deng, W., Nies, F., Feuer, A., Bocina, I., Oliver, D., and Jiang, D. (2013). Anion translocation through an Slc26 transporter mediates lumen expansion during tubulogenesis. Proc Natl Acad Sci USA 110, 14972–14977.
Denker, E., Bocina, I., and Jiang, D. (2013). Tubulogenesis in a simple cell cord requires the formation of bi-apical cells through two discrete Par domains. Development 140, 2985–2996.
Denker, E., Sehring, I.M., Dong, B., Audisso, J., Mathiesen, B., and Jiang, D. (2015). Regulation by a TGFβ-ROCK-actomyosin axis secures a non-linear lumen expansion that is essential for tubulogenesis. Development 142, 1639–1650.
Derelle, E., Ferraz, C., Rombauts, S., Rouzé, P., Worden, A.Z., Robbens, S., Partensky, F., Degroeve, S., Echeynié, S., Cooke, R., et al. (2006). Genome analysis of the smallest free-living eukaryote *Ostreococcus tauri* unveils many unique features. Proc Natl Acad Sci USA 103, 11647–11652.
Derycke, S., De Meester, N., Rigaux, A., Creer, S., Bik, H., Thomas, W.K., and Moens, T. (2016). Coexisting cryptic species of the *Litoditis marina* complex (Nematoda) show differential resource use and have distinct microbiomes with high intraspecific variability. Mol Ecol 25, 2093–2110.
Desban, L., Prendergast, A., Roussel, J., Rosello, M., Geny, D., Wyart, C., and Bardet, P.L. (2019). Regulation of the apical extension morphogenesis tunes the mechanosensory response of microvilliated neurons. PLoS Biol 17, e3000235.
Deschamps, P., and Moreira, D. (2012). Reevaluating the green contribution to diatom genomes. Genome Biol Evol 4, 683–688.
Diaz-Benjumea, F.J., and Cohen, S.M. (1993). Interaction between dorsal and ventral cells in the imaginal disc directs wing development in *Drosophila*. Cell 75, 741–752.
Doherty, K.M., van de Warrenburg, B.P., Peralta, M.C., Silveira-Moriyama, L., Azulay, J.P., Gershanik, O.S., and Bloem, B.R. (2011). Postural deformities in Parkinson's disease. Lancet Neurol 10, 538–549.
Dong, B., Horie, T., Denker, E., Kusakabe, T., Tsuda, M., Smith, W.C., and Jiang, D. (2009). Tube formation by complex cellular processes in *Ciona intestinalis* notochord. Dev Biol 330, 237–249.
Dong, B., Deng, W., and Jiang, D. (2011). Distinct cytoskeleton populations and extensive crosstalk control *Ciona* notochord tubulogenesis. Development 138, 1631–1641.
Dorrell, R.G., Gile, G., McCallum, G., Méheust, R., Bapteste, E.P., Klinger, C.M., Brillet-Guéguen, L., Freeman, K.D., Richter, D.J., and Bowler, C. (2017). Chimeric origins of ochrophytes and haptophytes revealed through an ancient plastid proteome. eLife 6, e23717.
Dumortier, J.G., Le Verge-Serandour, M., Tortorelli, A.F., Mielke, A., de Plater, L., Turlier, H., and Maître, J.L. (2019). Hydraulic fracturing and active coarsening position the lumen of the mouse blastocyst. Science 365, 465–468.
Duncan, B.K., and Miller, J.H. (1980). Mutagenic deamination of cytosine residues in DNA. Nature 287, 560–561.
Eisenhauer, N., and Guerra, C.A. (2019). Global maps of soil-dwelling nematode worms. Nature 572, 187–188.
Else, K.J., Keiser, J., Holland, C.V., Grencis, R.K., Sattelle, D.B., Fujiwara, R.T., Bueno, L.L., Asaolu, S.O., Sowemimo, O.A., and Cooper, P.J. (2020). Whipworm and roundworm infections. Nat Rev Dis Primers 6, 44.
Endo, T., Bryant, S.V., and Gardiner, D.M. (2004). A stepwise model system for limb regeneration. Dev Biol 270, 135–145.
Ettensohn, C.A. (2013). Encoding anatomy: developmental gene regulatory networks and morphogenesis. Genesis 51, 383–409.
Evans, T., Rosenthal, E.T., Youngblom, J., Distel, D., and Hunt, T. (1983). Cyclin: a protein specified by maternal mRNA in sea urchin eggs that is destroyed at each cleavage division. Cell 33, 389–396.
Eyres, I., Boschetti, C., Crisp, A., Smith, T.P., Fontaneto, D., Tunnacliffe, A., and Barraclough, T.G. (2015). Horizontal gene transfer in bdelloid rotifers is ancient, ongoing and more frequent in species from desiccating habitats. BMC Biol 13, 90.
Fadzan, M., and Bettany-Saltikov, J. (2017). Etiological theories of adolescent idiopathic scoliosis: past and present. Open Orthop J 11, 1466–1489.
Fan, X., Qiu, H., Han, W., Wang, Y., Xu, D., Zhang, X., Bhattacharya, D., and Ye, N. (2020). Phytoplankton pangenome reveals extensive prokaryotic horizontal gene transfer of diverse functions. Sci Adv 6, eaba0111.
Fang, Y., Lai, K.S., She, P., Sun, J., Tao, W., and Zhong, T.P. (2020). Tbx20 induction promotes zebrafish heart regeneration by inducing cardiomyocyte dedifferentiation and endocardial expansion. Front Cell Dev Biol 8, 738.
Fei, J.F., Schuez, M., Knapp, D., Taniguchi, Y., Drechsel, D.N., and Tanaka, E.M. (2017). Efficient gene knockin in axolotl and its use to test the role of satellite cells in limb regeneration. Proc Natl Acad Sci USA 114, 12501–12506.
Feldman, J.L., and Priess, J.R. (2012). A role for the centrosome and PAR-3 in the hand-off of MTOC function during epithelial polarization. Curr Biol 22, 575–582.
Feng, D., Chen, Z., Yang, K., Miao, S., Xu, B., Kang, Y., Xie, H., and Zhao, C. (2017). The cytoplasmic tail of rhodopsin triggers rapid rod degeneration in kinesin-2 mutants. J Biol Chem 292, 17375–17386.
Finn, R.D., Coggill, P., Eberhardt, R.Y., Eddy, S.R., Mistry, J., Mitchell, A. L., Potter, S.C., Punta, M., Qureshi, M., Sangrador-Vegas, A., et al. (2016). The Pfam protein families database: towards a more sustainable future. Nucleic Acids Res 44, D279–D285.
Flink, I.L. (2002). Cell cycle reentry of ventricular and atrial cardiomyocytes and cells within the epicardium following amputation of the ventricular apex in the axolotl, *Amblystoma mexicanum*: confocal

microscopic immunofluorescent image analysis of bromodeoxyuridine-labeled nuclei. Anat Embryol 205, 235–244.
Flores-Benitez, D., and Knust, E. (2016). Dynamics of epithelial cell polarity in *Drosophila*: how to regulate the regulators? Curr Opin Cell Biol 42, 13–21.
Foster, P.L., Hanson, A.J., Lee, H., Popodi, E.M., and Tang, H. (2013). On the mutational topology of the bacterial genome. G3 (Bethesda) 3, 399–407.
Fu, Y., Luo, G.Z., Chen, K., Deng, X., Yu, M., Han, D., Hao, Z., Liu, J., Lu, X., Dore, L.C., et al. (2015). N^6-methyldeoxyadenosine marks active transcription start sites in *Chlamydomonas*. Cell 161, 879–892.
Fukuda, R., Marín-Juez, R., El-Sammak, H., Beisaw, A., Ramadass, R., Kuenne, C., Guenther, S., Konzer, A., Bhagwat, A.M., Graumann, J., et al. (2020). Stimulation of glycolysis promotes cardiomyocyte proliferation after injury in adult zebrafish. EMBO Rep 21.
Funakoshi, Y., Minami, M., and Tabata, T. (2001). mtv shapes the activity gradient of the Dpp morphogen through regulation of thickveins. Development 128, 67–74.
Gálvez-Santisteban, M., Chen, D., Zhang, R., Serrano, R., Nguyen, C., Zhao, L., Nerb, L., Masutani, E.M., Vermot, J., Burns, C.G., et al. (2019). Hemodynamic-mediated endocardial signaling controls *in vivo* myocardial reprogramming. eLife 8, e44816.
Gao, F., Warren, A., Zhang, Q., Gong, J., Miao, M., Sun, P., Xu, D., Huang, J., Yi, Z., and Song, W. (2016). The all-data-based evolutionary hypothesis of ciliated protists with a revised classification of the phylum Ciliophora (Eukaryota, Alveolata). Sci Rep 6, 24874.
Gao, F., Roy, S.W., and Katz, L.A. (2015). Analyses of alternatively processed genes in ciliates provide insights into the origins of scrambled genomes and may provide a mechanism for speciation. mBio 6, e01998-14.
Gao, Y., Gong, R., Jiang, Y., Pan, B., Li, Y., Warren, A., Jiang, J., and Gao, F. (2020). Morphogenetic characters of the model ciliate *Euplotes vannus* (Ciliophora, Spirotrichea): Notes on cortical pattern formation during conjugational and postconjugational reorganization. Eur J Protistol 73, 125675.
Gemberling, M., Karra, R., Dickson, A.L., and Poss, K.D. (2015). Nrg1 is an injury-induced cardiomyocyte mitogen for the endogenous heart regeneration program in zebrafish. eLife 4, e05871.
Gerber, T., Murawala, P., Knapp, D., Masselink, W., Schuez, M., Hermann, S., Gac-Santel, M., Nowoshilow, S., Kageyama, J., Khattak, S., et al. (2018). Single-cell analysis uncovers convergence of cell identities during axolotl limb regeneration. Science 362, eaaq0681.
Godin, A.G., Lounis, B., and Cognet, L. (2014). Super-resolution microscopy approaches for live cell imaging. Biophys J 107, 1777–1784.
Godwin, J.W., Debuque, R., Salimova, E., and Rosenthal, N.A. (2017). Heart regeneration in the salamander relies on macrophage-mediated control of fibroblast activation and the extracellular landscape. NPJ Regen Med 2, 22.
Godwin, J.W., Pinto, A.R., and Rosenthal, N.A. (2013). Macrophages are required for adult salamander limb regeneration. Proc Natl Acad Sci USA 110, 9415–9420.
Gong, R., Jiang, Y., Vallesi, A., Gao, Y., and Gao, F. (2020). Conjugation in *Euplotes raikovi* (Protista, ciliophora): New insights into nuclear events and macronuclear development from micronucleate and amicronucleate cells. Microorganisms 8, 162.
González-Rosa, J.M., Martín, V., Peralta, M., Torres, M., and Mercader, N. (2011). Extensive scar formation and regression during heart regeneration after cryoinjury in zebrafish. Development 138, 1663–1674.
González-Rosa, J.M., Peralta, M., and Mercader, N. (2012). Pan-epicardial lineage tracing reveals that epicardium derived cells give rise to myofibroblasts and perivascular cells during zebrafish heart regeneration. Dev Biol 370, 173–186.
González-Rosa, J.M., Sharpe, M., Field, D., Soonpaa, M.H., Field, L.J., Burns, C.E., and Burns, C.G. (2018). Myocardial polyploidization creates a barrier to heart regeneration in zebrafish. Dev Cell 44, 433–446.e7.
Gorbman, A., Nozaki, M., and Kubokawa, K. (1999). A brain-Hatschek's pit connection in amphioxus. Gen Comp Endocrinol 113, 251–254.
Gorovsky, M.A., Hattman, S., and Pleger, G.L. (1973). [^{6}N]methyl adenine in the nuclear DNA of a eucaryote, *Tetrahymena pyriformis*. J Cell Biol 56, 697–701.
Greer, E.L., Blanco, M.A., Gu, L., Sendinc, E., Liu, J., Aristizábal-Corrales, D., Hsu, C.H., Aravind, L., He, C., and Shi, Y. (2015). DNA Methylation on N^6-adenine in *C. elegans*. Cell 161, 868–878.
Greider, C.W., and Blackburn, E.H. (1985). Identification of a specific telomere terminal transferase activity in *Tetrahymena* extracts. Cell 43, 405–413.
Greider, C.W., and Blackburn, E.H. (1989). A telomeric sequence in the RNA of *Tetrahymena* telomerase required for telomere repeat synthesis. Nature 337, 331–337.
Grimes, D.T., Boswell, C.W., Morante, N.F.C., Henkelman, R.M., Burdine, R.D., and Ciruna, B. (2016). Zebrafish models of idiopathic scoliosis link cerebrospinal fluid flow defects to spine curvature. Science 352, 1341–1344.
Grimm, M., Brünen-Nieweler, C., Junker, V., Heckmann, K., and Beier, H. (1998). The hypotrichous ciliate *Euplotes octocarinatus* has only one type of tRNACys with GCA anticodon encoded on a single macronuclear DNA molecule. Nucleic Acids Res 26, 4557–4565.
Grivas, J., Haag, M., Johnson, A., Manalo, T., Roell, J., Das, T.L., Brown, E., Burns, A.R., and Lafontant, P.J. (2014). Cardiac repair and regenerative potential in the goldfish (*Carassius auratus*) heart. Comp Biochem Physiol Part C Toxicol Pharmacol 163, 14–23.
Guillemette, B., Bataille, A.R., Gévry, N., Adam, M., Blanchette, M., Robert, F., and Gaudreau, L. (2005). Variant histone H2A.Z is globally localized to the promoters of inactive yeast genes and regulates nucleosome positioning. PLoS Biol 3, e384.
Guo, B., Zhang, S., Wang, S., and Liang, Y. (2009). Expression, mitogenic activity and regulation by growth hormone of growth hormone/insulin-like growth factor in *Branchiostoma belcheri*. Cell Tissue Res 338, 67–77.
Haft, D.H., Selengut, J.D., and White, O. (2003). The TIGRFAMs database of protein families. Nucleic Acids Res 31, 371–373.
Halder, G., Polaczyk, P., Kraus, M.E., Hudson, A., Kim, J., Laughon, A., and Carroll, S. (1998). The Vestigial and Scalloped proteins act together to directly regulate wing-specific gene expression in *Drosophila*. Genes Dev 12, 3900–3909.
Hamaratoglu, F., Affolter, M., and Pyrowolakis, G. (2014). Dpp/BMP signaling in flies: From molecules to biology. Semin Cell Dev Biol 32, 128–136.
Han, Y., Chen, A., Umansky, K.B., Oonk, K.A., Choi, W.Y., Dickson, A.L., Ou, J., Cigliola, V., Yifa, O., Cao, J., et al. (2019). Vitamin D stimulates cardiomyocyte proliferation and controls organ size and regeneration in zebrafish. Dev Cell 48, 853–863.e5.
Hao, Z., Wu, T., Cui, X., Zhu, P., Tan, C., Dou, X., Hsu, K.W., Lin, Y.T., Peng, P.H., Zhang, L.S., et al. (2020). N^6-deoxyadenosine methylation in mammalian mitochondrial DNA. Mol Cell 78, 382–395.e8.
Harrison, G.S., and Karrer, K.M. (1985). DNA synthesis, methylation and degradation during conjugation in *Tetrahymena thermophila*. Nucl Acids Res 13, 73–87.
Harrison, G.S., Findly, R.C., and Karrer, K.M. (1986). Site-specific methylation of adenine in the nuclear genome of a eucaryote, *Tetrahymena thermophila*. Mol Cell Biol 6, 2364–2370.
Hashimoto, H., Robin, F.B., Sherrard, K.M., and Munro, E.M. (2015). Sequential contraction and exchange of apical junctions drives zippering and neural tube closure in a simple chordate. Dev Cell 32, 241–255.
Hattman, S. (2005). DNA-[adenine] methylation in lower eukaryotes. Biochem (Moscow) 70, 550–558.
Hattman, S., Kenny, C., Berger, L., and Pratt, K. (1978). Comparative study of DNA methylation in three unicellular eucaryotes. J Bacteriol 135, 1156–1157.
Haubner, B.J., Schneider, J., Schweigmann, U., Schuetz, T., Dichtl, W.,

Velik-Salchner, C., Stein, J.I., and Penninger, J.M. (2016). Functional recovery of a human neonatal heart after severe myocardial infarction. Circ Res 118, 216–221.
Hayashi, S., and Dong, B. (2017). Shape and geometry control of the *Drosophila* tracheal tubule. Dev Growth Differ 59, 4–11.
Heaphy, S.M., Mariotti, M., Gladyshev, V.N., Atkins, J.F., and Baranov, P. V. (2016). Novel ciliate genetic code variants including the reassignment of all three stop codons to sense codons in *Condylostoma magnum*. Mol Biol Evol 33, 2885–2889.
Hein, S.J., Lehmann, L.H., Kossack, M., Juergensen, L., Fuchs, D., Katus, H.A., and Hassel, D. (2015). Advanced echocardiography in adult zebrafish reveals delayed recovery of heart function after myocardial cryoinjury. PLoS ONE 10, e0122665.
Herwig, L., Blum, Y., Krudewig, A., Ellertsdottir, E., Lenard, A., Belting, H.G., and Affolter, M. (2011). Distinct cellular mechanisms of blood vessel fusion in the zebrafish embryo. Curr Biol 21, 1942–1948.
Higgins, R.P., and Thiel, H. (1988). Introduction to the study of meiofauna. Eur J Protistol 25, 188–189.
Hildebrandt, F., Benzing, T., and Katsanis, N. (2011). Ciliopathies. N Engl J Med 364, 1533–1543.
Hodges, M.M., Zgheib, C., and Liechty, K.W. (2021). A large mammalian model of myocardial regeneration after myocardial infarction in fetal sheep. Adv Wound Care 10, 174–190.
Holland, L.Z., Albalat, R., Azumi, K., Benito-Gutiérrez, E., Blow, M.J., Bronner-Fraser, M., Brunet, F., Butts, T., Candiani, S., Dishaw, L.J., et al. (2008). The amphioxus genome illuminates vertebrate origins and cephalochordate biology. Genome Res 18, 1100–1111.
Honkoop, H., de Bakker, D.E., Aharonov, A., Kruse, F., Shakked, A., Nguyen, P.D., de Heus, C., Garric, L., Muraro, M.J., Shoffner, A., et al. (2019). Single-cell analysis uncovers that metabolic reprogramming by ErbB2 signaling is essential for cardiomyocyte proliferation in the regenerating heart. eLife 8, e50163.
Howe, K., Clark, M.D., Torroja, C.F., Torrance, J., Berthelot, C., Muffato, M., Collins, J.E., Humphray, S., McLaren, K., Matthews, L., et al. (2013). The zebrafish reference genome sequence and its relationship to the human genome. Nature 496, 498–503.
Hu, X. (2014). Ciliates in extreme environments. J Eukaryot Microbiol 61, 410–418.
Hu, X., Lin, X., and Song, W. (2019). Ciliate Atlas: Species Found in the South China Sea. Beijing: Science Press.
Huang, G.N., Thatcher, J.E., McAnally, J., Kong, Y., Qi, X., Tan, W., DiMaio, J.M., Amatruda, J.F., Gerard, R.D., Hill, J.A., et al. (2012). C/EBP transcription factors mediate epicardial activation during heart development and injury. Science 338, 1599–1603.
Huang, P., and Schier, A.F. (2009). Dampened Hedgehog signaling but normal Wnt signaling in zebrafish without cilia. Development 136, 3089–3098.
Huang, Y., Harrison, M.R., Osorio, A., Kim, J., Baugh, A., Duan, C., Sucov, H.M., and Lien, C.L. (2013). Igf signaling is required for cardiomyocyte proliferation during zebrafish heart development and regeneration. PLoS ONE 8, e67266.
Hugot, J.P., Baujard, P., and Morand, S. (2001). Biodiversity in helminths and nematodes as a field of study: an overview. Nematology 3, 199–208.
Husnik, F., and McCutcheon, J.P. (2017). Functional horizontal gene transfer from bacteria to eukaryotes. Nat Rev Microbiol 16, 67–79.
International Helminth Genomes Consortium. (2019). Comparative genomics of the major parasitic worms. Nat Genet 51, 163–174.
Iruela-Arispe, M.L., and Beitel, G.J. (2013). Tubulogenesis. Development 140, 2851–2855.
Ishikawa, H., and Marshall, W.F. (2011). Ciliogenesis: building the cell's antenna. Nat Rev Mol Cell Biol 12, 222–234.
Ito, K., Morioka, M., Kimura, S., Tasaki, M., Inohaya, K., and Kudo, A. (2014). Differential reparative phenotypes between zebrafish and medaka after cardiac injury. Dev Dyn 243, 1106–1115.
Iwamoto, M., Koujin, T., Osakada, H., Mori, C., Kojidani, T., Matsuda, A., Asakawa, H., Hiraoka, Y., and Haraguchi, T. (2015). Biased assembly of the nuclear pore complex is required for somatic and germline nuclear differentiation in *Tetrahymena*. J Cell Sci 128, 1812–1823.
Iyer, L.M., Abhiman, S., and Aravind, L. (2011). Natural history of eukaryotic DNA methylation systems. Prog Mol Biol Transl Sci, 101, 25–104.
Iyer, L.M., Zhang, D., and Aravind, L. (2016). Adenine methylation in eukaryotes: apprehending the complex evolutionary history and functional potential of an epigenetic modification. BioEssays 38, 27–40.
Izquierdo, E., Quinkler, T., and De Renzis, S. (2018). Guided morphogenesis through optogenetic activation of Rho signalling during early *Drosophila* embryogenesis. Nat Commun 9, 2366.
Jacobs, M.E., and Klobutcher, L.A. (1996). The long and the short of developmental DNA deletion in *Euplotes crassus*. J Eukaryot Microbiol 43, 442–452.
Jalalvand, E., Robertson, B., Wallén, P., and Grillner, S. (2016). Ciliated neurons lining the central canal sense both fluid movement and pH through ASIC3. Nat Commun 7, 10002.
Jeong, H., Sung, S., Kwon, T., Seo, M., Caetano-Anollés, K., Choi, S.H., Cho, S., Nasir, A., and Kim, H. (2016). HGTree: database of horizontally transferred genes determined by tree reconciliation. Nucleic Acids Res 44, D610–D619.
Jiang, D., and Smith, W.C. (2007). Ascidian notochord morphogenesis. Dev Dyn 236, 1748–1757.
Jiang, J., and Hui, C.C. (2008). Hedgehog signaling in development and cancer. Dev Cell 15, 801–812.
Jiang, J., Shao, C., Xu, H., and Al-Rasheid, K.A.S. (2010). Morphogenetic observations on the marine ciliate *Euplotes vannus* during cell division (Protozoa: Ciliophora). J Mar Biol Ass 90, 683–689.
Jiang, Y., Zhang, T., Vallesi, A., Yang, X., and Gao, F. (2019). Time-course analysis of nuclear events during conjugation in the marine ciliate *Euplotes vannus* and comparison with other ciliates (Protozoa, Ciliophora). Cell Cycle 18, 288–298.
Johnson, M.D., Tengs, T., Oldach, D.W., Delwiche, C.F., and Stoecker, D. K. (2004). Highly divergent SSU rRNA genes found in the marine ciliates *Myrionecta rubra* and *Mesodinium pulex*. Protist 155, 347–359.
Johnson, R.L., Grenier, J.K., and Scott, M.P. (1995). Patched overexpression alters wing disc size and pattern: transcriptional and post-transcriptional effects on hedgehog targets. Development 121, 4161–4170.
Jopling, C., Sleep, E., Raya, M., Martí, M., Raya, A., and Izpisúa Belmonte, J.C. (2010). Zebrafish heart regeneration occurs by cardiomyocyte dedifferentiation and proliferation. Nature 464, 606–609.
Jopling, C., Suñé, G., Faucherre, A., Fabregat, C., and Izpisua Belmonte, J. C. (2012). Hypoxia induces myocardial regeneration in zebrafish. Circulation 126, 3017–3027.
Joven, A., Elewa, A., and Simon, A. (2019). Model systems for regeneration: salamanders. Development 146, dev167700.
Karrer, K.M., and VanNuland, T.A. (2002). Methylation of adenine in the nuclear DNA of *Tetrahymena* is internucleosomal and independent of histone H1. Nucleic Acids Res 30, 1364–1370.
Kawauchi, H., and Sower, S.A. (2006). The dawn and evolution of hormones in the adenohypophysis. General Comp Endocrinol 148, 3–14.
Keeling, P.J., and Palmer, J.D. (2008). Horizontal gene transfer in eukaryotic evolution. Nat Rev Genet 9, 605–618.
Kikuchi, K., Gupta, V., Wang, J., Holdway, J.E., Wills, A.A., Fang, Y., and Poss, K.D. (2011a). *tcf21*$^{+}$ epicardial cells adopt non-myocardial fates during zebrafish heart development and regeneration. Development 138, 2895–2902.
Kikuchi, K., Holdway, J.E., Major, R.J., Blum, N., Dahn, R.D., Begemann, G., and Poss, K.D. (2011b). Retinoic acid production by endocardium and epicardium is an injury response essential for zebrafish heart regeneration. Dev Cell 20, 397–404.
Kikuchi, K., Holdway, J.E., Werdich, A.A., Anderson, R.M., Fang, Y., Egnaczyk, G.F., Evans, T., Macrae, C.A., Stainier, D.Y.R., and Poss, K. D. (2010). Primary contribution to zebrafish heart regeneration by

gata4^{+} cardiomyocytes. Nature 464, 601–605.
Kikuchi, T., Eves-van den Akker, S., and Jones, J.T. (2017). Genome evolution of plant-parasitic nematodes. Annu Rev Phytopathol 55, 333–354.
Kim, J., Wu, Q., Zhang, Y., Wiens, K.M., Huang, Y., Rubin, N., Shimada, H., Handin, R.I., Chao, M.Y., Tuan, T.L., et al. (2010). PDGF signaling is required for epicardial function and blood vessel formation in regenerating zebrafish hearts. Proc Natl Acad Sci USA 107, 17206–17210.
Kimura, W., Xiao, F., Canseco, D.C., Muralidhar, S., Thet, S.W., Zhang, H. M., Abderrahman, Y., Chen, R., Garcia, J.A., Shelton, J.M., et al. (2015). Hypoxia fate mapping identifies cycling cardiomyocytes in the adult heart. Nature 523, 226–230.
Klein, T., and Arias, A.M. (1998). Different spatial and temporal interactions between *Notch*, *wingless*, and *vestigial* specify proximal and distal pattern elements of the wing in *Drosophila*. Dev Biol 194, 196–212.
Klobutcher, L.A., and Farabaugh, P.J. (2002). Shifty ciliates: frequent programmed translational frameshifting in euplotids. Cell 111, 763–766.
Klobutcher, L.A., Gygax, S.E., Podoloff, J.D., Vermeesch, J.R., Price, C. M., Tebeau, C.M., and Jahn, C.L. (1998). Conserved DNA sequences adjacent to chromosome fragmentation and telomere addition sites in *Euplotes crassus*. Nucleic Acids Res 26, 4230–4240.
Kong, D., Lv, Z., Häring, M., Lin, B., Wolf, F., and Großhans, J. (2019). *In vivo* optochemical control of cell contractility at single-cell resolution. EMBO Rep 20, e47755.
Koutsovoulos, G., Makepeace, B., Tanya, V.N., and Blaxter, M. (2014). Palaeosymbiosis revealed by genomic fossils of *Wolbachia* in a strongyloidean nematode. PLoS Genet 10, e1004397.
Koziol, M.J., Bradshaw, C.R., Allen, G.E., Costa, A.S.H., Frezza, C., and Gurdon, J.B. (2016). Identification of methylated deoxyadenosines in vertebrates reveals diversity in DNA modifications. Nat Struct Mol Biol 23, 24–30.
Kragl, M., Knapp, D., Nacu, E., Khattak, S., Maden, M., Epperlein, H.H., and Tanaka, E.M. (2009). Cells keep a memory of their tissue origin during axolotl limb regeneration. Nature 460, 60–65.
Krzic, U., Gunther, S., Saunders, T.E., Streichan, S.J., and Hufnagel, L. (2012). Multiview light-sheet microscope for rapid in toto imaging. Nat Methods 9, 730–733.
Ku, C., Nelson-Sathi, S., Roettger, M., Sousa, F.L., Lockhart, P.J., Bryant, D., Hazkani-Covo, E., McInerney, J.O., Landan, G., and Martin, W.F. (2015). Endosymbiotic origin and differential loss of eukaryotic genes. Nature 524, 427–432.
Kumar, A., Godwin, J.W., Gates, P.B., Garza-Garcia, A.A., and Brockes, J. P. (2007). Molecular basis for the nerve dependence of limb regeneration in an adult vertebrate. Science 318, 772–777.
Knudson Jr, A.G. (1971). Mutation and cancer: statistical study of retinoblastoma. Proc Natl Acad Sci USA 68, 820–823.
Kurahashi, M. (2016). Solar energy storage using algae. In: Sugiyama, M., Fujii, K., and Nakamura, S., eds. Solar to Chemical Energy Conversion. Heidelberg: Springer. 455–478.
Lafontant, P.J., Burns, A.R., Grivas, J.A., Lesch, M.A., Lala, T.D., Reuter, S.P., Field, L.J., and Frounfelter, T.D. (2012). The giant danio (*D. aequipinnatus*) as a model of cardiac remodeling and regeneration. Anat Rec 295, 234–248.
Lai, S.L., Marín-Juez, R., Moura, P.L., Kuenne, C., Lai, J.K.H., Tsedeke, A. T., Guenther, S., Looso, M., and Stainier, D.Y. (2017). Reciprocal analyses in zebrafish and medaka reveal that harnessing the immune response promotes cardiac regeneration. eLife 6, e25605.
Lander, A.D., Nie, Q., Sanchez-Tapia, C., Simonyan, A., and Wan, F.Y.M. (2020). Regulatory feedback on receptor and non-receptor synthesis for robust signaling. Dev Dyn 249, 383–409.
Laube, F., Heister, M., Scholz, C., Borchardt, T., and Braun, T. (2006). Re-programming of newt cardiomyocytes is induced by tissue regeneration. J Cell Sci 119, 4719–4729.
Lecuit, T., and Wieschaus, E. (2000). Polarized insertion of new membrane from a cytoplasmic reservoir during cleavage of the *Drosophila* embryo. J Cell Biol 150, 849–860.
Leigh, N.D., Dunlap, G.S., Johnson, K., Mariano, R., Oshiro, R., Wong, A. Y., Bryant, D.M., Miller, B.M., Ratner, A., Chen, A., et al. (2018). Transcriptomic landscape of the blastema niche in regenerating adult axolotl limbs at single-cell resolution. Nat Commun 9, 5153.
Lepilina, A., Coon, A.N., Kikuchi, K., Holdway, J.E., Roberts, R.W., Burns, C.G., and Poss, K.D. (2006). A dynamic epicardial injury response supports progenitor cell activity during zebrafish heart regeneration. Cell 127, 607–619.
Leptin, M., and Grunewald, B. (1990). Cell shape changes during gastrulation in *Drosophila*. Development 110, 73–84.
Li, M., Gao, Z., Ji, D., and Zhang, S. (2014). Functional characterization of GH-like homolog in amphioxus reveals an ancient origin of GH/GH receptor system. Endocrinology 155, 4818–4830.
Li, M., Jiang, C., Zhang, Y., and Zhang, S. (2017). Activities of amphioxus GH-like protein in osmoregulation: insight into origin of vertebrate GH family. Int J Endocrinol 2017, 1–13.
Liang, Z., Shen, L., Cui, X., Bao, S., Geng, Y., Yu, G., Liang, F., Xie, S., Lu, T., Gu, X., et al. (2018). DNA N^6-adenine methylation in *Arabidopsis thaliana*. Dev Cell 45, 406–416.e3.
Liao, S., Dong, W., Lv, L., Guo, H., Yang, J., Zhao, H., Huang, R., Yuan, Z., Chen, Y., Feng, S., et al. (2017). Heart regeneration in adult *Xenopus tropicalis* after apical resection. Cell Biosci 7, 70.
Lindgren, D. (1972). The temperature influence on the spontaneous mutation rate. Hereditas 70, 179–184.
Liu, J., Zhu, Y., Luo, G.Z., Wang, X., Yue, Y., Wang, X., Zong, X., Chen, K., Yin, H., Fu, Y., et al. (2016). Abundant DNA 6mA methylation during early embryogenesis of zebrafish and pig. Nat Commun 7, 13052.
Liu, M., and Zhang, S. (2011). Amphioxus IGF-like peptide induces mouse muscle cell development via binding to IGF receptors and activating MAPK and PI3K/Akt signaling pathways. Mol Cell Endocrinol 343, 45–54.
Lobanov, A.V., Heaphy, S.M., Turanov, A.A., Gerashchenko, M.V., Pucciarelli, S., Devaraj, R.R., Xie, F., Petyuk, V.A., Smith, R.D., Klobutcher, L.A., et al. (2017). Position-dependent termination and widespread obligatory frameshifting in *Euplotes* translation. Nat Struct Mol Biol 24, 61–68.
Long, H., Miller, S.F., Strauss, C., Zhao, C., Cheng, L., Ye, Z., Griffin, K., Te, R., Lee, H., Chen, C.C., et al. (2016). Antibiotic treatment enhances the genome-wide mutation rate of target cells. Proc Natl Acad Sci USA 113, E2498–E2505.
Long, H., Sung, W., Miller, S.F., Ackerman, M.S., Doak, T.G., and Lynch, M. (2015). Mutation rate, spectrum, topology, and context-dependency in the DNA mismatch repair-deficient *Pseudomonas fluorescens* ATCC948. Genome Biol Evol 7, 262–271.
Lozupone, C.A., Knight, R.D., and Landweber, L.F. (2001). The molecular basis of nuclear genetic code change in ciliates. Curr Biol 11, 65–74.
Lu, Q., Bhattachan, P., and Dong, B. (2019). Ascidian notochord elongation. Dev Biol 448, 147–153.
Lu, Q., Gao, Y., Fu, Y., Peng, H., Shi, W., Li, B., Lv, Z., Feng, X.Q., and Dong, B. (2020). *Ciona* embryonic tail bending is driven by asymmetrical notochord contractility and coordinated by epithelial proliferation. Development 147, dev185868.
Lubarsky, B., and Krasnow, M.A. (2003). Tube morphogenesis: making and shaping biological tubes. Cell 112, 19–28.
Luo, G.Z., Hao, Z., Luo, L., Shen, M., Sparvoli, D., Zheng, Y., Zhang, Z., Weng, X., Chen, K., Cui, Q., et al. (2018). N^6-methyldeoxyadenosine directs nucleosome positioning in *Tetrahymena* DNA. Genome Biol 19, 200.
Luporini, P., Pedrini, B., Alimenti, C., and Vallesi, A. (2016). Revisiting fifty years of research on pheromone signaling in ciliates. Eur J Protistol 55, 26–38.
Luschnig, S., and Uv, A. (2014). Luminal matrices: an inside view on organ morphogenesis. Exp Cell Res 321, 64–70.
Lv, Z., Rosenbaum, J., Mohr, S., Zhang, X., Kong, D., Preiß, H., Kruss, S.,

Alim, K., Aspelmeier, T., and Großhans, J. (2020). The emergent yo-yo movement of nuclei driven by cytoskeletal remodeling in pseudo-synchronous mitotic cycles. Curr Biol 30, 2564–2573.e5.
Lv, Z., Lu, Q., and Dong, B. (2019). Morphogenesis: a focus on marine invertebrates. Mar Life Sci Technol 1, 28–40.
Magadum, A., Ding, Y., He, L., Kim, T., Vasudevarao, M.D., Long, Q., Yang, K., Wickramasinghe, N., Renikunta, H.V., Dubois, N., et al. (2017). Live cell screening platform identifies PPARδ as a regulator of cardiomyocyte proliferation and cardiac repair. Cell Res 27, 1002–1019.
Magiorkinis, G., Belshaw, R., and Katzourakis, A. (2013). 'There and back again': revisiting the pathophysiological roles of human endogenous retroviruses in the post-genomic era. Phil Trans R Soc B 368, 20120504.
Maharjan, R.P., and Ferenci, T. (2017). A shifting mutational landscape in 6 nutritional states: Stress-induced mutagenesis as a series of distinct stress input-mutation output relationships. PLoS Biol 15, e2001477.
Mann, F.A., Lv, Z., Großhans, J., Opazo, F., and Kruss, S. (2019). Nanobody-conjugated nanotubes for targeted near-infrared *in vivo* imaging and sensing. Angew Chem Int Ed 58, 11469–11473.
Marín-Juez, R., El-Sammak, H., Helker, C.S.M., Kamezaki, A., Mullapuli, S.T., Bibli, S.I., Foglia, M.J., Fleming, I., Poss, K.D., and Stainier, D.Y. R. (2019). Coronary revascularization during heart regeneration is regulated by epicardial and endocardial cues and forms a scaffold for cardiomyocyte repopulation. Dev Cell 51, 503–515.e4.
Marques, I.J., Lupi, E., and Mercader, N. (2019). Model systems for regeneration: zebrafish. Development 146, dev167692.
Marshall, L., Vivien, C., Girardot, F., Péricard, L., Demeneix, B.A., Coen, L., and Chai, N. (2017). Persistent fibrosis, hypertrophy and sarcomere disorganisation after endoscopy-guided heart resection in adult *Xenopus*. PLoS ONE 12, e0173418.
Marshall, L.N., Vivien, C.J., Girardot, F., Péricard, L., Scerbo, P., Palmier, K., Demeneix, B.A., and Coen, L. (2019). Stage-dependent cardiac regeneration in *Xenopus* is regulated by thyroid hormone availability. Proc Natl Acad Sci USA 116, 3614–3623.
Martín, M., Ostalé, C.M., and de Celis, J.F. (2017). Patterning of the *Drosophila* L2 vein is driven by regulatory interactions between region-specific transcription factors expressed in response to Dpp signalling. Development 144, 3168–3176.
Martindale, D., Allis, C., and Bruns, P. (1982). Conjugation in *Tetrahymena thermophile*: a temporal analysis of cytological stages. Exp Cell Res 140, 227–236.
Matamoro-Vidal, A., Salazar-Ciudad, I., and Houle, D. (2015). Making quantitative morphological variation from basic developmental processes: Where are we? The case of the *Drosophila* wing. Dev Dyn 244, 1058–1073.
Matsunobu, S., and Sasakura, Y. (2015). Time course for tail regression during metamorphosis of the ascidian *Ciona intestinalis*. Dev Biol 405, 71–81.
McCusker, C.D., and Gardiner, D.M. (2013). Positional information is reprogrammed in blastema cells of the regenerating limb of the axolotl (*Ambystoma mexicanum*). PLoS ONE 8, e77064.
McCusker, C.D., and Gardiner, D.M. (2014). Understanding positional cues in salamander limb regeneration: Implications for optimizing cell-based regenerative therapies. Dis Model Mech 7, 593–599.
Mescher, A.L., and Neff, A.W. (2005). Regenerative capacity and the developing immune system. Adv Biochem Eng Biotechnol 93, 39–66.
Meyer, F., Schmidt, H.J., Plümper, E., Hasilik, A., Mersmann, G., Meyer, H.E., Engström, A., and Heckmann, K. (1991). UGA is translated as cysteine in pheromone 3 of *Euplotes octocarinatus*. Proc Natl Acad Sci USA 88, 3758–3761.
Mizotani, Y., Suzuki, M., Hotta, K., Watanabe, H., Shiba, K., Inaba, K., Tashiro, E., Oka, K., and Imoto, M. (2018). 14-3-3εa directs the pulsatile transport of basal factors toward the apical domain for lumen growth in tubulogenesis. Proc Natl Acad Sci USA 115, E8873–E8881.
Mollova, M., Bersell, K., Walsh, S., Savla, J., Das, L.T., Park, S.Y., Silberstein, L.E., Dos Remedios, C.G., Graham, D., Colan, S., et al. (2013). Cardiomyocyte proliferation contributes to heart growth in young humans. Proc Natl Acad Sci USA 110, 1446–1451.
Mondo, S.J., Dannebaum, R.O., Kuo, R.C., Louie, K.B., Bewick, A.J., LaButti, K., Haridas, S., Kuo, A., Salamov, A., Ahrendt, S.R., et al. (2017). Widespread adenine N^6-methylation of active genes in fungi. Nat Genet 49, 964–968.
Moustafa, A., Beszteri, B., Maier, U.G., Bowler, C., Valentin, K., and Bhattacharya, D. (2009). Genomic footprints of a cryptic plastid endosymbiosis in diatoms. Science 324, 1724–1726.
Münch, J., Grivas, D., González-Rajal, Á., Torregrosa-Carrión, R., and de la Pompa, J.L. (2017). Notch signalling restricts inflammation and *serpine1* expression in the dynamic endocardium of the regenerating zebrafish heart. Development 144, 1425–1440.
Nakada, Y., Canseco, D.C., Thet, S.W., Abdisalaam, S., Asaithamby, A., Santos, C.X., Shah, A.M., Zhang, H., Faber, J.E., Kinter, M.T., et al. (2017). Hypoxia induces heart regeneration in adult mice. Nature 541, 222–227.
Nellen, D., Burke, R., Struhl, G., and Basler, K. (1996). Direct and long-range action of a DPP morphogen gradient. Cell 85, 357–368.
Neumann, C.J., and Cohen, S.M. (1997). Long-range action of Wingless organizes the dorsal-ventral axis of the *Drosophila* wing. Development 124, 871–880.
Ngo, T.T.M., Yoo, J., Dai, Q., Zhang, Q., He, C., Aksimentiev, A., and Ha, T. (2016). Effects of cytosine modifications on DNA flexibility and nucleosome mechanical stability. Nat Commun 7, 10813.
Notari, M., Ventura-Rubio, A., Bedford-Guaus, S.J., Jorba, I., Mulero, L., Navajas, D., Martí, M., and Raya, Á. (2018). The local microenvironment limits the regenerative potential of the mouse neonatal heart. Sci Adv 4, eaao5553.
Noto, T., and Mochizuki, K. (2017). Whats, hows and whys of programmed DNA elimination in *Tetrahymena*. Open Biol 7, 170172.
Novikov, A.I., and Khloponin, P.A. (1982). Reparative processes during embryonal and postembryonal myocardiogenesis in *Gallus domesticus* L. Arkh Anat Gistol Embriol 82, 59–67.
Oberpriller, J.O., and Oberpriller, J.C. (1974). Response of the adult newt ventricle to injury. J Exp Zool 187, 249–259.
Odagiri, Y., Uchida, H., Hosokawa, M., Takemoto, K., Morley, A.A., and Takeda, T. (1998). Accelerated accumulation of somatic mutations in the senescence-accelerated mouse. Nat Genet 19, 116–117.
Okitsu, C.Y., Hsieh, J.C.F., and Hsieh, C.L. (2010). Transcriptional activity affects the H3K4me3 level and distribution in the coding region. MCB 30, 2933–2946.
Orts-Del'Immagine, A., Cantaut-Belarif, Y., Thouvenin, O., Roussel, J., Baskaran, A., Langui, D., Koeth, F., Bivas, P., Lejeune, F.X., Bardet, P. L., et al. (2020). Sensory neurons contacting the cerebrospinal fluid require the reissner fiber to detect spinal curvature *in vivo*. Curr Biol 30, 827–839.e824.
Pagani, I., Liolios, K., Jansson, J., Chen, I.M.A., Smirnova, T., Nosrat, B., Markowitz, V.M., and Kyrpides, N.C. (2012). The Genomes OnLine Database (GOLD) v.4: status of genomic and metagenomic projects and their associated metadata. Nucleic Acids Res 40, D571–D579.
Palacios, G., Martin-Gonzalez, A., and Gutierrez, J.C. (1994). Macronuclear DNA demethylation is involved in the encystment process of the ciliate *Colpoda inflata*. Cell Biol Int 18, 223–228.
Pashmforoush, M., Chan, S.J., and Steiner, D.F. (1996). Structure and expression of the insulin-like peptide receptor from amphioxus. Mol Endocrinol 10, 857–866.
Peng, C., Ren, J.L., Deng, C., Jiang, D., Wang, J., Qu, J., Chang, J., Yan, C., Jiang, K., Murphy, R.W., et al. (2020a). The genome of Shaw's sea snake (*Hydrophis curtus*) reveals secondary adaptation to its marine environment. Mol Biol Evol 37, 1744–1760.
Peng, H., Qiao, R., and Dong, B. (2020b). Polarity establishment and maintenance in ascidian notochord. Front Cell Dev Biol 8, 597446.
Piatkowski, T., Mühlfeld, C., Borchardt, T., and Braun, T. (2013). Reconstitution of the myocardium in regenerating newt hearts is preceded by transient deposition of extracellular matrix components. Stem Cells Dev 22, 1921–1931.
Pope, K.L., and Harris, T.J.C. (2008). Control of cell flattening and

junctional remodeling during squamous epithelial morphogenesis in *Drosophila*. Development 135, 2227–2238.
Porrello, E.R., Mahmoud, A.I., Simpson, E., Hill, J.A., Richardson, J.A., Olson, E.N., and Sadek, H.A. (2011). Transient regenerative potential of the neonatal mouse heart. Science 331, 1078–1080.
Porrello, E.R., Mahmoud, A.I., Simpson, E., Johnson, B.A., Grinsfelder, D., Canseco, D., Mammen, P.P., Rothermel, B.A., Olson, E.N., and Sadek, H.A. (2013). Regulation of neonatal and adult mammalian heart regeneration by the miR-15 family. Proc Natl Acad Sci USA 110, 187–192.
Poss, K.D., Wilson, L.G., and Keating, M.T. (2002). Heart regeneration in zebrafish. Science 298, 2188–2190.
Pratt, K., and Hattman, S. (1981). Deoxyribonucleic acid methylation and chromatin organization in *Tetrahymena thermophila*. Mol Cell Biol 1, 600–608.
Prescott, D.M. (1994). The DNA of ciliated protozoa. Microbiol Rev 58, 233–267.
Prescott, D.M., Bostock, C.J., Murti, K.G., Lauth, M.R., and Gamow, E. (1971). DNA of ciliated protozoa. Chromosoma 34, 355–366.
Price, E.L., Vieira, J.M., and Riley, P.R. (2019). Model organisms at the heart of regeneration. Dis Model Mech 12, dmm040691.
Puente, B.N., Kimura, W., Muralidhar, S.A., Moon, J., Amatruda, J.F., Phelps, K.L., Grinsfelder, D., Rothermel, B.A., Chen, R., Garcia, J.A., et al. (2014). The oxygen-rich postnatal environment induces cardiomyocyte cell-cycle arrest through DNA damage response. Cell 157, 565–579.
Rae, P.M.M., and Spear, B.B. (1978). Macronuclear DNA of the hypotrichous ciliate *Oxytricha fallax*. Proc Natl Acad Sci USA 75, 4992–4996.
Raikov, I.B. (1982). The Protozoan Nucleus: Morphology and Evolution. Vienna: Springer.
Raya, A., Koth, C.M., Büscher, D., Kawakami, Y., Itoh, T., Raya, R.M., Sternik, G., Tsai, H.J., Rodríguez-Esteban, C., and Izpisúa-Belmonte, J. C. (2003). Activation of Notch signaling pathway precedes heart regeneration in zebrafish. Proc Natl Acad Sci USA 100, 11889–11895.
Reiter, J.F., and Leroux, M.R. (2017). Genes and molecular pathways underpinning ciliopathies. Nat Rev Mol Cell Biol 18, 533–547.
Riley, J.L., and Katz, L.A. (2001). Widespread distribution of extensive chromosomal fragmentation in ciliates. Mol Biol Evol 18, 1372–1377.
Román-Fernández, A., and Bryant, D.M. (2016). Complex polarity: building multicellular tissues through apical membrane traffic. Traffic 17, 1244–1261.
Rose, C.D., Pompili, D., Henke, K., Van Gennip, J.L.M., Meyer-Miner, A., Rana, R., Gobron, S., Harris, M.P., Nitz, M., and Ciruna, B. (2020). SCO-Spondin defects and neuroinflammation are conserved mechanisms driving spinal deformity across genetic models of idiopathic scoliosis. Curr Biol 30, 2363–2373.e6.
Rossoni, A.W., Price, D.C., Seger, M., Lyska, D., Lammers, P., Bhattacharya, D., and Weber, A.P. (2019). The genomes of polyextremophilic cyanidiales contain 1% horizontally transferred genes with diverse adaptive functions. eLife 8, e45017.
Rota-Stabelli, O., Daley, A.C., and Pisani, D. (2013). Molecular timetrees reveal a Cambrian colonization of land and a new scenario for ecdysozoan evolution. Curr Biol 23, 392–398.
Russell, J.J., Theriot, J.A., Sood, P., Marshall, W.F., Landweber, L.F., Fritz-Laylin, L., Polka, J.K., Oliferenko, S., Gerbich, T., Gladfelter, A., et al. (2017). Non-model model organisms. BMC Biol 15, 55.
Ryan, F.J., and Kiritani, K. (1959). Effect of temperature on natural mutation in *Escherichia coli*. J Gen Microbiol 20, 644–653.
Saker, D.M., Walsh-Sukys, M., Spector, M., and Zahka, K.G. (1997). Cardiac recovery and survival after neonatal myocardial infarction. Pediatr Cardiol 18, 139–142.
Salvini, M., Barone, E., Ronca, S., and Nobili, R. (1986). DNA methylation in vegetative and conjugating cells of a protozoan ciliate: *Blepharisma japonicum*. Dev Genet 7, 149–158.
Salzberg, S.L., White, O., Peterson, J., and Eisen, J.A. (2001). Microbial genes in the human genome: lateral transfer or gene loss? Science 292, 1903–1906.
Sande-Melón, M., Marques, I.J., Galardi-Castilla, M., Langa, X., Pérez-López, M., Botos, M.A., Sánchez-Iranzo, H., Guzmán-Martínez, G., Ferreira Francisco, D.M., Pavlinic, D., et al. (2019). Adult sox10^{+} cardiomyocytes contribute to myocardial regeneration in the zebrafish. Cell Rep 29, 1041–1054.e5.
Santosh, N., Windsor, L.J., Mahmoudi, B.S., Li, B., Zhang, W., Chernoff, E.A., Rao, N., Stocum, D.L., and Song, F. (2011). Matrix metalloproteinase expression during blastema formation in regeneration-competent versus regeneration-deficient amphibian limbs. Dev Dyn 240, 1127–1141.
Satoh, A., Cummings, G.M.C., Bryant, S.V., and Gardiner, D.M. (2010). Neurotrophic regulation of fibroblast dedifferentiation during limb skeletal regeneration in the axolotl (*Ambystoma mexicanum*). Dev Biol 337, 444–457.
Satoh, A., Graham, G.M.C., Bryant, S.V., and Gardiner, D.M. (2008). Neurotrophic regulation of epidermal dedifferentiation during wound healing and limb regeneration in the axolotl (*Ambystoma mexicanum*). Dev Biol 319, 321–335.
Satoh, N. (2008). An aboral-dorsalization hypothesis for chordate origin. Genesis 46, 614–622.
Satoh, N. (2009). An advanced filter-feeder hypothesis for urochordate evolution. Zool Sci 26, 97–111.
Schiffers, S., Ebert, C., Rahimoff, R., Kosmatchev, O., Steinbacher, J., Bohne, A.V., Spada, F., Michalakis, S., Nickelsen, J., Müller, M., et al. (2017). Quantitative LC-MS provides no evidence for m^{6}dA or m^{4}dC in the genome of mouse embryonic stem cells and tissues. Angew Chem Int Ed 56, 11268–11271.
Schmidt, A., and Grosshans, J. (2018). Dynamics of cortical domains in early *Drosophila* development. J Cell Sci 131, jcs212795.
Schmidt, A., Lv, Z., and Großhans, J. (2018). ELMO and Sponge specify subapical restriction of Canoe and formation of the subapical domain in early *Drosophila* embryos. Development 145, dev157909.
Schnabel, K., Wu, C.C., Kurth, T., and Weidinger, G. (2011). Regeneration of cryoinjury induced necrotic heart lesions in zebrafish is associated with epicardial activation and cardiomyocyte proliferation. PLoS ONE 6, e18503.
Schwank, G., Restrepo, S., and Basler, K. (2008). Growth regulation by Dpp: an essential role for Brinker and a non-essential role for graded signaling levels. Development 135, 4003–4013.
Sehring, I.M., Recho, P., Denker, E., Kourakis, M., Mathiesen, B., Hannezo, E., Dong, B., and Jiang, D. (2015). Assembly and positioning of actomyosin rings by contractility and planar cell polarity. eLife 4, e09206.
Senyo, S.E., Steinhauser, M.L., Pizzimenti, C.L., Yang, V.K., Cai, L., Wang, M., Wu, T.D., Guerquin-Kern, J.L., Lechene, C.P., and Lee, R.T. (2013). Mammalian heart renewal by pre-existing cardiomyocytes. Nature 493, 433–436.
Shen, H., Gan, P., Wang, K., Darehzereshki, A., Wang, K., Kumar, S.R., Lien, C.L., Patterson, M., Tao, G., and Sucov, H.M. (2020). Mononuclear diploid cardiomyocytes support neonatal mouse heart regeneration in response to paracrine IGF2 signaling. eLife 9, e53071.
Sheng, Y., Duan, L., Cheng, T., Qiao, Y., Stover, N.A., and Gao, S. (2020). The completed macronuclear genome of a model ciliate *Tetrahymena thermophila* and its application in genome scrambling and copy number analyses. Sci China Life Sci 63, 1534–1542.
Shewaramani, S., Finn, T.J., Leahy, S.C., Kassen, R., Rainey, P.B., and Moon, C.D. (2017). Anaerobically grown *Escherichia coli* has an enhanced mutation rate and distinct mutational spectra. PLoS Genet 13, e1006570.
Shibai, A., Takahashi, Y., Ishizawa, Y., Motooka, D., Nakamura, S., Ying, B.W., and Tsuru, S. (2017). Mutation accumulation under UV radiation in *Escherichia coli*. Sci Rep 7, 14531.
Singh, B.N., Koyano-Nakagawa, N., Gong, W., Moskowitz, I.P., Weaver, C.V., Braunlin, E., Das, S., van Berlo, J.H., Garry, M.G., and Garry, D.J. (2018). A conserved HH-Gli1-Mycn network regulates heart

regeneration from newt to human. Nat Commun 9, 4237.
Sladitschek, H.L., Fiuza, U.M., Pavlinic, D., Benes, V., Hufnagel, L., and Neveu, P.A. (2020). MorphoSeq: full single-cell transcriptome dynamics up to gastrulation in a chordate. Cell 181, 922–935.e21.
Song, W., and Shao, C. (2017). Ontogenetic Patterns of Hypotrich Ciliates (in Chinese). Beijing: Science Press.
Song, Z., Zhang, X., Jia, S., Yelick, P.C., and Zhao, C. (2016). Zebrafish as a model for human ciliopathies. J Genet Genomics 43, 107–120.
Stargell, L.A., Bowen, J., Dadd, C.A., Dedon, P.C., Davis, M., Cook, R.G., Allis, C.D., and Gorovsky, M.A. (1993). Temporal and spatial association of histone H2A variant hv1 with transcriptionally competent chromatin during nuclear development in *Tetrahymena thermophila*. Genes Dev 7, 2641–2651.
Stemple, D.L. (2005). Structure and function of the notochord: an essential organ for chordate development. Development 132, 2503–2512.
Stockdale, W.T., Lemieux, M.E., Killen, A.C., Zhao, J., Hu, Z., Riepsaame, J., Hamilton, N., Kudoh, T., Riley, P.R., van Aerle, R., et al. (2018). Heart regeneration in the Mexican cavefish. Cell Rep 25, 1997–2007.e7.
Stocum, D.L. (2011). The role of peripheral nerves in urodele limb regeneration. Eur J Neurosci 34, 908–916.
Stolfi, A., Gandhi, S., Salek, F., and Christiaen, L. (2014). Tissue-specific genome editing in *Ciona* embryos by CRISPR/Cas9. Development 141, 4115–4120.
Stolfi, A., Ryan, K., Meinertzhagen, I.A., and Christiaen, L. (2015). Migratory neuronal progenitors arise from the neural plate borders in tunicates. Nature 527, 371–374.
Strahl, B.D., Ohba, R., Cook, R.G., and Allis, C.D. (1999). Methylation of histone H3 at lysine 4 is highly conserved and correlates with transcriptionally active nuclei in *Tetrahymena*. Proc Natl Acad Sci USA 96, 14967–14972.
Strauss, C., Long, H., Patterson, C.E., Te, R., and Lynch, M. (2017). Genome-wide mutation rate response to pH change in the coral reef pathogen *Vibrio shilonii* AK1. mBio 8, e01021.
Sugawara, M., Epstein, B., Badgley, B.D., Unno, T., and Sadowsky, M.J. (2013). Comparative genomics of the core and accessory genomes of 48 sinorhizobium strains comprising five genospecies. Genome Biol 14, R17..
Sullivan, W., and Theurkauf, W.E. (1995). The cytoskeleton and morphogenesis of the early *Drosophila* embryo. Curr Opin Cell Biol 7, 18–22.
Swart, E.C., Serra, V., Petroni, G., and Nowacki, M. (2016). Genetic codes with no dedicated stop codon: context-dependent translation termination. Cell 166, 691–702.
Szostak, J.W., and Blackburn, E.H. (1982). Cloning yeast telomeres on linear plasmid vectors. Cell 29, 245–255.
Tabata, T., Eaton, S., and Kornberg, T.B. (1992). The *Drosophila* hedgehog gene is expressed specifically in posterior compartment cells and is a target of engrailed regulation. Genes Dev 6, 2635–2645.
Tang, D., Wang, X., Dong, J., Li, Y., Gao, F., Xie, H., and Zhao, C. (2020). Morpholino-mediated knockdown of ciliary genes in *Euplotes vannus*, a novel marine ciliated model organism. Front Microbiol 11, 549781.
Tang, W., Martik, M.L., Li, Y., and Bronner, M.E. (2019). Cardiac neural crest contributes to cardiomyocytes in amniotes and heart regeneration in zebrafish. eLife 8, e47929.
Tatusov, R.L., Fedorova, N.D., Jackson, J.D., Jacobs, A.R., Kiryutin, B., Koonin, E.V., Krylov, D.M., Mazumder, R., Mekhedov, S.L., Nikolskaya, A.N., et al. (2003). The COG database: an updated version includes eukaryotes. BMC BioInf 4, 41.
Tincher, C., Long, H., Behringer, M., Walker, N., and Lynch, M. (2017). The glyphosate-based herbicide roundup does not elevate genome-wide mutagenesis of *Escherichia coli*. G3 7, 3331–3335.
Treen, N., Yoshida, K., Sakuma, T., Sasaki, H., Kawai, N., Yamamoto, T., and Sasakura, Y. (2014). Tissue-specific and ubiquitous gene knockouts by TALEN electroporation provide new approaches to investigating gene function in *Ciona*. Development 141, 481–487.
Trielli, F., Amaroli, A., Sifredi, F., Marchi, B., Falugi, C., and Corrado, M. U.D. (2007). Effects of xenobiotic compounds on the cell activities of *Euplotes crassus*, a single-cell eukaryotic test organism for the study of the pollution of marine sediments. Aquat Toxicol 83, 272–283.
Tsujikawa, M., and Malicki, J. (2004). Intraflagellar transport genes are essential for differentiation and survival of vertebrate sensory neurons. Neuron 42, 703–716.
Upadhyay, A., Peterson, A.J., Kim, M.J., and O'Connor, M.B. (2020). Muscle-derived Myoglianin regulates *Drosophila* imaginal disc growth. eLife 9, e51710.
Van Etten, J., and Bhattacharya, D. (2020). Horizontal gene transfer in eukaryotes: not if, but how much? Trends Genet 36, 915–925.
van Megen, H., van den Elsen, S., Holterman, M., Karssen, G., Mooyman, P., Bongers, T., Holovachov, O., Bakker, J., and Helder, J. (2009). A phylogenetic tree of nematodes based on about 1200 full-length small subunit ribosomal DNA sequences. Nematology 11, 927–950.
van den Hoogen, J., Geisen, S., Routh, D., Ferris, H., Traunspurger, W., Wardle, D.A., de Goede, R.G.M., Adams, B.J., Ahmad, W., Andriuzzi, W.S., et al. (2019). Soil nematode abundance and functional group composition at a global scale. Nature 572, 194–198.
Van Gennip, J.L.M., Boswell, C.W., and Ciruna, B. (2018). Neuroinflammatory signals drive spinal curve formation in zebrafish models of idiopathic scoliosis. Sci Adv 4, eaav1781.
Verissimo, K.M., Perez, L.N., Dragalzew, A.C., Senevirathne, G., Darnet, S., Barroso Mendes, W.R., Ariel Dos Santos Neves, C., Monteiro Dos Santos, E., Nazare de Sousa Moraes, C., Elewa, A., et al. (2020). Salamander-like tail regeneration in the West African lungfish. Proc R Soc B 287, 20192939.
Vivien, C.J., Hudson, J.E., and Porrello, E.R. (2016). Evolution, comparative biology and ontogeny of vertebrate heart regeneration. NPJ Regen Med 1, 16012.
Wagner, A., Whitaker, R.J., Krause, D.J., Heilers, J.H., van Wolferen, M., van der Does, C., and Albers, S.V. (2017). Mechanisms of gene flow in archaea. Nat Rev Microbiol 15, 492–501.
Wang, J., Cao, J., Dickson, A.L., and Poss, K.D. (2015). Epicardial regeneration is guided by cardiac outflow tract and Hedgehog signalling. Nature 522, 226–230.
Wang, J., Karra, R., Dickson, A.L., and Poss, K.D. (2013). Fibronectin is deposited by injury-activated epicardial cells and is necessary for zebrafish heart regeneration. Dev Biol 382, 427–435.
Wang, J., Panáková, D., Kikuchi, K., Holdway, J.E., Gemberling, M., Burris, J.S., Singh, S.P., Dickson, A.L., Lin, Y.F., Sabeh, M.K., et al. (2011). The regenerative capacity of zebrafish reverses cardiac failure caused by genetic cardiomyocyte depletion. Development 138, 3421–3430.
Wang, R., Xiong, J., Wang, W., Miao, W., and Liang, A. (2016). High frequency of +1 programmed ribosomal frameshifting in *Euplotes octocarinatus*. Sci Rep 6, 21139.
Wang, W., Hu, C.K., Zeng, A., Alegre, D., Hu, D., Gotting, K., Ortega Granillo, A., Wang, Y., Robb, S., Schnittker, R., et al. (2020a). Changes in regeneration-responsive enhancers shape regenerative capacities in vertebrates. Science 369, eaaz3090.
Wang, X., Li, Z., Zhang, Q., Li, B., Lu, C., Li, W., Cheng, T., Xia, Q., and Zhao, P. (2018). DNA methylation on N^6-adenine in lepidopteran *Bombyx mori*. Biochim Biophys Acta 1861, 815–825.
Wang, X., Wang, S., Meng, Z., and Zhao, C. (2020b). Adrb1 and Adrb2b are the major β-adrenergic receptors regulating body axis straightening in zebrafish. J Genets Genomics doi: 10.1016/j.jgg.2020.10.009.
Wang, Y., Chen, X., Sheng, Y., Liu, Y., and Gao, S. (2017). N^6-adenine DNA methylation is associated with the linker DNA of H2A.Z-containing well-positioned nucleosomes in Pol II-transcribed genes in *Tetrahymena*. Nucleic Acids Res 45, 11594–11606.
Wang, Y., Sheng, Y., Liu, Y., Zhang, W., Cheng, T., Duan, L., Pan, B., Qiao, Y., Liu, Y., and Gao, S. (2019). A distinct class of eukaryotic MT-A70 methyltransferases maintain symmetric DNA N^6-adenine methylation at the ApT dinucleotides as an epigenetic mark associated with transcription. Nucleic Acids Res 47, 11771–11789.
Wei, F. (2020). A new era for evolutionary developmental biology in non-

model organisms. Sci China Life Sci 63, 1251–1253.
Wei, J., Wang, G., Li, X., Ren, P., Yu, H., and Dong, B. (2017). Architectural delineation and molecular identification of extracellular matrix in ascidian embryos and larvae. Biol Open 6, 1383–1390.
Wei, K., Serpooshan, V., Hurtado, C., Diez-Cuñado, M., Zhao, M., Maruyama, S., Zhu, W., Fajardo, G., Noseda, M., Nakamura, K., et al. (2015). Epicardial FSTL1 reconstitution regenerates the adult mammalian heart. Nature 525, 479–485.
Weinstein, S.L. (2019). The natural history of adolescent idiopathic scoliosis. J Pediatr Orthop 39, S44–S46.
Winkler, F., Gummalla, M., Künneke, L., Lv, Z., Zippelius, A., Aspelmeier, T., and Grosshans, J. (2015). Fluctuation analysis of centrosomes reveals a cortical function of kinesin-1. Biophys J 109, 856–868.
Witman, N., Murtuza, B., Davis, B., Arner, A., and Morrison, J.I. (2011). Recapitulation of developmental cardiogenesis governs the morphological and functional regeneration of adult newt hearts following injury. Dev Biol 354, 67–76.
Wu, T.P., Wang, T., Seetin, M.G., Lai, Y., Zhu, S., Lin, K., Liu, Y., Byrum, S.D., Mackintosh, S.G., Zhong, M., et al. (2016). DNA methylation on N^6-adenine in mammalian embryonic stem cells. Nature 532, 329–333.
Xiao, C., Gao, L., Hou, Y., Xu, C., Chang, N., Wang, F., Hu, K., He, A., Luo, Y., Wang, J., et al. (2016). Chromatin-remodelling factor Brg1 regulates myocardial proliferation and regeneration in zebrafish. Nat Commun 7, 13787.
Xiao, C.L., Zhu, S., He, M., Chen, D., Zhang, Q., Chen, Y., Yu, G., Liu, J., Xie, S.Q., Luo, F., et al. (2018). N^6-methyladenine DNA modification in the human genome. Mol Cell 71, 306–318.e7.
Xie, Q., Wu, T.P., Gimple, R.C., Li, Z., Prager, B.C., Wu, Q., Yu, Y., Wang, P., Wang, Y., Gorkin, D.U., et al. (2018). N^6-methyladenine DNA modification in glioblastoma. Cell 175, 1228–1243.e20.
Xie, Y., Zhang, P., Xue, B., Cao, X., Ren, X., Wang, L., Sun, Y., Yang, H., and Zhang, L. (2020). Establishment of a marine nematode model for animal functional genomics, environmental adaptation and developmental evolution. bioRxiv 980219.
Xu, J., Li, X., Song, W., Wang, W., and Gao, S. (2019). Cyclin Cyc2p is required for micronuclear bouquet formation in *Tetrahymena thermophila*. Sci China Life Sci 62, 668–680.
Yan, Y., Maurer-Alcalá, X.X., Knight, R., Kosakovsky Pond, S.L., and Katz, L.A. (2019). Single-cell transcriptomics reveal a correlation between genome architecture and gene family evolution in ciliates. mBio 10.
Yao, B., Cheng, Y., Wang, Z., Li, Y., Chen, L., Huang, L., Zhang, W., Chen, D., Wu, H., Tang, B., et al. (2017). DNA N^6-methyladenine is dynamically regulated in the mouse brain following environmental stress. Nat Commun 8, 1122.
Ye, L., D'Agostino, G., Loo, S.J., Wang, C.X., Su, L.P., Tan, S.H., Tee, G. Z., Pua, C.J., Pena, E.M., Cheng, R.B., et al. (2018). Early regenerative capacity in the porcine heart. Circulation 138, 2798–2808.
Zhang, G., Huang, H., Liu, D., Cheng, Y., Liu, X., Zhang, W., Yin, R., Zhang, D., Zhang, P., Liu, J., et al. (2015a). N^6-methyladenine DNA modification in *Drosophila*. Cell 161, 893–906.
Zhang, L., Gualberto, D.G., Guo, X., Correa, P., Jee, C., and Garcia, L.R. (2015b). TMC-1 attenuates *C. elegans* development and sexual behaviour in a chemically defined food environment. Nat Commun 6, 6345.
Zhang, R., Han, P., Yang, H., Ouyang, K., Lee, D., Lin, Y.F., Ocorr, K., Kang, G., Chen, J., Stainier, D.Y.R., et al. (2013). *In vivo* cardiac reprogramming contributes to zebrafish heart regeneration. Nature 498, 497–501.
Zhang, S., Zhao, J., Lv, X., Fan, J., Lu, Y., Zeng, T., Wu, H., Chen, L., and Zhao, Y. (2020). Analysis on gene modular network reveals morphogen-directed development robustness in *Drosophila*. Cell Discov 6, 43.
Zhang, X., Jia, S., Chen, Z., Chong, Y.L., Xie, H., Feng, D., Wu, X., Song, D.Z., Roy, S., and Zhao, C. (2018). Cilia-driven cerebrospinal fluid flow directs expression of urotensin neuropeptides to straighten the vertebrate body axis. Nat Genet 50, 1666–1673.
Zhao, C., and Malicki, J. (2007). Genetic defects of pronephric cilia in zebrafish. Mech Dev 124, 605–616.
Zhao, D., Liu, J., Wang, M., Zhang, X., and Zhou, M. (2019a). Epidemiology of cardiovascular disease in China: current features and implications. Nat Rev Cardiol 16, 203–212.
Zhao, L., Ben-Yair, R., Burns, C.E., and Burns, C.G. (2019b). Endocardial Notch signaling promotes cardiomyocyte proliferation in the regenerating zebrafish heart through Wnt pathway antagonism. Cell Rep 26, 546–554.e5.
Zhao, L., Borikova, A.L., Ben-Yair, R., Guner-Ataman, B., MacRae, C.A., Lee, R.T., Burns, C.G., and Burns, C.E. (2014). Notch signaling regulates cardiomyocyte proliferation during zebrafish heart regeneration. Proc Natl Acad Sci USA 111, 1403–1408.
Zhao, L., Wang, L., Chi, C., Lan, W., and Su, Y. (2017). The emerging roles of phosphatases in Hedgehog pathway. Cell Commun Signal 15, 35.
Zhou, C., Wang, C., Liu, H., Zhou, Q., Liu, Q., Guo, Y., Peng, T., Song, J., Zhang, J., Chen, L., et al. (2018). Identification and analysis of adenine N^6-methylation sites in the rice genome. Nat Plants 4, 554–563.
Zhu, C., Mahlich, Y., Miller, M., and Bromberg, Y. (2018a). fusionDB: assessing microbial diversity and environmental preferences via functional similarity networks. Nucleic Acids Res 46, D535–D541.
Zhu, W., Zhang, E., Zhao, M., Chong, Z., Fan, C., Tang, Y., Hunter, J.D., Borovjagin, A.V., Walcott, G.P., Chen, J.Y., et al. (2018b). Regenerative potential of neonatal porcine hearts. Circulation 138, 2809–2816.
Zhu, Y., Qiu, Y., Chen, W., Nie, Q., and Lander, A.D. (2020). Scaling a Dpp morphogen gradient through feedback control of receptors and co-receptors. Dev Cell 53, 724–739.e14.